PhD
PROGRAM IN TRANSLATIONAL
AND MOLECULAR MEDICINE

University of Milano-Bicocca
School of Medicine and Faculty of Science

Cell-based analysis of dynamic aspects of molecular mechanisms involved in the pathogenesis of Parkinson's Disease

Coordinator: Prof. Andrea Biondi
Tutor: Prof. Carlo Ferrarese

Dr. Dalila Ciceri
Matr. No. 037872

XXII CICLE
Academic year
2008-2009

Table of Contents:

Chapter 1
Introduction

1.1 Parkinson's Disease

In the Western countries Parkinson's Disease (PD) is the second most common neurodegenerative disorder after Alzheimer's Disease (AD). The World Health Organization estimates around one million of affected persons in Europe. The estimated prevalence if the disease in the world is 1-2% in people aged more than 65 years and it rises with age. The incidence of PD seems to be slightly higher in men than in women (lifetime risk 2,0% versus 1,3%, respectively) (Nutt and Wooten, 2005; Weintraub et al., 2008).

In general the age of onset is in the early 60s; however, in up to 10% of the cases, PD symptoms could appear also in 40-50 years old persons (Weintraub et al., 2008). Considering the current increase in life expectancy, PD will have a growing social and economical impact in the future.

1.1.1 Clinical aspects of PD

PD was first described as "shaking palsy" by James Parkinson, in 1817. Further studies led to a better definition of the clinical features of this progressive neurodegenerative disorder. Nowadays, the diagnosis of PD is linked to the presence of at least 2 of the following main clinical signs: tremor at rest (involuntary shaking that is reduced during voluntary movements), rigidity and bradykinesia/akinesia (slowness/failure in initiation and execution of the movements).

Other common manifestations of PD include the postural instability (due to impairment of postural reflexes), difficulties in maintaining the balance, in walking, in talking. Together with motor impairments, PD affects also the autonomic function, cognition and behaviour, indicating an involvement not only of dopaminergic, but also of noradrenergic, cholinergic and serotoninergic pathways; (Jankovic, 2008; Nutt and Wooten, 2005; Weintraub et al., 2008).

The onset of PD is often unilateral and mild, so sometimes it is difficult to define exactly the beginning of the disease. The tremor is in general the first symptom that is perceived, in up to 70% of the affected patients (Weintraub et al., 2008). Rigidity and bradykinesia often appear later. In general clinical observation is sufficient to make diagnosis; however, Positron Emission Tomography (PET) and the Single Positron Emission Computerized Tomography (SPECT) have proven as a useful help to the clinicians for differential diagnosis.

1.1.2 Pathological features of PD

The typical neuropathological hallmark of PD, and the cause of the motor dysfunctions in the affected, is the progressive loss of dopamine-producing neurons located in the pars compacta of the substantia nigra. The substantia nigra is part of a complex of neuronal structures, called basal ganglia, involved in the control and coordination of movements and connected to the cortex, the thalamus and other brain areas (Weintraub et al., 2008). The lack of dopamine production interferes with the regulatory functions of the basal ganglia (Fig.1).

During the progression of the disease, neurons from other brain areas become affected, giving rise to the large spectrum of symptoms (including the not-motor ones) observed in the patients (Braak et al., 2003).

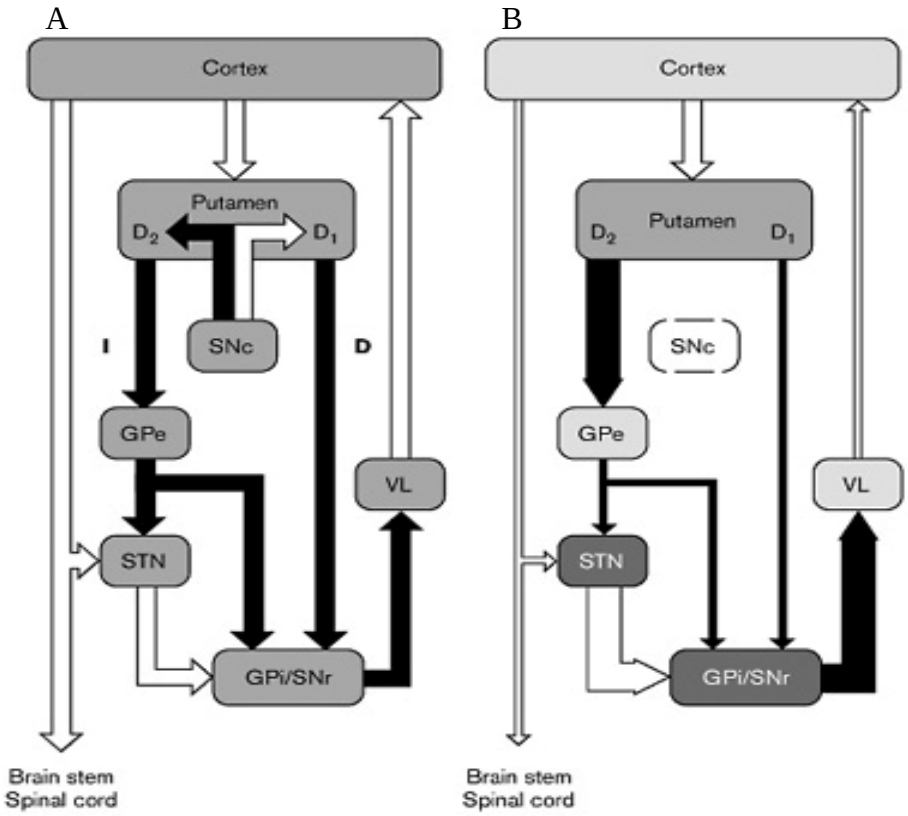

Figue 1: Schematic representation of the neuronal circuits of the basal ganglia in physiological conditions (A) and in PD (B). Black arrows indicate inhibitory signals, while white arrows indicate excitatory signals. SNc/r: substantia nigra pars compacta/reticulata; GPe/i: globus pallidus external/internal segment; VL: ventral lateral nucleus of the thalamus; STN: subthalamic nucleus (Adapted from http://www.unifr.ch/biochem).

It was calculated that the clinical symptoms of PD become evident only when at least 60% of the neurons in the substantia nigra are lost and the striatal levels of dopamine are reduced by 80% (Harrison, *Principles of Internal Medicine,* McGraw-Hill, 15st ed., 2002).

Post-mortem examination of PD patients usually reveals the presence of intracytoplasmic inclusions in the surviving neurons of the substantia nigra and in other areas of the brain. These inclusions develop as spindle- or thread-like Lewy neuritis (LN) in cellular processes or in the form of globular Lewy bodies (LB) in neuronal perikarya (Forno, 1996; Pollanen et al., 1993). LB are spherical, 8-30 μm in diameter, protein aggregates with a peripheral halo of radiating filaments and a dense core of granular material (Olanow et al., 2004). Their main components are insoluble fibrils of alpha-synuclein, a neuronal pre-synaptic protein (Polymeropoulos et al., 1997; Spillantini et al., 1997). LB contain also a variety of other proteins, such as neurofilaments (Schmidt et al., 1991), ubiquitin (Lennox et al., 1989), synphilin-1 (Wakabayashi et al., 2000), components of the ubiquitin-proteasome system (Ii et al., 1997; Lowe et al., 1990), heat shock proteins (Auluck et al., 2002) and centrosome-related proteins (McNaught et al., 2002a).

It's important to mention that LB have also been reported in other neurological disorders, such as dementia with Lewy bodies (Spillantini et al., 1998), multiple system atrophy (Burn and Jaros, 2001), Alzheimer's disease (Giasson et al., 2000) and even Down syndrome (Raghavan et al., 1993), grouping some of them under the term "synucleinopathies". Moreover, LB can be found in the neurons of the substantia nigra of 10-15% over 65 years old individuals who

died without any evidence of neurological illness (Braak et al., 2003; Gibb and Lees, 1988).

1.1.3 Aetiology of PD

Idiopathic PD is sporadic in 90% of cases, with a not well-defined aetiology. It is thought to be the result of a combination of environmental factors or toxins, genetic susceptibility, and the aging process (Weintraub et al., 2008).

Genetic mutations are responsible for 10% of cases of PD (Lesage and Brice, 2009). The SNCA gene, coding for alpha-synuclein, was the first one to be unequivocally associated with familial parkinsonism (Polymeropoulos et al., 1997). In addition to three point mutations, a group of families with PD were shown to carry duplications or triplications of the wild-type gene (reviewed in Hardy et al., 2009).

More than ten years after the identification of the first monogenic form of parkinsonism, clinical studies, genome-wide linkage analysis and positional cloning led to the discovery of several loci and genes linked to inherited forms of PD (Tab.1). Among them, six are established causative genes for PD (PARK1/4, PARK 2, 6, 7, 8 and 9), while the relevance to the disease of the others is not yet well defined (Lesage and Brice, 2009).

Genetic forms of PD are seen more frequently in young-onset PD (Simuni T. “Diagnosis and management of Parkinson’s Disease” Medscape Neurology, Aug. 2007).

Secondary forms of parkinsonism can be caused by medications, central nervous system infections, toxins, structural lesions (such as

stroke), trauma or vascular/metabolic disorders (Weintraub et al., 2008).

Table 1: current list of genes and loci for parkinsonism			
A. Loci and genes implicated in PD with conclusive evidence			
Locus	Map position	Gene	Inheritance
PARK1/4	4q21-q23	alpha-synuclein	dominant
PARK8	12p11-q13	LRRK2	dominant
PARK2	6q25-q27	Parkin	recessive
PARK6	1p36-p35	PINK1	recessive
PARK7	1p36	DJ-1	recessive
PARK9	1p36	ATP13A2	recessive
B. Loci identified in genome-wide linkage screens			
PARK3	2p13	unknown	dominant
PARK10	1p32	unknown	unclear
PARK11	2q36-q37	unknown	unclear
PARK12	Xq	unknown	unclear
Pending	2q35-q36	unknown	dominant
C. Genes proposed to be implicated in PD			
PARK5	4p14	UCHL1	unclear
PARK13	2p12	Omi/HtrA2	unclear
Pending	1q21	GBA	unclear
Pending	2q22-q23	NR4A2 (NURR1)	unclear
Pending	5q23	synphilin-1	unclear

Table adapted form: Bonifati, 2007.

1.1.4 Molecular pathogenesis of PD

Genetic studies of familiar PD cases, together with the useful information coming from the post-mortem examinations and the *in vivo* and *in vitro* models of PD shed light on the molecular pathogenesis of the disease. Nowadays, five main pathological mechanisms are thought to be responsible for PD in a coordinated and synergic way: mitochondrial dysfunctions, impairments of the

Ubiquitin-Proteasome System (UPS), oxidative stress, excitotoxicity and protein aggregation (Fig.2)

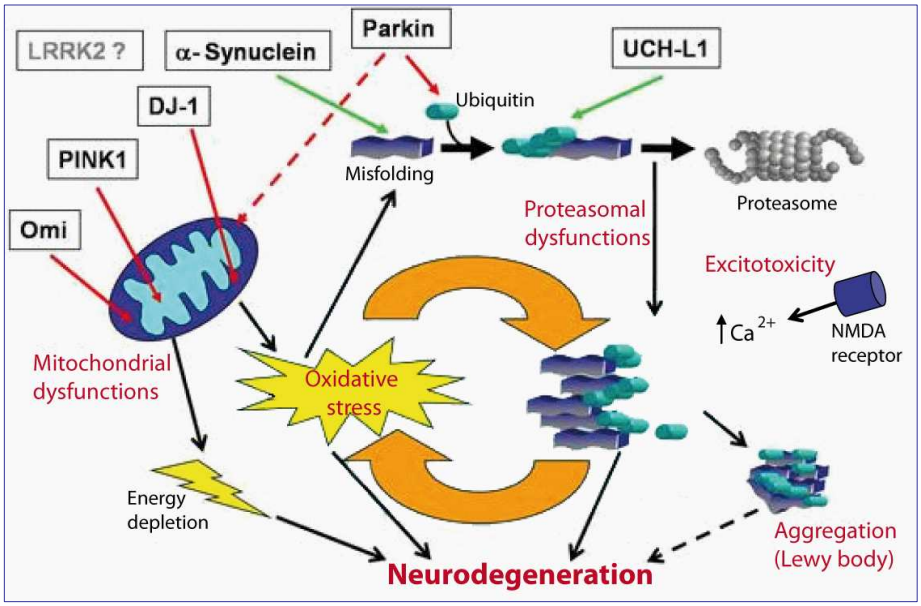

Figure 2: Schematic representation of the molecular pathogenetic mechanisms of PD. Red arrows indicate gain of function mutations, while green arrows indicate mutations leading to gain of toxic function (Adapted from www.hih-tuebingen.de).

Mitochondrial dysfunction:

The first hints of the involvement of mitochondria in the pathogenesis of PD came from the discovery of parkinsonian symptoms in people exposed to 1-methyl-4-phenyl-1,2,3,6-tetrahydropyridine (MPTP). In fact, its metabolite 1-methyl-4-phenylpyridinium (MPP^+) is a specific inhibitor of the complex I of the mitochondrial respiratory chain (Langston et al., 1983)

Later, it was discovered that also the exposition to other complex I inhibitors, such as the pesticides rotenone and paraquat (reviewed in

Cicchetti et al., 2009), together with aging, increases the risk to develop PD (Thiruchelvam et al., 2003).

Moreover, a significant reduction of the activity of the complex I of the mitochondrial respiratory chain has been observed in brain, muscles and platelets from PD patients (Schapira et al., 1990; Parker et al., 1989).

Finally, several studies reported mutations in genes coding for either mitochondrial protein or protein involved in mitochondrial function (such as Parkin, PTEN-induced kinase-1, DJ-1 and Omi/HtrA2) in familiar PD cases (Kitada et al., 1998; Valente et al., 2004; Bonifati et al., 2004; Strauss et al., 2005), further suggesting a role of mitochondrial impairments in PD.

Excitotoxicity:

The term excitotoxicity defines the excess of activity of the excitatoriy amino acids neurotransmitters abnormally released in pathological conditions, causing a calcium-dependent neurodegenerative process.

Glutamate-mediated excitotoxicity might occur via two different mechanisms in PD. The ‘fast mechanism’ hypothesis suggests that glutaminergic projections from the subthalamic nucleus to the sbstantia nigra pars compacta (SNc) are overactive, leading to increased glutamate release and over-activation of N-Methyl-D-Aspartate (NMDA) receptors that are present on dopaminergic neurons (Bergman et al., 1990).

The ‘slow mechanism’ hypothesis proposes that impairment of complex I activity in the SNc leads to loss of ATP, reversal of the Na^+/K^+ ATPase and loss of resting membrane potential. This causes

partial depolarization of dopaminergic cell membrane and relieves the voltage-dependent blockade of NMDA receptors by Mg^{2+}, causing these neurons to become susceptible to damage consequent to normal physiological levels of glutamate (Beal, 1998; Greene and Greenamyre, 1996).

Dysfunctions of the Ubiquitin-Proteasome System (UPS):

The main function of UPS is to prevent the accumulation of abnormal proteins in the cells. It performs a continuous monitoring activity on the newly-synthesized proteins in order to prevent excesses of protein from being damaged. Moreover, it degrades the protein with abnormal structures due to biosynthetic mistakes, misfolding or post-translational aberrant modifications (Jung et al., 2009).

The proteasome is a multi-subunit enzyme complex formed by a cylindrical catalytic 20S core bound on each side to a 19S regulatory protein. It specifically recognises and degrades only the proteins that have been previously tagged with a short chain made of a 76 amino acid protein, called ubiquitin. A group of protein named E1, E2 and E3 are responsible for the recognition and for the ubiquitination of the targets (Cook and Petrucelli, 2009).

In a process that requires energy (ATP), tagged proteins are unfolded and fed into the inner chamber. The proteins are then digested into 6 to 9 amino acids long peptides and released. The peptides can then be recycled (Cook and Petrucelli, 2009).

The evaluation of human post-mortem brain tissue has provided considerable amount of evidence implicating proteasomal dysfunction in PD. A significant decrement in proteasomal activity was detected in

the substantia nigra of PD patients, when compared to age-matched controls (Furukawa et al., 2002; McNaught et al., 2003; McNaught and Jenner, 2001; Tofaris et al., 2003). In addition, accumulation of ubiquitinated proteins and components of the UPS has been detected in LB (Ii et al., 1997; Lennox et al., 1989; Lowe et al., 1990; McNaught et al., 2002b; Schlossmacher et al., 2002).

Treatment with the proteasomal inhibitor lactacystin dose-dependently leads to the degeneration and to the formation of synuclein- and ubiquitin-positive inclusions in cultured neurons (McNaught et al., 2002b). Moreover, a behavioural and pathological phenotype reminiscent of PD was observed also in rats after systemic administration of proteasomal inhibitors (McNaught et al., 2004; Schapira et al., 2006; Zeng et al., 2006).

The link between proteasomal dysfunctions and PD was further solidified by genetic studies of inherited forms of PD. In particular, mutations in the genes coding for Parkin (an E3 ubiquitin lygase) and UCH-L1 (a Ubiquitin-C terminal Hydroxilase necessary for ubiquitin recycling), found in rare familiar forms of PD, provide further support for a central role of UPS dysfunction in the aetiopathogenesis of PD (Leroy et al., 1998; Kitada et al., 1998).

Oxidative stress:

Reactive Oxygen Species (ROS) and free radicals are really dangerous, since they can irreversibly damage proteins, DNA and the lipids of the membranes.

Several signs of oxidative stress were observed in *post-mortem* PD brains: in particular, increased levels of lipid peroxidation, protein

nytrosylation (Andersen, 2004) and depletion of antioxidants (Sian et al., 1994) were reported in the substantia nigra of PD patients. Also elevated levels of iron (leading to production of hydrogen peroxide through the so-called Fenton's reaction) were found in the substantia nigra of affected people (Sofic et al., 1991; Gerlach et al., 1997). Moreover, loss-of-function mutations in DJ-1, a protein that has anti-oxidant properties, have been described in inherited PD cases, further suggesting a role of oxidative stress in PD (Bonifati et al., 2004).

Finally, it is important to remind that the oxidative load of the neurons of the substantia nigra is normally higher than other brain regions, since the physiological enzymatic metabolism and auto-oxidation of dopamine involves free radical productions (Graham, 1978).

Protein aggregation:

The involvement of protein aggregation in the pathogenesis of PD is obviously supported by the presence of LB and LN in PD brains and by the evidence of PD-causing mutations in alpha-synuclein as well (see above). In fact, alpha-synuclein has a physiological tendency to aggregate (Wood et al., 1999) and it forms inclusions not only in PD, but also in other neurological disorders, generally referred as alpha-synucleophaties (reviewed in Recchia et al., 2004).

In PD patients, there is no evidence of an increase in the mRNA levels of any aggregate-prone protein, not even the ones found in LB. (Hill et al., 1993; Kingsbury et al., 2004). Rather, as mention in the above paragraphs, several research groups reported increased level of oxidative stress, dysfunction of the UPS and of mitochondria, which could trigger and enhance the mechanisms of protein aggregation.

Indeed, it has been shown that free radical attack on macromolecules is an important cause of protein damage, misfolding and aggregation (Grune et al., 2004) and also pharmacological inhibition of mitochondrial function can induce alpha-synuclein aggregation in various models (Betarbet et al., 2000; Fornai et al., 2005; Lee et al., 2002b). In addition, as mention above, proteasomal dysfunction has been shown to enhance protein aggregation in both *in vitro* and *in vivo* studies.

In conclusion, protein aggregation is more likely to represent an indirect secondary effect due to the combination of other dysfunctions and abnormalities observed in PD than a primary cause of PD. A growing amount of publications suggests that the formation of inclusions bodies could have a protective role (Tanaka et al., 2004; Tompkins and Hill, 1997; McNaught et al., 2002b).

1.2 Autophagy

Autophagy is an evolutionary conserved pathway involved in the degradation and turnover of protein, organelles and macromolecules in the lysosomes, apart from the already-mentioned UPS. It encompasses at least three pathways, all of them ending in the lysosomes: microautophagy, chaperone-mediated autophagy and macroautophagy, also referred as autophagy (reviewed in Martinez-Vicente and Cuervo, 2007). Microautophagy takes place constitutively and it is characterized by a direct engulfment of portion of the cytoplasm in the lysosomes via encocytotic-like mechanisms. Chaperone-mediated autophagy is responsible for the degradation of unfolded proteins: they are carried to the membranes of the lysosomes by specific chaperones and then inside the lysosomes through the Lamp2a receptor. It is enhanced under stress conditions. Macroautophagy is thought to be responsible for the degradation of aggregates and organelles (Rideout et al., 2004), including mitochondria. It involves the formation of double membrane vesicles, called autophagosomes, which fuse with lysosomes to form autophagolysosomes, where the content is degraded (Martinez-Vicente and Cuervo, 2007) (Fig.3).

Autophagy is regulated principally via two signalling pathways: the class I and III phosphatidylinositol 3-kinases (PI3K) pathways; the first one, which involves the kinase mammalian Target Of Rapamycin (mTOR), promotes normal cell growth but it has a repressive effect on

autophagy, while the second is essential for autophagy induction (Todde et al., 2009)

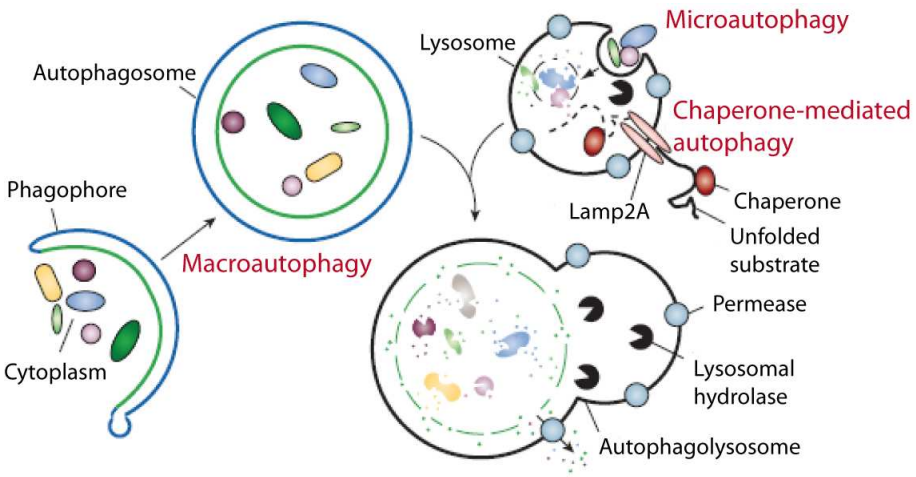

Figure 3: Schematic overview of the autophagic pathways (adapted from Mizushima et al., 2008).

Growing evidence proposes that impairments of autophagy-related catabolic mechanisms could be involved in the pathogenesis of PD. For example, loss-of-function mutations in the lysosomal ATPase ATP13A2 have been recently described in an autosomal recessive form of an early-onset parkinsonian syndrome with degeneration and dementia (Ramirez et al., 2006). Furthermore, it was demonstrated that the suppression of basal autophagy in mice was sufficient to induce neurodegeneration and deficits in motor function, accompanied by the presence of inclusion bodies in neurons (Hara et al., 2006).

1.3 Synphilin-1

Synphilin-1 is a 919 amino acid protein predominantly expressed in neurons, mainly at the pre-synaptic terminals (Krüger, 2004). In human brain, synphilin-1 is mainly found in Purkinje, nigral and pyramidal neurons (Engelender et al., 2000; Ribeiro et al., 2002; Murray et al., 2003). It can be detected predominantly as a 90 kDa isoform; however, some variants with different molecular weight (120, 65 and 50 kDa) are also detectable, suggesting the possibility of alternative splicing or post-translational processing of synphilin-1 (Murray et al., 2003).

Several domains have been identified in synphilin-1 structure, including six ankyrin-like domains, a coiled-coil domain and an ATP/GTP-binding motif (Krüger, 2004). The physiological function of synphilin-1 is still unknown. It has been identified as an alpha-synuclein-interacting protein by using yeast two-hybrid screenings (Neystat et al., 2002; Engelender et al., 1999) and a report suggested that it may play a role in the control of vesicle trafficking, possibly by mediating the interaction of alpha-synuclein with the membranes of the synaptic vesicles (Ribeiro et al., 2002). A potential role of synphilin-1 in modulating the proteasomal function was suggested by a study reporting a direct interaction of synphilin-1 with the regulatory S6 subunit of the proteasome (Marx et al., 2007). Other members of regulatory components of the proteasome were previously implicated in other neurodegenerative disorders, i.e. spastic paraplegia and ataxia

(SCA3) (Hazan et al., 1999; Doss-Pepe et al., 2003; Matsumoto et al., 2004).

The identification of synphilin-1 as a substrate of the PD-associated ubiquitin E3 ligase Parkin (Chung et al., 2001) for its degradation by the proteasome (Chung et al., 2001; Lee et al., 2002a) established the first link of synphilin-1 with the pathogenesis of PD. Furthermore, it has been shown that synphilin-1 can be ubiquitinated also by other three E3 ligases: dorfin, SIAH-1 and SIAH-2 (Ito et al., 2003; Nagano et al., 2003; Liani et al., 2004). Interestingly, all these ligases (and Parkin as well) are components of LB in the brain of PD patients and therefore they may be related to neurodegeneration (Schlossmacher et al., 2002; Ito et al., 2003; Liani et al., 2004).

In addition, synphilin-1 itself is present in the majority of LB in PD brains (Wakabayashi et al., 2000) and it can spontaneously form LB-like inclusions also when it is overexpressed *in vitro* (O'Farrell et al., 2001) and *in vivo* (Nuber et al., 2010).

Besides protein aggregates, transgenic overexpression of synphilin-1 in mice caused also neuronal degeneration and mitochondrial abnormalities, together with significant reduction of both motor skill learning and motor performance (Nuber et al., 2010).

The amino acid substitution R621C of synphilin-1, which was identified in two German PD patients, was related to an increased susceptibility to cellular stress *in vitro* (Marx et al., 2003) and to a more severe pathological phenotype *in vivo* (Nuber et al., 2010). Moreover, recent studies focused on the aggregate-forming properties of synphilin-1 showed that the ankyrin-repeat domain harbouring the

R621C substitution is critical for the aggregation of the protein (Zaarur et al., 2008).

However, subsequent genetic studies observed the same rare variant also in healthy controls, allowing no firm confirmation of the relevance of the mutation in PD pathogenesis (Myhre et al., 2008).

1.4 Mitochondrial morphology, fission and fusion

The central nervous system has an intense demand for mitochondria: the human brain consumes 20% of resting metabolic energy while comprising only 2% of total body mass (Silver and Erecinska, 1998). More than 95% of ATP used by the brain is produced by mitochondria. In neurons, ATP is needed for essential functions, such as the maintenance of ionic gradients, neurotransmitter synthesis, synaptic vesicle mobilization, release, and recycling, and local protein translation and degradation (Yang and Lu, 2009).

Mitochondria exhibit dynamic structural changes in vivo: in addition to the classical kidney bean shape of individual mitochondrion, they are commonly found as extended reticular and tubular networks. These elaborate mitochondrial networks are extremely dynamic, undergoing frequent processes of fission and fusion in order to serve the needs of the cells and to respond to the environmental cues (Okamoto and Shaw, 2005).

Fission and fusion of mitochondria require distinct conserved GTPase proteins and their binding partners acting at mitochondrial membranes (Fig.4). In mammals, the key molecules for mitochondrial fission are hFis1 and Drp1 (dynamin-related protein 1). The opposing process, mitochondrial fusion, is controlled by mitofusins (Mfn) and OPA1 in mammalian cells. Mfn1 and Mfn2 localize on the outer membrane of mitochondria and may directly mediate mitochondrial outer-membrane fusion. OPA1 resides in the intermembrane space and it is essential for inner-membrane fusion (Chan, 2006).

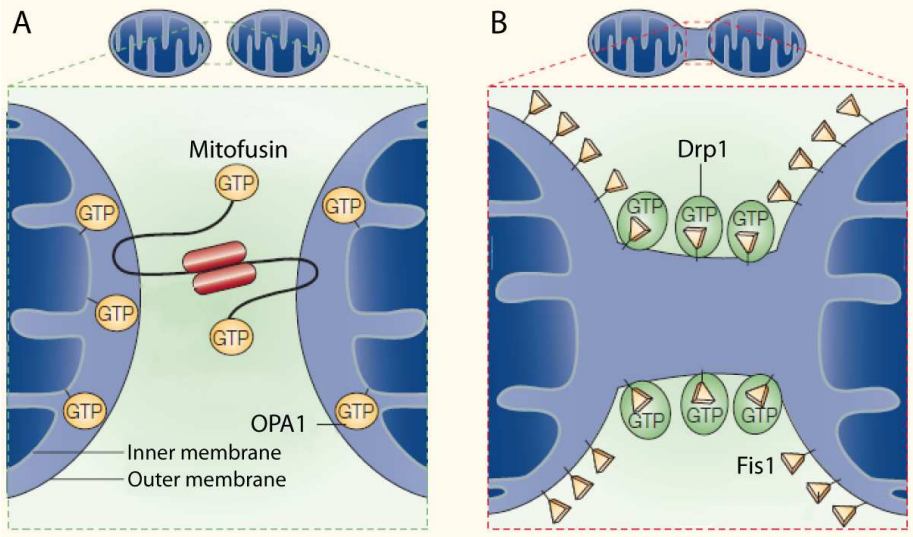

Figure 4: Schematic overview of the processes of mitochondrial fusion (A) and fission (B). (Adapted from Youle and Karbowski, 2005).

OPA1 has further been implicated in maintaining the cristae structure in mitochondria, by forming a complex including soluble and membrane-bound forms of OPA1 at the cristae junctions (Griparic et al., 2004).

Nevertheless, the physiological advantages of a dynamic mitochondrial population are still unclear. It was speculated that fission facilitates mitochondrial biogenesis, promotes the compartmentalization of mitochondrial functions (Yang and Lu, 2009) and facilitates mitochondrial transport in axon and dendrites (Misgeld et al., 2007). Fusion is thought to promote intermitochondrial cooperation, such as the transmission of membrane potential and the exchange of mitochondria contents (Yang and Lu, 2009). In particular, mitochondrial DNA (mtDNA) exchange between mitochondria could lead to complementation of mtDNA lesions (Ono et al., 2001).

Moreover, two key functions of mitochondria, electron transport and regulation of apoptosis, are affected by disruption of molecules involved in mitochondrial fusion and fission (Chan, 2006).

The importance of fission and fusion mechanisms, especially for the neurons, is confirmed by several genetic studies focused on their molecular regulators. In particular, mutations of OPA1 have been linked to an autosomal-dominant optic atrophy, which is characterized by loss of visual acuity caused by degeneration of retinal ganglion neurons (Delettre et al., 2000). Waterham and co-workers recently identified a lethal mutation in the Drp1 gene in a newborn human with microcephaly, lactic acidemia, and optic atrophy (Waterham et al., 2007). Deficiency of the Drosophila homologue of fission molecule Drp1 caused a severe loss of presynaptic mitochondria in neuromuscular junctions, leading to neurotransmission failure after intense stimulation (Verstreken et al., 2005). Finally, mutations of Mfn2 are implicated in the Charcot-Marie-Tooth disease-subtype 2A (CMT2A) neuropathy, characterized by aggregation of axonal mitochondria in the peripheral nerves (Verhoeven et al., 2006).

1.5 HtrA2/Omi

High temperature requirement A2 (HtrA2)/Omi is a 49 kDa nuclear encoded serine protease that localizes principally to the intermembrane space of mitochondria. Small amounts of HtrA2/Omi are found also in the nucleus and in the endoplasmic reticulum (Gray et al., 2000; Kuninaka et al., 2007; Martins et al., 2002).

It was first isolated in yeast two hybrid screenings using Mxi2, a splice variant of the stress-activated kinase p38, as bait (Faccio et al., 2000). HtrA2/Omi is a member of a well-conserved family (called HtrA) of serine proteases which are found in most eukaryotes and prokaryotes (Koonin and Aravind, 2002; Sagan, 1967).

HtrA2/Omi is expressed as a pre-peptide with the following domains (Fig.5): a C-terminal mitochondrial targeting sequence, a putative transmembrane domain, a protease catalytic domain and a PDZ (Post synaptic density protein PSD95, Drosophila disc large tumour suppressor DIgA and Zonula occludens-1 protein zo-1) protein interaction domain.

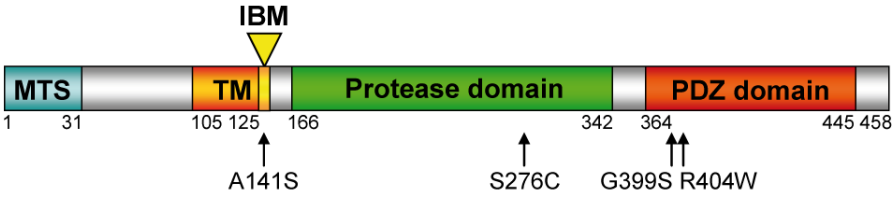

Figure 5: Schematic overview of the domain structure of HtrA2/Omi. Arrows indicate the PD-associated mutations described by Strauss, Bogaerts and colleagues and the mutation identified in the mnd2 mice. MTS: Mitochondrial Targeting Sequence; TM: TransMembrane domain; IBM: Inhibitor of apoptosis proteins Binding Motif.

The amino acids Tyr147, Phe149 and Phe256 constitute a trimerization motif responsible for the trimeric three-dimensional structure of the protein, necessary for its activity (Li et al., 2002).

The activity of the protease domain appeared to be modulated by the PDZ domain (Li et al., 2002; Wilken et al., 2004). The transmembrane domain is cleaved off during the proteolytic maturation process, revealing a highly conserved inhibitor of apoptosis proteins (IAPs) binding motif (IBM) in the mature HtrA2/Omi (Li et al., 2002).

Apoptotic stimuli that involve mitochondria (such as increased Ca^{2+}, ROS or decreased mitochondrial membrane potential) lead to the release of HtrA2/Omi from the intermembrane space to the cytosol. Once in the cytoplasm, HtrA2/Omi is known to cleave some anti-apoptotic proteins, including the IAPs, promoting apoptosis in both a caspase-dependent and -independent way (Kroemer et al., 2007).

However, recent evidence shed light also on the potential protective effects of HtrA2/Omi. It has been reported that the interaction of HtrA2/Omi with the mitochondrial Mpv17-like protein protects the mitochondria against cellular stress, reducing ROS levels and stabilizing the mitochondrial membrane potential (Krick et al., 2008). On the other way round, loss of HtrA2/Omi causes accumulation of misfolded proteins in the mitochondria, defective respiration, increased ROS an eventually neuronal cell death (Moisoi et al., 2009). The role of HtrA2/Omi in the protein quality control within mitochondria is also supported by a further study showing that HtrA2/Omi plays a role in the clearance of accumulating misfolded proteins upon inhibition of the proteasome (Radke et al., 2008).

A first link between HtrA2/Omi and neurodegeneration has been established by the identification of Omi/HtrA2 as a presenilin-1-interacting protein in yeast two-hybrid assays (Gupta et al., 2004). Mutations in presenilin-1 are responsible for inherited forms of early-onset Alzheimer's disease. Furthermore, HtrA2/Omi was shown to interact with the AD-associated amyloid precursor protein (Park et al., 2006; Huttunen et al., 2007). Recent evidence suggested also a link of HtrA2/Omi with Huntington's disease (Inagaki et al., 2008).

The characterization of the mnd2 mouse model of motor neuron disease led to the identification of a loss-of-function mutation (S276C) of HtrA2/Omi. Interestingly, the mutant mice displayed a clear, early-onset neurodegeneration, muscle wasting and death by 40 days of age (Jones et al., 2003). Recently, a neurodegenerative phenotype with parkinsonian features has been defined also in Omi/HtrA2 knockout mice (Martins et al., 2004). On the other hand, the neuron-specific overexpression of HtrA2/Omi in mice did not induce increased cell death (Liu et al., 2007). Taken together, the pathological phenotype resulting from loss of function of HtrA2/Omi and the lack of toxic effects of overexpressed HtrA2/Omi in mice, highlight the physiological relevance of HtrA2/Omi in mitochondrial homeostasis, rather than its pro-apoptotic function, in neurons.

Two missense mutation of HtrA2/Omi affecting its enzymatic activity were identified in a cohort of sporadic German PD patients (Strauss et al., 2005). An additional missense mutation was described in a Belgian population of sporadic PD patients (Bogaerts et al., 2008). These results, however, were not confirmed by two other studies (Ross et al., 2008; Simon-Sanchez and Singleton, 2008), which found

the same mutations also in healthy controls, raising a debate about the role of genetic mutations of HtrA2/Omi in PD.

1.6 Scope of the thesis

Here, we aimed at enhancing our understanding of the mechanisms of protein aggregation and mitochondrial dysfunctions and its potential interplay contributing to the pathogenesis of PD. In addition, we wanted to elucidate the possible pathogenetic role of two proteins whose involvement in PD is not yet well defined: synphilin-1 and HtrA2/Omi.

In particular, we used HEK293 cells overexpressing wild type or R621C mutant synphilin-1 to study the dynamics of protein aggregation and to evaluate if autophagy activation may influence cell viability by modulating synphilin-1 aggregation. We investigated also the effects synphilin-1 overexpression and aggregation on mitochondrial function.

Moreover, we studied the consequence of loss of HtrA2/Omi protein on mitochondrial function, morphology and homeostasis in fibroblasts from knockout mice, as well as in HeLa cells and in *Drosophila melanogaster* cells.

1.7 References of chapter 1

Andersen JK (2004) Oxidative stress in neurodegeneration: cause or consequence? Nat Med 10 Suppl:S18-25.

Auluck PK, Chan HY, Trojanowski JQ, Lee VM, Bonini NM (2002) Chaperone suppression of alpha-synuclein toxicity in a Drosophila model for Parkinson's disease. Science 295:865-868.

Beal MF (1998) Excitotoxicity and nitric oxide in Parkinson's disease pathogenesis. Ann Neurol 44:S110-114.

Bergman H, Wichmann T, DeLong MR (1990) Reversal of experimental parkinsonism by lesions of the subthalamic nucleus. Science 249:1436-1438.

Betarbet R, Sherer TB, MacKenzie G, Garcia-Osuna M, Panov AV, Greenamyre JT (2000) Chronic systemic pesticide exposure reproduces features of Parkinson's disease. Nat Neurosci 3:1301-1306.

Bogaerts V, Nuytemans K, Reumers J, Pals P, Engelborghs S, Pickut B, Corsmit E, Peeters K, Schymkowitz J, De Deyn PP, Cras P, Rousseau F, Theuns J, Van Broeckhoven C (2008) Genetic variability in the mitochondrial serine protease HTRA2 contributes to risk for Parkinson disease. Hum Mutat 29:832-840.

Bonifati V (2007) Genetics of parkinsonism. Parkinsonism Relat Disord 13 Suppl 3:S233-241.

Bonifati V, Oostra BA, Heutink P (2004) Linking DJ-1 to neurodegeneration offers novel insights for understanding the pathogenesis of Parkinson's disease. J Mol Med 82:163-174.

Braak H, Rub U, Gai WP, Del Tredici K (2003) Idiopathic Parkinson's disease: possible routes by which vulnerable neuronal types may be subject to neuroinvasion by an unknown pathogen. J Neural Transm 110:517-536.

Burn DJ, Jaros E (2001) Multiple system atrophy: cellular and molecular pathology. Mol Pathol 54:419-426.

Chan DC (2006) Mitochondria: dynamic organelles in disease, aging, and development. Cell 125:1241-1252.

Chung KK, Zhang Y, Lim KL, Tanaka Y, Huang H, Gao J, Ross CA, Dawson VL, Dawson TM (2001) Parkin ubiquitinates the alpha-synuclein-interacting protein, synphilin-1: implications for Lewy-body formation in Parkinson disease. Nat Med 7:1144-1150.

Cicchetti F, Drouin-Ouellet J, Gross RE (2009) Environmental toxins and Parkinson's disease: what have we learned from pesticide-induced animal models? Trends Pharmacol Sci 30:475-483.

Cook C, Petrucelli L (2009) A critical evaluation of the ubiquitin-proteasome system in Parkinson's disease. Biochim Biophys Acta 1792:664-675.

Delettre C, Lenaers G, Griffoin JM, Gigarel N, Lorenzo C, Belenguer P, Pelloquin L, Grosgeorge J, Turc-Carel C, Perret E, Astarie-Dequeker C, Lasquellec L, Arnaud B, Ducommun B, Kaplan J, Hamel CP (2000) Nuclear gene OPA1, encoding a

mitochondrial dynamin-related protein, is mutated in dominant optic atrophy. Nat Genet 26:207-210.

Doss-Pepe EW, Stenroos ES, Johnson WG, Madura K (2003) Ataxin-3 interactions with rad23 and valosin-containing protein and its associations with ubiquitin chains and the proteasome are consistent with a role in ubiquitin-mediated proteolysis. Mol Cell Biol 23:6469-6483.

Engelender S, Wanner T, Kleiderlein JJ, Wakabayashi K, Tsuji S, Takahashi H, Ashworth R, Margolis RL, Ross CA (2000) Organization of the human synphilin-1 gene, a candidate for Parkinson's disease. Mamm Genome 11:763-766.

Engelender S, Kaminsky Z, Guo X, Sharp AH, Amaravi RK, Kleiderlein JJ, Margolis RL, Troncoso JC, Lanahan AA, Worley PF, Dawson VL, Dawson TM, Ross CA (1999) Synphilin-1 associates with alpha-synuclein and promotes the formation of cytosolic inclusions. Nat Genet 22:110-114.

Faccio L, Fusco C, Chen A, Martinotti S, Bonventre JV, Zervos AS (2000) Characterization of a novel human serine protease that has extensive homology to bacterial heat shock endoprotease HtrA and is regulated by kidney ischemia. J Biol Chem 275:2581-2588.

Fornai F, Schluter OM, Lenzi P, Gesi M, Ruffoli R, Ferrucci M, Lazzeri G, Busceti CL, Pontarelli F, Battaglia G, Pellegrini A, Nicoletti F, Ruggieri S, Paparelli A, Sudhof TC (2005) Parkinson-like syndrome induced by continuous MPTP infusion: convergent roles of the ubiquitin-proteasome system

and alpha-synuclein. Proc Natl Acad Sci U S A 102:3413-3418.

Forno LS (1996) Neuropathology of Parkinson's disease. J Neuropathol Exp Neurol 55:259-272.

Furukawa Y, Vigouroux S, Wong H, Guttman M, Rajput AH, Ang L, Briand M, Kish SJ, Briand Y (2002) Brain proteasomal function in sporadic Parkinson's disease and related disorders. Ann Neurol 51:779-782.

Gerlach M, Double K, Riederer P, Hirsch E, Jellinger K, Jenner P, Trautwein A, Youdim MB (1997) Iron in the Parkinsonian substantia nigra. Mov Disord 12:258-260.

Giasson BI, Duda JE, Murray IV, Chen Q, Souza JM, Hurtig HI, Ischiropoulos H, Trojanowski JQ, Lee VM (2000) Oxidative damage linked to neurodegeneration by selective alpha-synuclein nitration in synucleinopathy lesions. Science 290:985-989.

Gibb WR, Lees AJ (1988) The relevance of the Lewy body to the pathogenesis of idiopathic Parkinson's disease. J Neurol Neurosurg Psychiatry 51:745-752.

Graham DG (1978) Oxidative pathways for catecholamines in the genesis of neuromelanin and cytotoxic quinones. Mol Pharmacol 14:633-643.

Gray CW, Ward RV, Karran E, Turconi S, Rowles A, Viglienghi D, Southan C, Barton A, Fantom KG, West A, Savopoulos J, Hassan NJ, Clinkenbeard H, Hanning C, Amegadzie B, Davis JB, Dingwall C, Livi GP, Creasy CL (2000) Characterization of human HtrA2, a novel serine protease involved in the

mammalian cellular stress response. Eur J Biochem 267:5699-5710.

Greene JG, Greenamyre JT (1996) Bioenergetics and glutamate excitotoxicity. Prog Neurobiol 48:613-634.

Griparic L, van der Wel NN, Orozco IJ, Peters PJ, van der Bliek AM (2004) Loss of the intermembrane space protein Mgm1/OPA1 induces swelling and localized constrictions along the lengths of mitochondria. J Biol Chem 279:18792-18798.

Grune T, Jung T, Merker K, Davies KJ (2004) Decreased proteolysis caused by protein aggregates, inclusion bodies, plaques, lipofuscin, ceroid, and 'aggresomes' during oxidative stress, aging, and disease. Int J Biochem Cell Biol 36:2519-2530.

Gupta S, Singh R, Datta P, Zhang Z, Orr C, Lu Z, Dubois G, Zervos AS, Meisler MH, Srinivasula SM, Fernandes-Alnemri T, Alnemri ES (2004) The C-terminal tail of presenilin regulates Omi/HtrA2 protease activity. J Biol Chem 279:45844-45854.

Hara T, Nakamura K, Matsui M, Yamamoto A, Nakahara Y, Suzuki-Migishima R, Yokoyama M, Mishima K, Saito I, Okano H, Mizushima N (2006) Suppression of basal autophagy in neural cells causes neurodegenerative disease in mice. Nature 441:885-889.

Hardy J, Lewis P, Revesz T, Lees A, Paisan-Ruiz C (2009) The genetics of Parkinson's syndromes: a critical review. Curr Opin Genet Dev 19:254-265.

Hazan J, Fonknechten N, Mavel D, Paternotte C, Samson D, Artiguenave F, Davoine CS, Cruaud C, Durr A, Wincker P, Brottier P, Cattolico L, Barbe V, Burgunder JM, Prud'homme

JF, Brice A, Fontaine B, Heilig B, Weissenbach J (1999) Spastin, a new AAA protein, is altered in the most frequent form of autosomal dominant spastic paraplegia. Nat Genet 23:296-303.

Hill WD, Arai M, Cohen JA, Trojanowski JQ (1993) Neurofilament mRNA is reduced in Parkinson's disease substantia nigra pars compacta neurons. J Comp Neurol 329:328-336.

Huttunen HJ, Guenette SY, Peach C, Greco C, Xia W, Kim DY, Barren C, Tanzi RE, Kovacs DM (2007) HtrA2 regulates beta-amyloid precursor protein (APP) metabolism through endoplasmic reticulum-associated degradation. J Biol Chem 282:28285-28295.

Ii K, Ito H, Tanaka K, Hirano A (1997) Immunocytochemical co-localization of the proteasome in ubiquitinated structures in neurodegenerative diseases and the elderly. J Neuropathol Exp Neurol 56:125-131.

Inagaki R, Tagawa K, Qi ML, Enokido Y, Ito H, Tamura T, Shimizu S, Oyanagi K, Arai N, Kanazawa I, Wanker EE, Okazawa H (2008) Omi / HtrA2 is relevant to the selective vulnerability of striatal neurons in Huntington's disease. Eur J Neurosci 28:30-40.

Ito T, Niwa J, Hishikawa N, Ishigaki S, Doyu M, Sobue G (2003) Dorfin localizes to Lewy bodies and ubiquitylates synphilin-1. J Biol Chem 278:29106-29114.

Jankovic J (2008) Parkinson's disease: clinical features and diagnosis. J Neurol Neurosurg Psychiatry 79:368-376.

Jones JM, Datta P, Srinivasula SM, Ji W, Gupta S, Zhang Z, Davies E, Hajnoczky G, Saunders TL, Van Keuren ML, Fernandes-Alnemri T, Meisler MH, Alnemri ES (2003) Loss of Omi mitochondrial protease activity causes the neuromuscular disorder of mnd2 mutant mice. Nature 425:721-727.

Jung T, Catalgol B, Grune T (2009) The proteasomal system. Mol Aspects Med 30:191-296.

Kingsbury AE, Daniel SE, Sangha H, Eisen S, Lees AJ, Foster OJ (2004) Alteration in alpha-synuclein mRNA expression in Parkinson's disease. Mov Disord 19:162-170.

Kitada T, Asakawa S, Hattori N, Matsumine H, Yamamura Y, Minoshima S, Yokochi M, Mizuno Y, Shimizu N (1998) Mutations in the parkin gene cause autosomal recessive juvenile parkinsonism. Nature 392:605-608.

Koonin EV, Aravind L (2002) Origin and evolution of eukaryotic apoptosis: the bacterial connection. Cell Death Differ 9:394-404.

Krick S, Shi S, Ju W, Faul C, Tsai SY, Mundel P, Bottinger EP (2008) Mpv17l protects against mitochondrial oxidative stress and apoptosis by activation of Omi/HtrA2 protease. Proc Natl Acad Sci U S A 105:14106-14111.

Kroemer G, Galluzzi L, Brenner C (2007) Mitochondrial membrane permeabilization in cell death. Physiol Rev 87:99-163.

Kruger R (2004) The role of synphilin-1 in synaptic function and protein degradation. Cell Tissue Res 318:195-199.

Kuninaka S, Iida SI, Hara T, Nomura M, Naoe H, Morisaki T, Nitta M, Arima Y, Mimori T, Yonehara S, Saya H (2007) Serine

protease Omi/HtrA2 targets WARTS kinase to control cell proliferation. Oncogene 26:2395-2406.

Langston JW, Ballard P, Tetrud JW, Irwin I (1983) Chronic Parkinsonism in humans due to a product of meperidine-analog synthesis. Science 219:979-980.

Lee G, Junn E, Tanaka M, Kim YM, Mouradian MM (2002a) Synphilin-1 degradation by the ubiquitin-proteasome pathway and effects on cell survival. J Neurochem 83:346-352.

Lee HJ, Shin SY, Choi C, Lee YH, Lee SJ (2002b) Formation and removal of alpha-synuclein aggregates in cells exposed to mitochondrial inhibitors. J Biol Chem 277:5411-5417.

Lennox G, Lowe J, Morrell K, Landon M, Mayer RJ (1989) Anti-ubiquitin immunocytochemistry is more sensitive than conventional techniques in the detection of diffuse Lewy body disease. J Neurol Neurosurg Psychiatry 52:67-71.

Leroy E, Boyer R, Auburger G, Leube B, Ulm G, Mezey E, Harta G, Brownstein MJ, Jonnalagada S, Chernova T, Dehejia A, Lavedan C, Gasser T, Steinbach PJ, Wilkinson KD, Polymeropoulos MH (1998) The ubiquitin pathway in Parkinson's disease. Nature 395:451-452.

Lesage S, Brice A (2009) Parkinson's disease: from monogenic forms to genetic susceptibility factors. Hum Mol Genet 18:R48-59.

Li W, Srinivasula SM, Chai J, Li P, Wu JW, Zhang Z, Alnemri ES, Shi Y (2002) Structural insights into the pro-apoptotic function of mitochondrial serine protease HtrA2/Omi. Nat Struct Biol 9:436-441.

Liani E, Eyal A, Avraham E, Shemer R, Szargel R, Berg D, Bornemann A, Riess O, Ross CA, Rott R, Engelender S (2004) Ubiquitylation of synphilin-1 and alpha-synuclein by SIAH and its presence in cellular inclusions and Lewy bodies imply a role in Parkinson's disease. Proc Natl Acad Sci U S A 101:5500-5505.

Liu MJ, Liu ML, Shen YF, Kim JM, Lee BH, Lee YS, Hong ST (2007) Transgenic mice with neuron-specific overexpression of HtrA2/Omi suggest a neuroprotective role for HtrA2/Omi. Biochem Biophys Res Commun 362:295-300.

Lowe J, McDermott H, Landon M, Mayer RJ, Wilkinson KD (1990) Ubiquitin carboxyl-terminal hydrolase (PGP 9.5) is selectively present in ubiquitinated inclusion bodies characteristic of human neurodegenerative diseases. J Pathol 161:153-160.

Martinez-Vicente M, Cuervo AM (2007) Autophagy and neurodegeneration: when the cleaning crew goes on strike. Lancet Neurol 6:352-361.

Martins LM, Iaccarino I, Tenev T, Gschmeissner S, Totty NF, Lemoine NR, Savopoulos J, Gray CW, Creasy CL, Dingwall C, Downward J (2002) The serine protease Omi/HtrA2 regulates apoptosis by binding XIAP through a reaper-like motif. J Biol Chem 277:439-444.

Martins LM, Morrison A, Klupsch K, Fedele V, Moisoi N, Teismann P, Abuin A, Grau E, Geppert M, Livi GP, Creasy CL, Martin A, Hargreaves I, Heales SJ, Okada H, Brandner S, Schulz JB, Mak T, Downward J (2004) Neuroprotective role of the

Reaper-related serine protease HtrA2/Omi revealed by targeted deletion in mice. Mol Cell Biol 24:9848-9862.

Marx FP, Soehn AS, Berg D, Melle C, Schiesling C, Lang M, Kautzmann S, Strauss KM, Franck T, Engelender S, Pahnke J, Dawson S, von Eggeling F, Schulz JB, Riess O, Kruger R (2007) The proteasomal subunit S6 ATPase is a novel synphilin-1 interacting protein--implications for Parkinson's disease. FASEB J 21:1759-1767.

Marx FP, Holzmann C, Strauss KM, Li L, Eberhardt O, Gerhardt E, Cookson MR, Hernandez D, Farrer MJ, Kachergus J, Engelender S, Ross CA, Berger K, Schols L, Schulz JB, Riess O, Kruger R (2003) Identification and functional characterization of a novel R621C mutation in the synphilin-1 gene in Parkinson's disease. Hum Mol Genet 12:1223-1231.

Matsumoto M, Yada M, Hatakeyama S, Ishimoto H, Tanimura T, Tsuji S, Kakizuka A, Kitagawa M, Nakayama KI (2004) Molecular clearance of ataxin-3 is regulated by a mammalian E4. EMBO J 23:659-669.

McNaught KS, Jenner P (2001) Proteasomal function is impaired in substantia nigra in Parkinson's disease. Neurosci Lett 297:191-194.

McNaught KS, Perl DP, Brownell AL, Olanow CW (2004) Systemic exposure to proteasome inhibitors causes a progressive model of Parkinson's disease. Ann Neurol 56:149-162.

McNaught KS, Shashidharan P, Perl DP, Jenner P, Olanow CW (2002a) Aggresome-related biogenesis of Lewy bodies. Eur J Neurosci 16:2136-2148.

McNaught KS, Belizaire R, Isacson O, Jenner P, Olanow CW (2003) Altered proteasomal function in sporadic Parkinson's disease. Exp Neurol 179:38-46.

McNaught KS, Mytilineou C, Jnobaptiste R, Yabut J, Shashidharan P, Jennert P, Olanow CW (2002b) Impairment of the ubiquitin-proteasome system causes dopaminergic cell death and inclusion body formation in ventral mesencephalic cultures. J Neurochem 81:301-306.

Misgeld T, Kerschensteiner M, Bareyre FM, Burgess RW, Lichtman JW (2007) Imaging axonal transport of mitochondria in vivo. Nat Methods 4:559-561.

Mizushima N, Levine B, Cuervo AM, Klionsky DJ (2008) Autophagy fights disease through cellular self-digestion. Nature 451:1069-1075.

Moisoi N, Klupsch K, Fedele V, East P, Sharma S, Renton A, Plun-Favreau H, Edwards RE, Teismann P, Esposti MD, Morrison AD, Wood NW, Downward J, Martins LM (2009) Mitochondrial dysfunction triggered by loss of HtrA2 results in the activation of a brain-specific transcriptional stress response. Cell Death Differ 16:449-464.

Murray IJ, Medford MA, Guan HP, Rueter SM, Trojanowski JQ, Lee VM (2003) Synphilin in normal human brains and in synucleinopathies: studies with new antibodies. Acta Neuropathol 105:177-184.

Myhre R, Klungland H, Farrer MJ, Aasly JO (2008) Genetic association study of synphilin-1 in idiopathic Parkinson's disease. BMC Med Genet 9:19.

Nagano Y, Yamashita H, Takahashi T, Kishida S, Nakamura T, Iseki E, Hattori N, Mizuno Y, Kikuchi A, Matsumoto M (2003) Siah-1 facilitates ubiquitination and degradation of synphilin-1. J Biol Chem 278:51504-51514.

Neystat M, Rzhetskaya M, Kholodilov N, Burke RE (2002) Analysis of synphilin-1 and synuclein interactions by yeast two-hybrid beta-galactosidase liquid assay. Neurosci Lett 325:119-123.

Nuber S, Franck T, Wolburg H, Schumann U, Casadei N, Fischer K, Calaminus C, Pichler BJ, Chanarat S, Teismann P, Schulz JB, Luft AR, Tomiuk J, Wilbertz J, Bornemann A, Kruger R, Riess O Transgenic overexpression of the alpha-synuclein interacting protein synphilin-1 leads to behavioral and neuropathological alterations in mice. Neurogenetics 11:107-120.

Nutt JG, Wooten GF (2005) Clinical practice. Diagnosis and initial management of Parkinson's disease. N Engl J Med 353:1021-1027.

O'Farrell C, Murphy DD, Petrucelli L, Singleton AB, Hussey J, Farrer M, Hardy J, Dickson DW, Cookson MR (2001) Transfected synphilin-1 forms cytoplasmic inclusions in HEK293 cells. Brain Res Mol Brain Res 97:94-102.

Okamoto K, Shaw JM (2005) Mitochondrial morphology and dynamics in yeast and multicellular eukaryotes. Annu Rev Genet 39:503-536.

Olanow CW, Perl DP, DeMartino GN, McNaught KS (2004) Lewy-body formation is an aggresome-related process: a hypothesis. Lancet Neurol 3:496-503.

Ono T, Isobe K, Nakada K, Hayashi JI (2001) Human cells are protected from mitochondrial dysfunction by complementation of DNA products in fused mitochondria. Nat Genet 28:272-275.

Park HJ, Kim SS, Seong YM, Kim KH, Goo HG, Yoon EJ, Min do S, Kang S, Rhim H (2006) Beta-amyloid precursor protein is a direct cleavage target of HtrA2 serine protease. Implications for the physiological function of HtrA2 in the mitochondria. J Biol Chem 281:34277-34287.

Parker WD, Jr., Boyson SJ, Parks JK (1989) Abnormalities of the electron transport chain in idiopathic Parkinson's disease. Ann Neurol 26:719-723.

Pollanen MS, Dickson DW, Bergeron C (1993) Pathology and biology of the Lewy body. J Neuropathol Exp Neurol 52:183-191.

Polymeropoulos MH, Lavedan C, Leroy E, Ide SE, Dehejia A, Dutra A, Pike B, Root H, Rubenstein J, Boyer R, Stenroos ES, Chandrasekharappa S, Athanassiadou A, Papapetropoulos T, Johnson WG, Lazzarini AM, Duvoisin RC, Di Iorio G, Golbe LI, Nussbaum RL (1997) Mutation in the alpha-synuclein gene identified in families with Parkinson's disease. Science 276:2045-2047.

Radke S, Chander H, Schafer P, Meiss G, Kruger R, Schulz JB, Germain D (2008) Mitochondrial protein quality control by the proteasome involves ubiquitination and the protease Omi. J Biol Chem 283:12681-12685.

Raghavan R, Khin-Nu C, Brown A, Irving D, Ince PG, Day K, Tyrer SP, Perry RH (1993) Detection of Lewy bodies in Trisomy 21 (Down's syndrome). Can J Neurol Sci 20:48-51.

Ramirez A, Heimbach A, Grundemann J, Stiller B, Hampshire D, Cid LP, Goebel I, Mubaidin AF, Wriekat AL, Roeper J, Al-Din A, Hillmer AM, Karsak M, Liss B, Woods CG, Behrens MI, Kubisch C (2006) Hereditary parkinsonism with dementia is caused by mutations in ATP13A2, encoding a lysosomal type 5 P-type ATPase. Nat Genet 38:1184-1191.

Recchia A, Debetto P, Negro A, Guidolin D, Skaper SD, Giusti P (2004) Alpha-synuclein and Parkinson's disease. FASEB J 18:617-626.

Ribeiro CS, Carneiro K, Ross CA, Menezes JR, Engelender S (2002) Synphilin-1 is developmentally localized to synaptic terminals, and its association with synaptic vesicles is modulated by alpha-synuclein. J Biol Chem 277:23927-23933.

Rideout HJ, Lang-Rollin I, Stefanis L (2004) Involvement of macroautophagy in the dissolution of neuronal inclusions. Int J Biochem Cell Biol 36:2551-2562.

Ross OA, Soto AI, Vilarino-Guell C, Heckman MG, Diehl NN, Hulihan MM, Aasly JO, Sando S, Gibson JM, Lynch T, Krygowska-Wajs A, Opala G, Barcikowska M, Czyzewski K, Uitti RJ, Wszolek ZK, Farrer MJ (2008) Genetic variation of Omi/HtrA2 and Parkinson's disease. Parkinsonism Relat Disord 14:539-543.

Sagan L (1967) On the origin of mitosing cells. J Theor Biol 14:255-274.

Schapira AH, Cooper JM, Dexter D, Clark JB, Jenner P, Marsden CD (1990) Mitochondrial complex I deficiency in Parkinson's disease. J Neurochem 54:823-827.

Schapira AH, Cleeter MW, Muddle JR, Workman JM, Cooper JM, King RH (2006) Proteasomal inhibition causes loss of nigral tyrosine hydroxylase neurons. Ann Neurol 60:253-255.

Schlossmacher MG, Frosch MP, Gai WP, Medina M, Sharma N, Forno L, Ochiishi T, Shimura H, Sharon R, Hattori N, Langston JW, Mizuno Y, Hyman BT, Selkoe DJ, Kosik KS (2002) Parkin localizes to the Lewy bodies of Parkinson disease and dementia with Lewy bodies. Am J Pathol 160:1655-1667.

Schmidt ML, Murray J, Lee VM, Hill WD, Wertkin A, Trojanowski JQ (1991) Epitope map of neurofilament protein domains in cortical and peripheral nervous system Lewy bodies. Am J Pathol 139:53-65.

Sian J, Dexter DT, Lees AJ, Daniel S, Agid Y, Javoy-Agid F, Jenner P, Marsden CD (1994) Alterations in glutathione levels in Parkinson's disease and other neurodegenerative disorders affecting basal ganglia. Ann Neurol 36:348-355.

Silver IA, Erecinska M (1998) Glucose-induced intracellular ion changes in sugar-sensitive hypothalamic neurons. J Neurophysiol 79:1733-1745.

Simon-Sanchez J, Singleton AB (2008) Sequencing analysis of OMI/HTRA2 shows previously reported pathogenic mutations in neurologically normal controls. Hum Mol Genet 17:1988-1993.

Sofic E, Paulus W, Jellinger K, Riederer P, Youdim MB (1991) Selective increase of iron in substantia nigra zona compacta of parkinsonian brains. J Neurochem 56:978-982.

Spillantini MG, Crowther RA, Jakes R, Hasegawa M, Goedert M (1998) alpha-Synuclein in filamentous inclusions of Lewy bodies from Parkinson's disease and dementia with lewy bodies. Proc Natl Acad Sci U S A 95:6469-6473.

Spillantini MG, Schmidt ML, Lee VM, Trojanowski JQ, Jakes R, Goedert M (1997) Alpha-synuclein in Lewy bodies. Nature 388:839-840.

Strauss KM, Martins LM, Plun-Favreau H, Marx FP, Kautzmann S, Berg D, Gasser T, Wszolek Z, Muller T, Bornemann A, Wolburg H, Downward J, Riess O, Schulz JB, Kruger R (2005) Loss of function mutations in the gene encoding Omi/HtrA2 in Parkinson's disease. Hum Mol Genet 14:2099-2111.

Tanaka M, Kim YM, Lee G, Junn E, Iwatsubo T, Mouradian MM (2004) Aggresomes formed by alpha-synuclein and synphilin-1 are cytoprotective. J Biol Chem 279:4625-4631.

Thiruchelvam M, McCormack A, Richfield EK, Baggs RB, Tank AW, Di Monte DA, Cory-Slechta DA (2003) Age-related irreversible progressive nigrostriatal dopaminergic neurotoxicity in the paraquat and maneb model of the Parkinson's disease phenotype. Eur J Neurosci 18:589-600.

Todde V, Veenhuis M, van der Klei IJ (2009) Autophagy: principles and significance in health and disease. Biochim Biophys Acta 1792:3-13.

Tofaris GK, Razzaq A, Ghetti B, Lilley KS, Spillantini MG (2003) Ubiquitination of alpha-synuclein in Lewy bodies is a pathological event not associated with impairment of proteasome function. J Biol Chem 278:44405-44411.

Tompkins MM, Hill WD (1997) Contribution of somal Lewy bodies to neuronal death. Brain Res 775:24-29.

Valente EM et al. (2004) Hereditary early-onset Parkinson's disease caused by mutations in PINK1. Science 304:1158-1160.

Verhoeven K et al. (2006) MFN2 mutation distribution and genotype/phenotype correlation in Charcot-Marie-Tooth type 2. Brain 129:2093-2102.

Verstreken P, Ly CV, Venken KJ, Koh TW, Zhou Y, Bellen HJ (2005) Synaptic mitochondria are critical for mobilization of reserve pool vesicles at Drosophila neuromuscular junctions. Neuron 47:365-378.

Wakabayashi K, Engelender S, Yoshimoto M, Tsuji S, Ross CA, Takahashi H (2000) Synphilin-1 is present in Lewy bodies in Parkinson's disease. Ann Neurol 47:521-523.

Waterham HR, Koster J, van Roermund CW, Mooyer PA, Wanders RJ, Leonard JV (2007) A lethal defect of mitochondrial and peroxisomal fission. N Engl J Med 356:1736-1741.

Weintraub D, Comella CL, Horn S (2008) Parkinson's disease--Part 1: Pathophysiology, symptoms, burden, diagnosis, and assessment. Am J Manag Care 14:S40-48.

Wilken C, Kitzing K, Kurzbauer R, Ehrmann M, Clausen T (2004) Crystal structure of the DegS stress sensor: How a PDZ

domain recognizes misfolded protein and activates a protease. Cell 117:483-494.

Wood SJ, Wypych J, Steavenson S, Louis JC, Citron M, Biere AL (1999) alpha-synuclein fibrillogenesis is nucleation-dependent. Implications for the pathogenesis of Parkinson's disease. J Biol Chem 274:19509-19512.

Yang Y, Lu B (2009) Mitochondrial morphogenesis, distribution, and Parkinson disease: insights from PINK1. J Neuropathol Exp Neurol 68:953-963.

Youle RJ, Karbowski M (2005) Mitochondrial fission in apoptosis. Nat Rev Mol Cell Biol 6:657-663.

Zaarur N, Meriin AB, Gabai VL, Sherman MY (2008) Triggering aggresome formation. Dissecting aggresome-targeting and aggregation signals in synphilin 1. J Biol Chem 283:27575-27584.

Zeng BY, Bukhatwa S, Hikima A, Rose S, Jenner P (2006) Reproducible nigral cell loss after systemic proteasomal inhibitor administration to rats. Ann Neurol 60:248-252.

Chapter 2

Chapter 2

Aggregate dynamics and mitochondrial function in synphilin-1 overexpressing cells

Authors:

Dalila Ciceri (1, 2), Guido K. Krebiehl (1), Nicole Kieper (1), Lena F. Burbulla (1, 4), Ellen Gerhardt (5), Jörg B. Schulz (5), Carlo Ferrarese (2, 3) and Rejko Krüger (1)

1: Centre of Neurology, Hertie Institute for Clinical Brain Research and German Research Centre for Neurodegenerative Disorders, University of Tübingen, Tübingen, Germany 2: Department of Neuroscience and Biomedical Technologies, University of Milano-Bicocca, Monza, Italy; 3: Department of Neurology, San Gerardo Hospital, Monza, Italy; 4: Graduate School of Cellular & Molecular Neuroscience, University of Tübingen, Tübingen, Germany; 5: DFG Research Centre for Molecular Physiology of Brain and Centre for Neurological Medicine, University of Göttingen, Göttingen, Germany.

Neuroscience

Submitted, March, 2010

Corresponding author:

Prof. Dr. Rejko Krueger, MD

Laboratory of Functional Neurogenomics,

Center of Neurology, Hertie-Institute for Clinical Brain Research and German Research Center for Neurodegenerative Diseases, University of Tübingen

Hoppe-Seyler-Str. 3

72076 Tuebingen, Germany

phone: +49-7071-2982141

fax: +49-7071-295260

e-mail: rejko.krueger@uni-tuebingen.de

Abbreviations used in the text:

PD: Parkinson's Disease; WT: wild type; LB: Lewy Bodies; ROS: Reactive Oxygen Species; MMP: Mitochondrial Membrane Potential; EGFP: Enhanced Green Fluorescent Protein; LC3: microtubule-associated protein 1 light chain 3; PCR: Polymerase Chain Reaction; PI3K: phosphatidilinhositol-3-phosphate kinase; UPS: Ubiquitin-Proteasome System; TMRE: TetraMethylRhodamineEthylester; FACS: Fluorescence-Activated Cell Sorting; GAP-DH: GlycerAldehyde-3-Phosphate DeHydrogenase, mTOR: mammalian Target Of Rapamycin Ac-DEVD-AMC: Acetyl-Asp-Glu-Val-Asp-Chloromethylcoumarin.

Abstract:

Intracytoplasmic protein aggregates called Lewy Bodies (LB) characterize the neurodegeneration in Parkinson's Disease (PD). However, whether aggregates are linked to cell death or they represent a protective mechanism is debated. Recent studies suggest that autophagy participates in the degradation of cytoplasmic protein inclusions.

Synphilin-1 is a protein that is present in LB and that interacts with key elements of PD pathogenesis, such as α-synuclein. Our group described a point mutation in synphilin-1 in two German PD patients. Overexpression of synphilin-1 in various cellular models leads to cytoplasmatic inclusions that fulfil the criteria of aggresomes, dynamic structures formed under proteolytic stress conditions.

We used HEK293 cells overexpressing wild type (WT) or R621C mutant synphilin-1 to evaluate if autophagy activation may influence cell viability by modulating synphilin-1 inclusions. Moreover, we studied also the effects synphilin-1-overexpression and aggregation on mitochondria.

We observed co-localization of synphilin-1 inclusions with autophagic structures under basal conditions. Moreover, the activation of autophagy by rapamycin and trehalose reduced the percentage of cells bearing WT and R621C synphilin-1 inclusions. However, this treatment couldn't protect the cells from apoptosis induced by MG132-mediated proteasome inhibition.

Synphilin-1-overexpressing cells revealed higher levels of mitochondrial reactive oxygen species and reduced mitochondrial

membrane potential compared to empty vector controls. Rapamycin treatments were not able to compensate for these impairments.

To conclude, we demonstrated that synphilin-1 aggresomes are a target of lysosomal degradation and that their clearance can be modulated by autophagic pathways. However, the activation of autophagy couldn't rescue synphilin-1-overexpressing cells from MG132-induced apoptosis or from mitochondrial dysfunction related to synphilin-1-overexpression. Thus, our findings support the view that aggresomes are actively built to remove excesses of noxious proteins; however, the enhancement of their clearance via autophagy is not sufficient to protect against proteasome inhibition and mitochondrial impairments in the presence of high levels of aggregate-prone proteins.

Key words: Aggregation, clearance, autophagy, apoptosis, mitochondria.

Introduction:

Parkinson's disease (PD) is a neurodegenerative disorder characterized by severe motor impairments. Clinical symptoms appear upon loss of the majority of dopaminergic neurons in the substantia nigra pars compacta and neurodegeneration is pathoanatomically characterized by neuronal cytoplasmatic inclusions called Lewy Bodies (LB). Mutations identified by genetic studies in rare inherited forms of PD suggested that protein aggregation and dysfunction of protein degradation machinery, together with mitochondrial impairments, could be important features of the pathogenesis of PD (Betarbet et al., 2002). In particular, mutations in the gene encoding alpha-synuclein shed light on this cytoplasmic protein, which has a tendency to aggregate also in its physiological form and represents the major component of the LB in brains of mutation carriers and sporadic PD patients (Polymeropoulos et al., 1997; Singleton et al., 2003).

Synphilin-1 is a presynaptic protein predominantly expressed in neurons whose function is still unknown. It has been first described as an alpha-synuclein-interacting protein (Engelender et al., 1999) and a report suggested that it is related to the synaptic functions of alpha-synuclein and involved in controlling the trafficking of synaptic vesicles (Ribeiro et al., 2002). First evidence for a relation to PD pathogenesis came from studies showing that synphilin-1 is a substrate of the PD-associated ubiquitin E3 ligase Parkin (Chung et al., 2001), and that ubiquitination of synphilin-1 leads to its degradation by the proteasome (Chung et al., 2001; Lee et al., 2002). More evidence for an involvement of synphilin-1 in proteasomal

degradation comes from its interaction with the ubiquitin E3 ligase SIAH-1 and the proteasomal subunit S6 ATPase (Liani et al., 2004; Marx et al., 2007). An amino acid substitution R621C of synphilin-1 that was first identified in two German PD patients was related to an increased susceptibility to cellular stress in vitro (Marx et al., 2003). However, subsequent genetic studies observed the same rare variant also in non-affected controls, allowing no firm conclusion on the pathogenic relevance of the mutation. Recent in vivo studies revealed that mice overexpressing synphilin-1 display significant motor impairments and neuronal degeneration with mitochondrial alterations, more pronounced in mice overexpressing the R621C variant (Nuber et al., 2010).

Synphilin-1 is present in of the majority of LB in brains of PD patients (Wakabayashi et al., 2000) and it was reported that it can spontaneously form LB-like inclusions when it is overexpressed *in vitro* (O'Farrell et al., 2001) and *in vivo* (Nuber et al., 2010). Interestingly, previous publications showed that the aggregates formed by synphilin-1 display the key features of the so called “aggresomes” due to their perinuclear localization and their positive staining for typical markers (Tanaka et al., 2004; Marx et al., 2007).

Aggresomes have been characterized as inclusions bodies that form at the centrosome in response to proteolytic stress (Johnston et al., 1998). They probably represent an active attempt to enhance the degradation of aggregated proteins involved in several neurodegenerative disorders (PD, multiple system atrophy and polyglutamine-repeat disorders such as Huntington's Disease; reviewed in Schulz and Dichgans, 1999); in fact, they are enriched of

chaperones and components of UPS (Garcia-Mata et al., 1999; Junn et al., 2002). Supporting the protective role of aggresomes, it was reported that there is a close correlation between aggresome formation and cell survival (Taylor et al., 2003; Muchowski et al., 2002).

It was further demonstrated that aggresomes trigger autophagy-related mechanisms to promote the clearance of the aggregated material in basal conditions (Wong et al., 2008; Fortun et al., 2003) and upon proteasomal dysfunctions (Lim et al., 2006; Rideout et al., 2004). In particular macroautophagy (also called autophagy) is thought to be responsible for the degradation of aggregates and organelles, including mitochondria. It involves the formation of double membrane vesicles called autophagosomes, which fuse with lysosomes to form autophagolysosomes, where the content is degraded (Martinez-Vicente and Cuervo, 2007).

There is evidence that LB may represent the in vivo correlate of aggresomes observed in cell culture models. In fact, LB contain typical markers of aggresomes (McNaught et al., 2002). Moreover, it was observed LB-bearing neurons appear generally healthier that the ones without aggregates in the substantia nigra of PD patients (Tompkins and Hill, 1997). It was suggested also that LB could represent aggresomes that failed to be properly handled or removed (Olanow et al., 2004). Thus, the dynamics of protein aggregation and the possible mechanisms responsible for the correct processing and eventually degradation of the aggresomes is of major interest to understand molecular mechanisms of neurodegeneration in PD.

In our study we used HEK cells stably overexpressing synphilin-1 as a cellular model to evaluate the possible role of autophagy in the

degradation of aggresomes and the effects of the pharmacological modulation of autophagic pathways on cell viability.

Dysfunctions of mitochondria represent a typical feature of PD; for example, a significant reduction of the activity of the complex I of the mitochondrial respiratory chain has been observed in PD patients (Schapira et al., 1990; Parker et al., 1989). In addition, mutations in genes encoding either mitochondrial proteins or proteins involved in mitochondrial function (such as Parkin, PTEN-induced kinase-1, DJ-1 and Omi/HtrA2) were identified in PD (Kitada et al., 1998; Valente et al., 2004; Bonifati et al., 2004; Strauss et al., 2005). Since also the first transgenic models of synphilin-1 overexpression in mice showed mitochondrial dysfunction and protein aggregation (Nuber et al., 2010), we included analyses on the status of the mitochondria in our synphilin-1-overexpressing cells and we evaluated whether the manipulation of synphilin-1 aggregation may influence mitochondrial homeostasis.

Experimental procedures:

Cellular model and chemicals:

The cloning process of human synphilin-1 (GenBank accession number NP_005451) into the pEGFP-N1 expression vector (Clontech Laboratories, CA, USA) has been described previously (O'Farrell et al., 2001). Mutagenesis to introduce the R621C amino acid change was performed using a transformer site directed mutagenesis kit (Clontech Laboratories, CA, USA) and then the plasmids were sequenced to verify their identity. FLAG-tagged expression constructs of wild-type (WT) and R621C synphilin-1 were generated by PCR using primers introducing a 5' FLAG tag. The constructs were cloned into the pcDNA3.1 vector (Invitrogen, CA, USA) between XhoI and HindIII sites.

To generate stable polyclonal cellular lines overexpressing WT and R621C mutant synphilin-1-EGFP fusion protein and WT and R621C mutant FLAG-tagged synphilin-1, HEK293 cells were transfected with 2μg of the corresponding construct using FuGENE (Roche, Germany) according to the manufacturer's instructions. In addition, the empty vectors were transfected in HEK293 cells in order to generate control cell lines. Transfected cells were selected adding 0,7mg/ml G418 (Clontech Laboratories, CA, USA) to the culture medium.

FLAG- and EGFP-tagged synphilin-1 overexpressing HEK cells were cultured in Dulbecco's Modified Eagle's Medium (DMEM) supplemented with 10% foetal bovine serum (FBS), 1% penicillin and

streptomycin (Invitrogen, CA, USA) and 0,7mg/ml G418. Cells were grown at 37° C in a humidified atmosphere containing 5% CO_2.
Concerning the chemicals that were used in this study, rapamycin was purchased from Calbiochem (CA, USA), while trehalose dihydrate, MG132 and wortmannin were from Sigma (MO, USA).

Western Blotting:

Western blot experiments were performed as previously described (Marx et al., 2003). Briefly, cells were washed with cold PBS, harvested by centrifugation and then resuspended in lysis buffer (1% Triton X-100 in PBS and Complete protease inhibitor, Roche, Germany). After incubation for 30 min on ice, the lysates were centrifuged at 13000 rpm for 30 min at 4° C to remove insoluble matters. Total protein concentration was measured by using Bio-Rad protein assay kit (Bio-Rad, Germany). Equal amounts of protein (30μg per lane) were loaded on SDS–PAGE gels and subjected to immunoblot analysis using the following antibodies: rabbit anti-synphilin-1 polyclonal antibody, mouse anti-β actin polyclonal antibody (Sigma, MO, USA), rabbit anti-PARP polyclonal antibody, rabbit anti-GFP monoclonal antibody, rabbit anti-phospho-mTOR polyclonal antibody, rabbit anti-mTOR polyclonal antibody (Cell Signaling, MA, USA) and anti-Complex IV-subunit-1 monoclonal antibody (MitoSciences, OR, USA). For densitometric analyses of the signals, the ImageJ software (Rasband, W.S., ImageJ, U.S. National Institutes of Health, USA, http://rsb.info.nih.gov/ij/, 1997-2007) was used.

Fluorescence microscopy in living cells:

The inclusions formed by synphilin-1 and the acidic organelles were studied using a Cell Observer inverted microscope (Carl Zeiss, Germany) at 37° C with 5% CO in living cells. EGFP-synphilin-1 overexpressing HEK cells and empty vector control cells were cultured in Lab-Tek® II chambered coverglasses (Nalge Nunc International, NY, USA). 1μg/ml Hoechst 33342 (Molecular Probes, USA) in culture medium was used to stain nuclei, while lysosomes and acidic organelles were stained with 200 nM LysoTracker® Red (Invitrogen, USA) in culture medium for 10 minutes at 37° C.

Pictures were taken with an AxioCamMRm camera (Zeiss, Germany) and then analyzed with AxioVision software (Zeiss, Germany). For the quantification of synphilin-1-positive inclusions more than 100 cells for each sample in randomly selected microscopic fields were analyzed; the experiments were performed three times with similar results.

Immunocytochemistry:

To study the co-localization of synphilin-1-positive inclusions with γ-tubulin, WT and R621C EGFP-synphilin-1 overexpressing cells and the empty vector control cells were grown on collagen-coated glass coverslips for two days and then fixed with 4% formaldehyde in PBS for 15 min and incubated with 0.3% Triton X-100 in PBS for 30 min. After blocking with 10% FCS in PBS for 30 min, the cells were labelled at 4°C overnight with a mouse anti-γ-tubulin monoclonal antibody (Sigma, MO, USA). The next day the cells were washed with PBS and labelled with a Cy2-conjugated anti-mouse secondary

antibody (Dianova, Germany). The nuclei were stained with 1µg/ml Hoechst 33342 (Molecular Probes, USA).

To study the co-localization of synphilin-1-positive inclusions with the marker of autophagosomes microtubule-associated protein 1 light chain 3 (LC3), WT and R621C FLAG-synphilin-1 overexpressing cells and the empty vector control cells were grown on collagen-coated glass coverslips and transfected with GFP-LC3 (kindly provided by Tassula Proikas-Cezanne, University of Tübingen, Germany) using FuGENE HD (Roche, Germany) according to the manufacturer's instructions. Forty eight hours after transfection, the cells were fixed, permeabilized and blocked as described above. To detect FLAG-synphilin-1, an anti-FLAG rabbit polyclonal antibody (Sigma, Germany) and a Cy3-conjugated anti-rabbit secondary antibody (Dianova, Germany) were used.

Caspase-3 activity assay:

Caspase-3 activity was measured monitoring the Caspase-3-dependent cleavage of Acetyl-Asp-Glu-Val-Asp-Chloromethylcoumarin (Ac-DEVD-AMC; Bachem, Switzerland) with a fluorescence-based method. Briefly, WT and R621C EGFP-tagged synphilin-1 overexpressing HEK cells and empty vector control cells were cultured in 96-well plates. After the treatments, the cells were lysed in a specific lysis buffer (50 mM Tris-HCl, 120 mM NaCl, 5mM EDTA, 0.5% NP-40) for 10 minutes at 37° C and then 12,5µM Ac-DEVD-AMC was added. Afterwards, the lysates were incubated for 1 hour and 15 minutes at 37° C and then the emission of fluorescence from the cleaved Ac-DEVD-AMC was measured by a Mithras LB 940

cytofluorimeter (Berthold Technologies, Germany) using excitation and emission wavelengths 360nM and 480nM, respectively. The records were analyzed using the Mikro Win 2000 software.

Assessment of Mitochondrial Parameters by Fluorescence-Activated Cell Sorting (FACS):

Analysis of Reactive Oxygen Species (ROS) production in the mitochondria and of the Mitochondrial Membrane Potential (MMP) in synphilin-1 overexpressing HEK cells compared to the empty vector control cells was performed using a FACS-based method. Cells were harvested with 2mM EDTA solution in PBS and washed once with PBS. To evaluate the production of intramitochondrial ROS the cells were incubated with 2µM MitoSOX® (Invitrogen, CA, USA) in PBS for 20 min at 37° C. The cells were then washed once with PBS and resuspended in PBS.

To study the MMP, cells were incubated with 200nM TetraMethylRhodamineEthylester (TMRE; Invitrogen, CA, USA) in Dulbecco's Modified Eagle Medium (DMEM, Invitrogen, CA, USA) for 30 min at 37°C. After staining, the cells were washed twice with PBS and then resuspended in PBS. For each sample ~70,000 cells were analyzed in a CyAnADP apparatus (Beckman Coulter) using the 488 argon laser and emission through the PE Texas Red filter (613nm) and the FITC filter (530nm). For all the flow-cytometry measurements, HEK cells stably overexpressing WT and R621C EGFP-synphilin-1 cells were compared to the empty-vector control cells. The threshold was set using unstained HEK cells and the percentage of shift in the fluorescent signals was determined with the

Summit version 4.2 software (Dako Cytomation). The results are presented as relative change compared to the empty-vector controls and they represent the means of three independent experiments performed in duplicate.

Subcellular fractionation:

Cellular fractionations were performed using a mitochondrial isolation kit for cultured cells (Pierce, IL, USA), according to the manufacturer's instructions. The cytosolic and mitochondrial fractions obtained were analyzed by Western blot. In order to check the quality of the fractionation and the purity of the mitochondrial and cytosolic fraction, a mouse monoclonal antibody against prohibitin (Thermo Scientific, MA, USA) and a mouse monoclonal antibody against GlycerAldehyde-3-Phosphate DeHydrogenase (GAP-DH; Millipore, MA, USA) were used, respectively.

Results:

Aggregates formed by synphilin-1 in HEK cells are aggresomes:

Consistent with our previous report (Marx et al., 2003), HEK cells stably overexpressing EGFP-tagged synphilin-1 spontaneously developed perinuclear circular structures even in the absence of treatment (Fig.1A). It has been previously shown that synphilin-1-positive inclusions are immunoreactive to antibodies against ubiquitin, 20S proteasome subunit, Hsp-70, and to the centromeric proteins vimentin and γ-tubulin (Tanaka et al., 2004; Marx et al., 2007), all of which are markers of aggresomes and found in LB (Ii et al., 1997; Auluck et al., 2002; Kuzuhara et al., 1988).

To confirm that synphilin-1 inclusions in our cellular model represent aggresomes, and that they are located at the centrosome, immunofluorescence experiments with antibodies against γ-tubulin were performed. Immunoreactivity to γ-tubulin localized intensely to the EGFP-positive inclusions formed by both WT and R621C synphilin-1 (Fig.1A).

Another typical feature of aggresomes is their tendency to increase in number and size in response to proteasomal inhibition (Johnston et al., 1998). Therefore, WT and R621C EGFP-synphilin-1 overexpressing cells were treated with MG132 to inhibit the proteasomal activity and analysed by florescence microscopy using live cell imaging. A significantly higher percentage of cells bearing EGFP-positive inclusions were counted after 5 hours treatments with 5μM MG132 in both WT and R621C synphilin-1 overexpressing cells compared to the untreated controls (Fig.1B). In order to study potential effects of the

MG132 treatment on cell viability, Western blot experiments were performed to monitor Poly-ADP-Ribose-Polymerase (PARP) cleavage, since PARP is cleaved by Caspase-3 upon induction of apoptosis. We observed no induction of apoptosis upon the treatment paradigm; indeed, no difference in PARP cleavage between WT and R621C synphilin-1 overexpressing cells and empty vector controls was observed upon treatment for 5 hours with 5μM MG132 (Fig.4).

Synphilin-1 inclusions are target of autophagic clearance:

To assess whether synphilin-1 inclusions were a substrate of lysosomal degradation via autophagy, we monitored lysosomes and the formation of autophagosomes in synphylin-1 overexpressing cells under basal condition.

Stably FLAG-tagged synphilin-1-overexpressing HEK cells and empty vector controls were transiently transfected with an expression vector coding for GFP-LC3-fusion protein and then fixed and stained with an anti-FLAG antibody. We observed co-localization of the synphilin-1-positive inclusions with LC3-positive structures in a subset of both WT and R621C synphilin-1 overexpressing cells. In the empty vector controls, GFP-LC3 was diffusely localized in the cytoplasm (Fig.2A).

In addition, acidic organelles and lysosomes (stained with LysoTracker® Red) co-localized with synphilin-1-positive inclusions in living WT and R621C EGFP-synphilin-1-overexpressing HEK cells (Fig.2B). In a subset of cells we observed only partial co-localization; however, in these cells the area around the aggresomes was enriched

of lysosomal structures. Lysosomes were more diffused in the cytoplasm in the empty vector cells (Fig.2B).

Effects on synphilin-1 inclusions due to modulation of autophagic pathways:

To investigate an involvement of autophagy in the clearance of synphilin-1 inclusions, WT and R621C EGFP-synphilin-1-stably overexpressing HEK cells were treated with 5μM MG132 for 5 hours (to increase the amount of aggresomes) and subsequently cultured for additional 24 hours either in normal medium or in the presence of 200nM rapamycin or 100mM trehalose. To check for specific effects on autophagic induction, co-treatments with either rapamycin or trehalose together with the autophagy inhibitor wortmannin were performed.

We observed that treatment of cells overexpressing WT or R621C synphilin-1 with rapamycin and trehalose resulted in a significant reduction of the number of inclusions. This effect was reversed in the presence of wortmannin (Fig.3) that blocks autophagy by inhibiting the components of the Phosphatidyl-Inositol-3-Kinase (PI3K) family. This indicates that the observed reduction of inclusions was specifically due to an autophagy-dependent degradation mechanism (Fig.3).

To confirm that the modulation of lysosomal pathways in our experimental condition was mTOR-mediated, we analysed the levels of phosphorylation of the mTOR kinase in response to rapamycin treatment. Stably WT and R621C EGFP-synphilin-1-overexpressing cells and empty vector controls were treated with rapamycin and then

the phosphorylation of the mTOR kinase was evaluated by Western blot. After 24 hours of treatment with either 100 or 200nM rapamycin the posphorylation of mTOR was significantly decreased compared to the respective untreated controls (Supplementary Fig.1), demonstrating that our treatments are effective in blocking the mTOR pathway.

Effects on cell viability due to activation of autopagy:

To test if the enhancement of autophagy could be protective in cells that overexpress synphilin-1 as a model of aggregation-prone protein, we investigated the effects of pre-treatments with rapamycin against apoptosis induced by MG132 in our cellular model. Cells stably overexpressing WT and R621C and empty vector controls were treated with 200nM rapamycin for 24 hours and subsequently proteasomal inhibition was induced by 1μM MG132 for 16 hours. To evaluate the levels of apoptosis the cleavage of PARP was monitored by Western blot analyses. The ratio of cleaved PARP/full-length PARP was not different in the cells pre-treated with rapamycin compared to the cells cultivated in normal medium before the pro-apoptotic treatment with MG132 (Fig.5). We observed a tendency towards a reduced cytotoxic effect of MG132 in the WT synphilin-1-overexpressing cells, especially compared to the empty vector control cells.

Next, we examined whether the activation of autophagy could be beneficial after exposure to a toxic stimulus. For this purpose, WT and R621C EGFP-synphilin-1-stably overexpressing HEK cells and empty vector controls were treated with 1μM MG132 for 16 hours to in order

to induce cell death. Afterwards, the cells were cultured for additional 24 hours either in normal medium or in the presence of either 100nM rapamycin or 50mM trehalose. The cleavage of PARP was analysed by immunoblotting. Neither rapamycin nor trehalose was able to rescue the cells from the toxicity induced by MG132. In fact, the amount of PARP cleavage in the cells that recovered with the normal culture medium was not different from the cells treated with either rapamycin or trehalose (Fig.6A). Interestingly, the densitometric analysis of the immunoblots in Fig.6A revealed a tendency towards a better recovery from the cytotoxic effect of MG132 in the HEK cells overexpressing the WT form of synphilin-1, especially compared to the empty vector control cells.

To further investigate the effects of the pharmacological enhancement of autophagy on apoptosis, we analysed the activity of the Caspase-3 in the same experimental setting as shown in Fig.6A. According to the results on PARP cleavage, also the enzymatic activity of Caspase-3 was not different in the cells that recovered in the normal culture medium compared with the cells treated with either rapamycin or trehalose after MG132-treatment (Fig.6B).

Cells overexpressing WT synphilin-1 that were treated with MG132 and that then recovered in the presence of normal culture medium or rapamycin or trehalose showed the same levels of caspase-3 activation as the respective untreated control cells (Fig.6B).

Effect of apoptosis induction on autopagy-mediated clearance of aggregates:

We were interested in studying whether the efficacy of the clearance of synphilin-1 via autophagy could be affected by pro-apoptotic treatments. For this purpose, we used the same paradigm of treatments shown in Fig.6: WT and R621C EGFP-synphilin-1-stably overexpressing HEK were treated with 1μM MG132 for 16 hours to in order to trigger cell death. Afterwards, the cells had 24 hours-washout either in normal medium or in the presence of 100nM rapamycin or 50mM trehalose; then, the percentage of the cells bearing synphilin-1-positive inclusion was evaluated by live cell imaging. We found that the post-treatment with rapamycin significantly reduced the number of cells bearing aggresomes (compared with the cells that recovered in the normal culture medium) only in the cells overexpressing WT synphilin-1 (Fig.7).

Mitochondrial function in synphilin-1-overexpressing cells:

To study the effects of synphilin-1 overexpression and of the modulation of its aggregate-forming properties on the cellular homeostasis, we focused on mitochondrial function as an important interface between energy metabolism and cell death.

The MMP and the content of ROS in the mitochondria of WT and R621C EGFP-synphilin-1-overexpressing HEK cells compared to empty vector control cells were analysed by FACS using TMRE and MitoSOX® staining, respectively.

WT and R621C EGFP-synphilin-1-overexpressing cells revealed a significant increase of the intra-mitochondrial ROS levels and a

reduction of the MMP compared with the empty vector controls in basal condition (Fig.8).

Neither treatments with rapamycin (in the same conditions that were effective in clearing protein inclusion) nor treatments with MG132 (in both, pro-apoptotic and not toxic conditions) caused significant effects of the above-mentioned mitochondrial impairments (data not shown).

We performed fractionation experiments to isolate the mitochondria from lysates of WT and R621C EGFP-synphilin-1-overexpressing cells and empty vector controls. Then the expression of synphilin-1 in the two fractions was assayed by immunoblotting. We found no immunoreactivity for synphilin-1 in the mitochondrial fraction (Fig.9).

Discussion:

Aggresomes have been characterised as inclusions bodies that form in response to proteasome inhibition (Johnston et al., 1998) and in the presence of high levels of aggregate-prone proteins (Wong et al., 2008). Here we confirmed previous reports showing that synphilin-1-positive inclusions fulfil the criteria of aggresomes (Marx et al., 2003; Tanaka et al., 2004) showing that synphilin-1-positive inclusions in WT and R621C synphilin-1-stably overexpressing cells co-localize with γ-tubulin as a marker of the centrosome (Fig.1A) and that the formation of aggresomes is enhanced by MG132-induced inhibition of the proteasome (Fig.1B).

The formation of aggresomes was found to be cytoprotective against cytotoxicity mediated by polyglutamine-containig proteins (Taylor et al., 2003; Arrasate et al., 2004; Muchowski et al., 2002). Moreover, it was described that bearing aggresomes formed by synphilin-1 and alpha-synuclein confers resistance to apoptotic cell death in conditions of proteasomal inhibition (Tanaka et al, 2004).

In this context, it was speculated that aggresomes may be protective by promoting alternative clearance pathways of the aggregated material in conditions of proteasomal dysfunction, i.e. by triggering autophagy-related mechanisms (Wong et al., 2008; Fortun et al., 2003). Indeed, here we observed co-localization of synphilin-1-positive inclusions with autophagosomes and lysosomal structures in WT and R621C synphilin-1-overexpressing cells, also in basal conditions (Fig.2).

Genetic studies and experiments with animal models showed that impairments of autophagic clearance could be involved in neurodegeneration in PD (Ramirez et al., 2006; Hara et al., 2006) and that modulation of autophagy could be beneficial (Sarkar et al., 2009).

Autophagy is regulated by the class I and III PI3 kinase pathways; the first one, which involves the kinase mammalian Target Of Rapamycin (mTOR), represses autophagy, while the second one induces it (Todde et al., 2009). Rapamycin is a macrolide antibiotic that activates autophagy by inhibiting the kinase activity of mTOR (Kim et al., 2002). Trehalose is disaccharide that stimulates autophagy in an mTOR-independent way. Both of these chemicals are effective in stimulating the clearance of various aggregate-prone proteins (Sarkar et al., 2009; Sarkar et al., 2007).

In this study we observed that both rapamycin and trehalose were effective in reducing the number of aggregates formed by WT and R621C mutant synphilin-1 in an autophagy-dependent way (Fig.3).

We studied also the possible protective effect of autophagy induction in terms of cell death. Since the experimental settings for treatments with MG132 shown in figure 3 didn't induce apoptosis (Fig.4) and dysfunctions of the UPS are involved in PD (reviewed in Ross and Pickart, 2004), we changed our conditions in order to induce apoptosis via MG132-mediated proteasomal inhibition.

Pre-treatments with rapamycin were not able to rescue synphilin-1 overexpressing cells from MG132-induced apoptosis (Fig.5). This result is in contrast with a recent report showing that autophagy activation by rapamycin has a protective role in a paradigm of rotenone-induced cell death in alpha-synuclein-overexpressing

dopaminergic cells (Dadakhujaev et al., 2010). This indicates that prolonged blockage of proteasome by MG132 may lead to a failure of the protective effect of rapamycin, while the effects of rotenone (that targets complex I of the mitochondrial respiratory chain) may be compensated by previous activation of autophagy.

We also observed no protective effect of trehalose and rapamycin after apoptosis induction by MG132 in synphilin-1-overexpressing cells (Fig.6). This is in line with another study that revealed a failure of activation of autophagy to rescue cultured embryonic rat cortical neurons from apoptosis previously induced by proteasome inhibition (Rideout et al., 2004).

Interestingly, we observed significantly reduced levels of caspase-3 activation in WT synphilin-1 overexpressing cells compared to R621C synphilin-1 overexpressing cells and empty vector controls after treatment with MG132. This supports recent observations that overexpressed WT synphilin-1 promotes cell growth and confers protection against cellular stress by reducing caspase-3 activation and PARP cleavage (Li et al., 2010). Indeed, it was shown that, under apoptosis induction, caspase-3 cleaves synphilin-1; then, the C-terminal fragment of synphilin-1 is able to inhibit further pro-caspase-3 activation leading to reduced levels of active caspase-3 and cleaved PARP (Giaime et al., 2006). Accordingly, we also observed protection from MG132-induced apoptosis in cells overexpressing WT synphilin-1 (Fig. 6B). Moreover, it can be speculated that the lack of protection observed in the R621C synphilin-1 overexpressing cells may be due to an impairment of the pro-survival function of C-terminal synphilin-1 fragment due to interference with caspase-

mediated cleavage, as the R621C amino acid-substitution is located in the critical C-terminal fragment of synphilin-1.

After inducing cell death with MG132, subsequent rapamycin-mediated activation of autophagy effectively reduced the level of aggregates only in WT synphilin-1-overexpressing cells, while no effective clearance of R621C synphilin-1 aggregates was observed (Fig.7). Considering that R621C synphilin-1-overexpressing cells were more susceptible to MG132-induced apoptosis compared to the WT cells (Fig.6B), this result is in line with a recent publication showing that autophagy-dependent clearance of aggregates is linked to metabolic activity of the cells (Yu et al., 2009). We hypothesize that, after the toxic treatment with MG132, R621C synphilin-1-overexpressing cells are more compromised compared to the WT synphilin-1-overexpressing cells. As a consequence, R621C synphilin-1-overexpressing cells could lack the energy resources to actively remove synphilin-1 aggregates via autophagy after pro-apoptotic treatment with MG132.

Interestingly, we observed that cells treated with 1μM MG132 for 16 hours and then cultured in normal growth medium had the same levels of aggregates as the untreated controls (Fig.7). This indicates important differences compared to an alternative, non-toxic treatment paradigm with shorter incubation and higher doses of MG132 (shown in Fig.1B). This difference may mean that a prolonged MG132-incuced inhibition of the proteasome itself is sufficient to stimulate the autophagic clearance of the aggregates, as recently shown (Rideout et al., 2004; Y. Bang, K. Kim and H. Choi “Role of autophagy in the pathogenesis of Parkinson’s disease” Program No 828.14, 2009

Neuroscience Meeting Planner, Chicago, IL, Society for Neuroscience 2009. Online).

As mentioned in the introduction, synphilin-1 was identified as the first alpha-synuclein-interacting protein that shares the same subcellular localization under physiological conditions and that is involved in protein aggregation in relevant brain areas in PD together with alpha-synuclein (Ribeiro et al., 2002; Neystat et al., 2002). Recently, direct effects of alpha-synuclein overexpression on mitochondrial function, i.e. reduced activity of the mitochondrial complex I and increased oxidative load were described (Hsu et al., 2000; Devi et al., 2008). Moreover, it was demonstrated that alpha-synuclein possesses a potential N-terminal mitochondrial targeting sequence that mediates its direct translocation to the mitochondria (Devi et al., 2008; Li et al., 2007).

Here we report first evidence for a functional impairment of mitochondria due to overexpression of WT and R621C synphilin-1, as delineated by increased levels of intramitochondrial ROS and decreased mitochondrial membrane potential compared to controls (Fig.8). This correlates with ultrastructural morphological changes of the mitochondrial network observed in synphilin-1-overexpressing mice (Nuber et al., 2010). This effect was not due to direct effects of synphilin-1 in the mitochondria, as no translocation of the protein to the mitochondria was found based on subcellular fractionation (Fig.9). This argues in favour of indirect effects on mitochondrial function.

It is well-known that mitochondria are carried along the microtubules using kinesin and dynein (Zinsmaier et al., 2009). Furthermore, it was published that dynein could be involved also in the processes of

fission and fusion, which are essential for the maintenance of the correct morphology and function of the mitochondria (Varadi et al., 2004).

Since aggresomes are also transported along microtubules in a dynein-dependent way (Garcia-Mata et al., 2002; Iwata et al., 2005) and dynein is involved also in autophagy-related dynamics (Cai et al., 2009), we hypothesize that both the abnormal expression of synphilin-1 and the presence and formation of aggregates might interfere with the dynein-dependent system for aggresome transport along the microtubules to the centrosome for autophagic degradation. Therefore, impaired mitochondria could not be transported effectively to the sites of lysosomal degradation. This condition could lead to a progressive accumulation of dysfunctional mitochondria and explain the observed mitochondrial phenotype in synphilin-1-overexpressing cells.

In this context, inhibitory effects of alpha-synuclein on mitochondrial function were not influenced by alpha-synuclein aggregation (Loeb et al., 2010). In line with these observations, we found that neither treatment with rapamycin (in the same experimental condition that reduced synphilin-1 inclusions, Fig.3) nor with MG132 (in the same condition that caused increased synphilin-1 aggregation, Fig.1B) were able to rescue mitochondrial deficits observed in synphilin-1-overexpressing cells (data not shown).

These data suggest dissociation between mitochondrial dysfunction and aggregate dynamics and indicate that the pharmacological activation of autophagy may not prevent mitochondrial dysfunction due to overexpression of synphilin-1.

To summarize, we observed that synphilin-1 aggresomes are a target of lysosomal degradation and that their clearance can be enhanced by activating autophagic pathways. However, we found that the pharmacological activation of autophagy was not effective to rescue synphilin-1-overexpressing cells from apoptosis triggered by proteasomal inhibition or from mitochondrial dysfunction related to synphilin-1-overexpression. Moreover, we observed a protective effect of overexpressed WT synphilin-1 against MG132-induced apoptosis. Our findings suggest that future therapies in PD that focus on modulation of the formation of protein inclusions may not be effective to provide protection from mitochondrial dysfunction and cell death.

Acknowledgements:

This work was supported by grants from the German Research Council [DFG, KR2119/3-1]; the Federal Ministry for Education and Research [BMBF, NGFNplus; 01GS08134] and a pilot grant from the Hertie-Institute to RK. LFB is supported by a doctoral scholarship of the charitable Hertie Foundation.

References:

Arrasate M, Mitra S, Schweitzer ES, Segal MR, Finkbeiner S (Inclusion body formation reduces levels of mutant huntingtin and the risk of neuronal death. Nature 431:805-810.2004).

Auluck PK, Chan HY, Trojanowski JQ, Lee VM, Bonini NM (Chaperone suppression of alpha-synuclein toxicity in a Drosophila model for Parkinson's disease. Science 295:865-868.2002).

Betarbet R, Sherer TB, Di Monte DA, Greenamyre JT (Mechanistic approaches to Parkinson's disease pathogenesis. Brain Pathol 12:499-510.2002).

Bonifati V, Oostra BA, Heutink P (Linking DJ-1 to neurodegeneration offers novel insights for understanding the pathogenesis of Parkinson's disease. J Mol Med 82:163-174.2004).

Cai ZL, Shi JJ, Yang YP, Cao BY, Wang F, Huang JZ, Yang F, Zhang P, Liu CF (MPP+ impairs autophagic clearance of alpha-synuclein by impairing the activity of dynein. Neuroreport 20:569-573.2009).

Chung KK, Zhang Y, Lim KL, Tanaka Y, Huang H, Gao J, Ross CA, Dawson VL, Dawson TM (Parkin ubiquitinates the alpha-synuclein-interacting protein, synphilin-1: implications for Lewy-body formation in Parkinson disease. Nat Med 7:1144-1150.2001).

Dadakhujaev S, Noh HS, Jung EJ, Cha JY, Baek SM, Ha JH, Kim DR (Autophagy protects the rotenone-induced cell death in alpha-

synuclein overexpressing SH-SY5Y cells. Neurosci Lett 472:47-52).

Devi L, Raghavendran V, Prabhu BM, Avadhani NG, Anandatheerthavarada HK (Mitochondrial import and accumulation of alpha-synuclein impair complex I in human dopaminergic neuronal cultures and Parkinson disease brain. J Biol Chem 283:9089-9100.2008).

Engelender S, Kaminsky Z, Guo X, Sharp AH, Amaravi RK, Kleiderlein JJ, Margolis RL, Troncoso JC, Lanahan AA, Worley PF, Dawson VL, Dawson TM, Ross CA (Synphilin-1 associates with alpha-synuclein and promotes the formation of cytosolic inclusions. Nat Genet 22:110-114.1999).

Fortun J, Dunn WA, Jr., Joy S, Li J, Notterpek L (Emerging role for autophagy in the removal of aggresomes in Schwann cells. J Neurosci 23:10672-10680.2003).

Garcia-Mata R, Bebok Z, Sorscher EJ, Sztul ES (Characterization and dynamics of aggresome formation by a cytosolic GFP-chimera. J Cell Biol 146:1239-1254.1999).

Garcia-Mata R, Gao YS, Sztul E (Hassles with taking out the garbage: aggravating aggresomes. Traffic 3:388-396.2002).

Giaime E, Sunyach C, Herrant M, Grosso S, Auberger P, McLean PJ, Checler F, da Costa CA (Caspase-3-derived C-terminal product of synphilin-1 displays antiapoptotic function via modulation of the p53-dependent cell death pathway. J Biol Chem 281:11515-11522.2006).

Hara T, Nakamura K, Matsui M, Yamamoto A, Nakahara Y, Suzuki-Migishima R, Yokoyama M, Mishima K, Saito I, Okano H,

Mizushima N (Suppression of basal autophagy in neural cells causes neurodegenerative disease in mice. Nature 441:885-889.2006).

Hsu LJ, Sagara Y, Arroyo A, Rockenstein E, Sisk A, Mallory M, Wong J, Takenouchi T, Hashimoto M, Masliah E (alpha-synuclein promotes mitochondrial deficit and oxidative stress. Am J Pathol 157:401-410.2000).

Ii K, Ito H, Tanaka K, Hirano A (Immunocytochemical co-localization of the proteasome in ubiquitinated structures in neurodegenerative diseases and the elderly. J Neuropathol Exp Neurol 56:125-131.1997).

Iwata A, Riley BE, Johnston JA, Kopito RR (HDAC6 and microtubules are required for autophagic degradation of aggregated huntingtin. J Biol Chem 280:40282-40292.2005).

Johnston JA, Ward CL, Kopito RR (Aggresomes: a cellular response to misfolded proteins. J Cell Biol 143:1883-1898.1998).

Junn E, Lee SS, Suhr UT, Mouradian MM (Parkin accumulation in aggresomes due to proteasome impairment. J Biol Chem 277:47870-47877.2002).

Kim DH, Sarbassov DD, Ali SM, King JE, Latek RR, Erdjument-Bromage H, Tempst P, Sabatini DM (mTOR interacts with raptor to form a nutrient-sensitive complex that signals to the cell growth machinery. Cell 110:163-175.2002).

Kitada T, Asakawa S, Hattori N, Matsumine H, Yamamura Y, Minoshima S, Yokochi M, Mizuno Y, Shimizu N (Mutations in the parkin gene cause autosomal recessive juvenile parkinsonism. Nature 392:605-608.1998).

Kuzuhara S, Mori H, Izumiyama N, Yoshimura M, Ihara Y (Lewy bodies are ubiquitinated. A light and electron microscopic immunocytochemical study. Acta Neuropathol 75:345-353.1988).

Lee G, Junn E, Tanaka M, Kim YM, Mouradian MM (Synphilin-1 degradation by the ubiquitin-proteasome pathway and effects on cell survival. J Neurochem 83:346-352.2002).

Li WW, Yang R, Guo JC, Ren HM, Zha XL, Cheng JS, Cai DF (Localization of alpha-synuclein to mitochondria within midbrain of mice. Neuroreport 18:1543-1546.2007).

Li X, Liu Z, Tamashiro K, Shi B, Rudnicki DD, Ross CA, Moran TH, Smith WW (Synphilin-1 exhibits trophic and protective effects against Rotenone toxicity. Neuroscience 165:455-462.2010).

Liani E, Eyal A, Avraham E, Shemer R, Szargel R, Berg D, Bornemann A, Riess O, Ross CA, Rott R, Engelender S (Ubiquitylation of synphilin-1 and alpha-synuclein by SIAH and its presence in cellular inclusions and Lewy bodies imply a role in Parkinson's disease. Proc Natl Acad Sci U S A 101:5500-5505.2004).

Lim KL, Dawson VL, Dawson TM (Parkin-mediated lysine 63-linked polyubiquitination: a link to protein inclusions formation in Parkinson's and other conformational diseases? Neurobiol Aging 27:524-529.2006).

Loeb V, Yakunin E, Saada A, Sharon R (The transgenic over expression of {alpha}-Synuclein and not its related pathology, associates with complex I inhibition. J Biol Chem.2010).

Martinez-Vicente M, Cuervo AM (Autophagy and neurodegeneration: when the cleaning crew goes on strike. Lancet Neurol 6:352-361.2007).

Marx FP, Holzmann C, Strauss KM, Li L, Eberhardt O, Gerhardt E, Cookson MR, Hernandez D, Farrer MJ, Kachergus J, Engelender S, Ross CA, Berger K, Schols L, Schulz JB, Riess O, Kruger R (Identification and functional characterization of a novel R621C mutation in the synphilin-1 gene in Parkinson's disease. Hum Mol Genet 12:1223-1231.2003).

Marx FP, Soehn AS, Berg D, Melle C, Schiesling C, Lang M, Kautzmann S, Strauss KM, Franck T, Engelender S, Pahnke J, Dawson S, von Eggeling F, Schulz JB, Riess O, Kruger R (The proteasomal subunit S6 ATPase is a novel synphilin-1 interacting protein--implications for Parkinson's disease. FASEB J 21:1759-1767.2007).

McNaught KS, Mytilineou C, Jnobaptiste R, Yabut J, Shashidharan P, Jennert P, Olanow CW (Impairment of the ubiquitin-proteasome system causes dopaminergic cell death and inclusion body formation in ventral mesencephalic cultures. J Neurochem 81:301-306.2002).

Muchowski PJ, Ning K, D'Souza-Schorey C, Fields S (Requirement of an intact microtubule cytoskeleton for aggregation and inclusion body formation by a mutant huntingtin fragment. Proc Natl Acad Sci U S A 99:727-732.2002).

Neystat M, Rzhetskaya M, Kholodilov N, Burke RE (Analysis of synphilin-1 and synuclein interactions by yeast two-hybrid

beta-galactosidase liquid assay. Neurosci Lett 325:119-123.2002).

Nuber S, Franck T, Wolburg H, Schumann U, Casadei N, Fischer K, Calaminus C, Pichler BJ, Chanarat S, Teismann P, Schulz JB, Luft AR, Tomiuk J, Wilbertz J, Bornemann A, Kruger R, Riess O (Transgenic overexpression of the alpha-synuclein interacting protein synphilin-1 leads to behavioral and neuropathological alterations in mice. Neurogenetics 11:107-120.2010).

O'Farrell C, Murphy DD, Petrucelli L, Singleton AB, Hussey J, Farrer M, Hardy J, Dickson DW, Cookson MR (Transfected synphilin-1 forms cytoplasmic inclusions in HEK293 cells. Brain Res Mol Brain Res 97:94-102.2001).

Olanow CW, Perl DP, DeMartino GN, McNaught KS (Lewy-body formation is an aggresome-related process: a hypothesis. Lancet Neurol 3:496-503.2004).

Parker WD, Jr., Boyson SJ, Parks JK (Abnormalities of the electron transport chain in idiopathic Parkinson's disease. Ann Neurol 26:719-723.1989).

Polymeropoulos MH, Lavedan C, Leroy E, Ide SE, Dehejia A, Dutra A, Pike B, Root H, Rubenstein J, Boyer R, Stenroos ES, Chandrasekharappa S, Athanassiadou A, Papapetropoulos T, Johnson WG, Lazzarini AM, Duvoisin RC, Di Iorio G, Golbe LI, Nussbaum RL (Mutation in the alpha-synuclein gene identified in families with Parkinson's disease. Science 276:2045-2047.1997).

Ramirez A, Heimbach A, Grundemann J, Stiller B, Hampshire D, Cid LP, Goebel I, Mubaidin AF, Wriekat AL, Roeper J, Al-Din A, Hillmer AM, Karsak M, Liss B, Woods CG, Behrens MI, Kubisch C (Hereditary parkinsonism with dementia is caused by mutations in ATP13A2, encoding a lysosomal type 5 P-type ATPase. Nat Genet 38:1184-1191.2006).

Ribeiro CS, Carneiro K, Ross CA, Menezes JR, Engelender S (Synphilin-1 is developmentally localized to synaptic terminals, and its association with synaptic vesicles is modulated by alpha-synuclein. J Biol Chem 277:23927-23933.2002).

Rideout HJ, Lang-Rollin I, Stefanis L (Involvement of macroautophagy in the dissolution of neuronal inclusions. Int J Biochem Cell Biol 36:2551-2562.2004).

Ross CA, Pickart CM (The ubiquitin-proteasome pathway in Parkinson's disease and other neurodegenerative diseases. Trends Cell Biol 14:703-711.2004).

Sarkar S, Davies JE, Huang Z, Tunnacliffe A, Rubinsztein DC (Trehalose, a novel mTOR-independent autophagy enhancer, accelerates the clearance of mutant huntingtin and alpha-synuclein. J Biol Chem 282:5641-5652.2007).

Sarkar S, Ravikumar B, Floto RA, Rubinsztein DC (Rapamycin and mTOR-independent autophagy inducers ameliorate toxicity of polyglutamine-expanded huntingtin and related proteinopathies. Cell Death Differ 16:46-56.2009).

Schapira AH, Cooper JM, Dexter D, Clark JB, Jenner P, Marsden CD (Mitochondrial complex I deficiency in Parkinson's disease. J Neurochem 54:823-827.1990).

Schulz JB, Dichgans J (Molecular pathogenesis of movement disorders: are protein aggregates a common link in neuronal degeneration? Curr Opin Neurol 12:433-439.1999).

Singleton AB, Farrer M, Johnson J, Singleton A, Hague S, Kachergus J, Hulihan M, Peuralinna T, Dutra A, Nussbaum R, Lincoln S, Crawley A, Hanson M, Maraganore D, Adler C, Cookson MR, Muenter M, Baptista M, Miller D, Blancato J, Hardy J, Gwinn-Hardy K (alpha-Synuclein locus triplication causes Parkinson's disease. Science 302:841.2003).

Strauss KM, Martins LM, Plun-Favreau H, Marx FP, Kautzmann S, Berg D, Gasser T, Wszolek Z, Muller T, Bornemann A, Wolburg H, Downward J, Riess O, Schulz JB, Kruger R (Loss of function mutations in the gene encoding Omi/HtrA2 in Parkinson's disease. Hum Mol Genet 14:2099-2111.2005).

Tanaka M, Kim YM, Lee G, Junn E, Iwatsubo T, Mouradian MM (Aggresomes formed by alpha-synuclein and synphilin-1 are cytoprotective. J Biol Chem 279:4625-4631.2004).

Taylor JP, Tanaka F, Robitschek J, Sandoval CM, Taye A, Markovic-Plese S, Fischbeck KH (Aggresomes protect cells by enhancing the degradation of toxic polyglutamine-containing protein. Hum Mol Genet 12:749-757.2003).

Todde V, Veenhuis M, van der Klei IJ (Autophagy: principles and significance in health and disease. Biochim Biophys Acta 1792:3-13.2009).

Tompkins MM, Hill WD (Contribution of somal Lewy bodies to neuronal death. Brain Res 775:24-29.1997).

Valente EM, Abou-Sleiman PM, Caputo V, Muqit MM, Harvey K, Gispert S, Ali Z, Del Turco D, Bentivoglio AR, Healy DG, Albanese A, Nussbaum R, Gonzalez-Maldonado R, Deller T, Salvi S, Cortelli P, Gilks WP, Latchman DS, Harvey RJ, Dallapiccola B, Auburger G, Wood NW (Hereditary early-onset Parkinson's disease caused by mutations in PINK1. Science 304:1158-1160.2004).

Varadi A, Johnson-Cadwell LI, Cirulli V, Yoon Y, Allan VJ, Rutter GA (Cytoplasmic dynein regulates the subcellular distribution of mitochondria by controlling the recruitment of the fission factor dynamin-related protein-1. J Cell Sci 117:4389-4400.2004).

Wakabayashi K, Engelender S, Yoshimoto M, Tsuji S, Ross CA, Takahashi H (Synphilin-1 is present in Lewy bodies in Parkinson's disease. Ann Neurol 47:521-523.2000).

Wong ES, Tan JM, Soong WE, Hussein K, Nukina N, Dawson VL, Dawson TM, Cuervo AM, Lim KL (Autophagy-mediated clearance of aggresomes is not a universal phenomenon. Hum Mol Genet 17:2570-2582.2008).

Yu WH, Dorado B, Figueroa HY, Wang L, Planel E, Cookson MR, Clark LN, Duff KE (Metabolic activity determines efficacy of macroautophagic clearance of pathological oligomeric alpha-synuclein. Am J Pathol 175:736-747.2009).

Zinsmaier KE, Babic M, Russo GJ (Mitochondrial transport dynamics in axons and dendrites. Results Probl Cell Differ 48:107-139.2009).

Figure legends:

Figure 1: Study of the characteristics of synphilin-1-positive inclusions. **A**: Immunofluorescent staining for γ-tubulin (red) of untreated HEK cells stably overexpressing WT and R621C mutant EGFP-synphilin-1 (green). Synphilin-1-positive inclusions co-localize with γ-tubulin at the centrosome. Scale bar: 10μm. **B**: Analysis via live cell imaging of the effects of 5 hours treatments with 5μM MG132 on the aggresomes in WT and R621C mutant EGFP-synphilin-1 overexpressing HEK cells stained with 1μg/ml Hoechst 33342. The results are represented as mean percentages of cells bearing EGFP-positive aggregates on the total amount of cells in three independent experiments ± standard deviation. The treated cells showed increased levels of synphilin-1 aggregates compared to the untreated controls (* $p < 0.05$ vs respective untreated controls, Student t test).

Figure 2: Co-localization of synphilin-1-positive inclusions with autophagic structures in untreated cells. **A**: Immunofluorescent staining for FLAG-tagged synphilin-1 of untreated HEK cells stably overexpressing WT and R621C mutant FLAG-synphilin-1 (red) and on empty vector controls after transient transfection with EGFP-LC-3 (green) The nuclei (blue) were stained with Hoechst 33342. Scale bar: 10μm. **B**: Analysis via live cell imaging of untreated HEK cells stably overexpressing WT and R621C mutant EGFP-synphilin-1 (green) and of empty vector controls stained with LysoTracker® Red (red) and Hoechst 33342 (blue) Scale bar: 10μm. Synphilin-1-positive

inclusions appeared to co-localize with the autophagosomes and with lysosomal structures.

Figure 3: Effects of the modulation of autophagy-regulating pathways on synphilin-1-aggregates. WT and R621C mutant EGFP-synphilin-1 overexpressing HEK cells were treated with 5μM MG132 for 5 hours and then cultured for additional 24 hours with either normal culture medium or in the presence of 200nM rapamycin or 100mM trehalose. As a negative control, treatments with 5μM MG132 for 5 hours followed by 24 hours-co-treatments with either 200nM rapamycin or 100mM trehalose together with 233nM wortmannin were performed. The nuclei were stained with Hoechst 33342 and live cell imaging-study of the amount of synphilin-1-positive inclusions was carried out. Values represent the mean percentage of cells bearing EGFP-positive aggregates in three independent experiments ± standard deviation. The pharmacological enhancement of autophagy resulted effective in reducing the amount of synphilin-1 aggregates (* $p < 0.05$ vs cells treated with 5uM MG132 for 5h and then cultured with either normal medium or in the presence of wortmannin for additional 24 hours, Student t test).

Figure 4: Western blot analysis of PARP cleavage in WT and R621C mutant EGFP-synphilin-1-overexpressing HEK cells and in empty vector-control cells after treatments with 5μM MG132 for 5 hours. PARP resulted not significantly cleaved in any of the analysed samples.

Figure 5: Effects of pre-treatment with rapamycin on cell viability against subsequent MG132-induced apoptosis. WT and R621C mutant EGFP-synphilin-1 overexpressing HEK cells and empty vector-control cells were either treated with 200nM rapamycin for 24 hours or cultured in normal medium for 24 hours and afterwards 1μM MG132 was added for 16 hours. Then, the cleavage of PARP was evaluated by immunoblotting. The densitometric analysis of three independent experiments shows that the ratio of cleaved PARP/full-length PARP in the cells pre-treated with rapamycin is not statistically different from the cells that did not receive any particular treatment before MG132-triggered apoptosis.

Figure 6: Effects of rapamycin and trehalose on cell viability after MG132-induced apoptosis. WT and R621C mutant EGFP-synphilin-1 overexpressing HEK cells and empty vector control cells were treated with 1μM MG132 for 16 hours and then they were cultured either in normal medium or in the presence of 100nM rapamycin or 50mM trehalose for 24 hours. **A:** The cleavage of PARP was evaluated by immunoblotting. The densitometric analysis of three independent experiments shows that the ratio of cleaved PARP/full-length PARP in the cells treated with rapamycin and trehalose after MG132-treatment resulted not statistically different from the cells that recovered in normal medium. **B:** The activity of Caspase-3 was measured. Values represent the ratio of the mean optic density/the protein concentration measured in three independent experiments ± the standard deviation (normalized to the respective untreated controls). Caspase-3-activity resulted not different in the cells that

recovered in the normal culture medium compared with the cells treated with either rapamycin or trehalose (data not shown) after MG132-treatment. (* $p < 0.05$ vs respective untreated controls, Student t test).

Figure 7: Effects of rapamycin on synphilin-1-aggregates after MG132-induced apoptosis. WT and R621C mutant EGFP-synphilin-1 overexpressing HEK cells were treated with 1μM MG132 for 16 hours and then cultured either in normal medium or in the presence of 100nM rapamycin for 24 hours. Afterwards, the nuclei were stained with Hoechst 33342 and live cell imaging-study of synphilin-1-positive inclusions was performed. Values represent the mean percentage of cells bearing EGFP-positive aggregates in three independent experiments ± standard deviation. The treatment with rapamycin resulted effective in reducing the amount of synphilin-1 aggregates after cytotoxic MG132-treatment compared to the cells that recovered in the normal medium only in the WT synphilin-1 overexpressing cells (* $p < 0.05$ vs cells cultured in normal medium after MG132-treatment, Student t test).

Figure 8: Analysis of mitochondrial parameters via FACS. The levels of ROS in the mitochondria and the mitochondrial membrane potential in untreated WT and R621C mutant EGFP-synphilin-1 overexpressing HEK and empty-vector control cells were analysed by FACS staining the cells with MitoSOX® and TMRE, respectively. Values represent the mean percentage of MitoSOX- and TMRE-positive cells in three independent experiments ± standard deviation.

WT and R621C mutant EGFP-synphilin-1 overexpressing HEK showed increased levels of ROS in the mitochondria and decreased mitochondrial membrane potential compared to the empty-vector control cells (* $p < 0.05$ vs empty vector control cells, Student t test).

Figure 9: Study of the expression of synphilin-1 in the cytosolic and mitochondrial cellular fraction. Untreated WT and R621C mutant EGFP-synphilin-1 overexpressing HEK and empty vector control HEK cells were subjected to fractionation experiments and then the expression of synphilin-1 in the cytoplasm and in the mitochondria was assayed by immunoblotting using an anti- GFP antibody. GAP-DH and prohibitin were used as markers of the cytoplasm and of the mitochondrial fraction, respectively, to asses the quality of the experiment.

Supplementary figure 1: Effects of rapamycin on the mTOR pathway in our experimental settings. Western blot analysis of the phosphorylation of mTOR in WT and R621C mutant EGFP-synphilin-1-overexpressing HEK cells in basal conditions and after treatment with either 100nM or 200nM rapamycin for 24 hours. The densitometric analysis of three independent experiments showed a significant reduction of the ratio of phosphorylated mTOR/total mTOR in the treated cells ($p < 0.05$ vs respective untreated controls, Student t test).

Figure 1

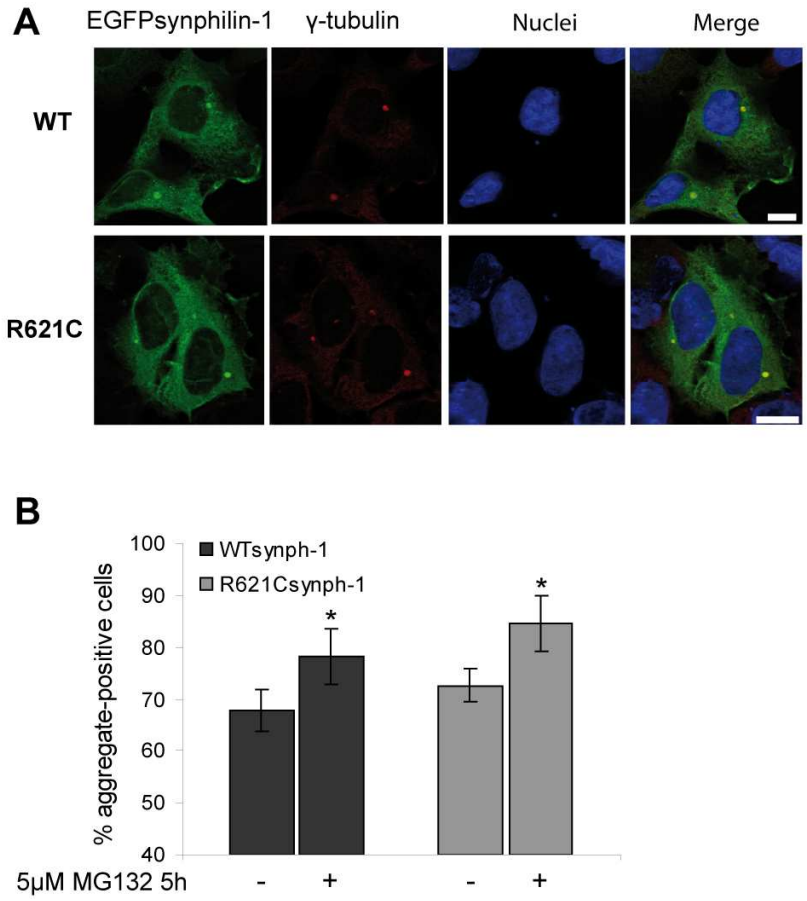
A
EGFPsynphilin-1
γ-tubulin
Nuclei
Merge
WT
R621C
B
WTsynph-1
R621Csynph-1
% aggregate-positive cells
100
90
80
70
60
50
40
*
*
5μM MG132 5h
-
+
-
+

Figure 2

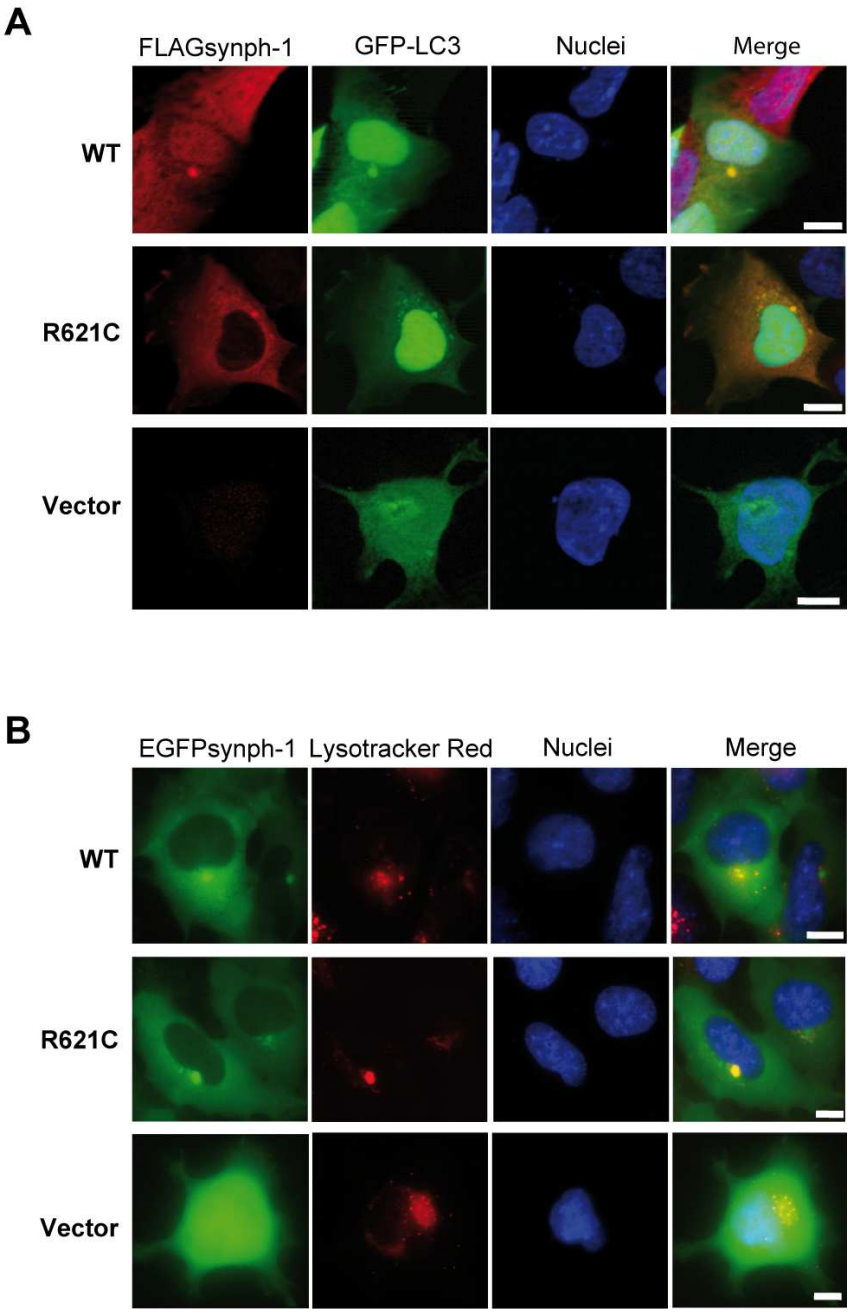
A
FLAGsynph-1
GFP-LC3
Nuclei
Merge
WT
R621C
Vector
B
EGFPsynph-1
Lysotracker Red
Nuclei
Merge
WT
R621C
Vector

Figure 3

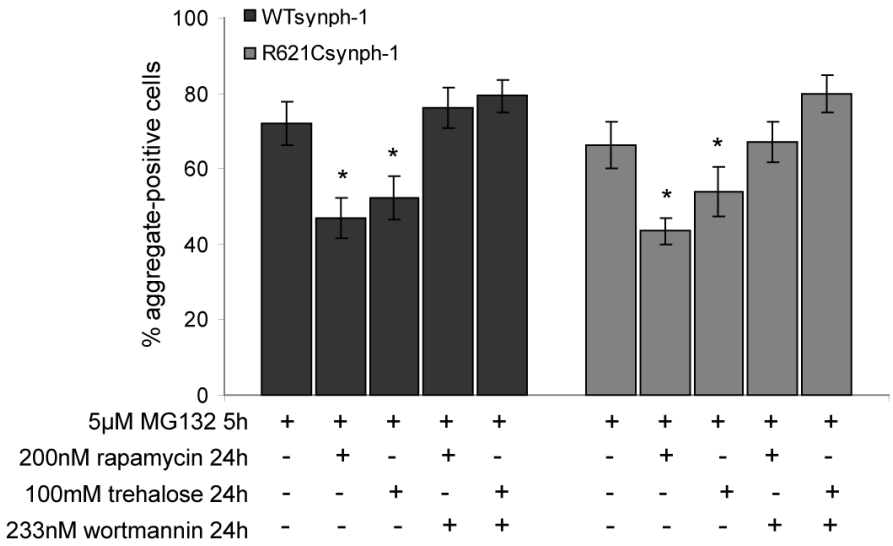

Figure 4

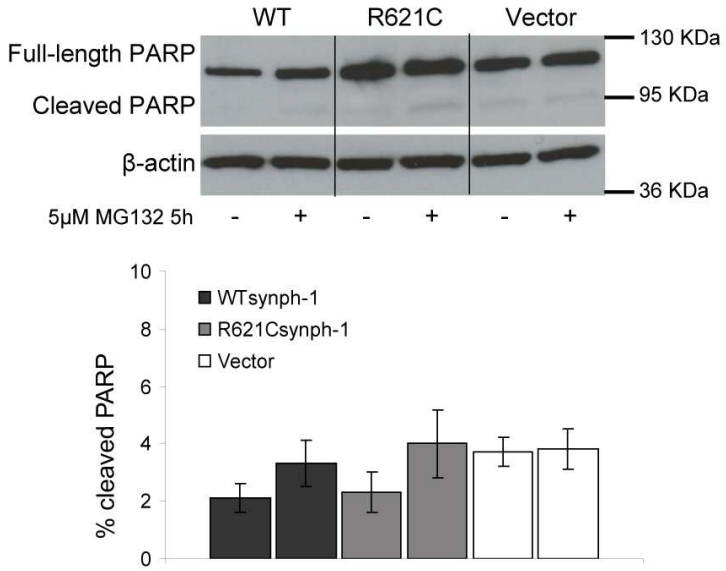

Figure 5

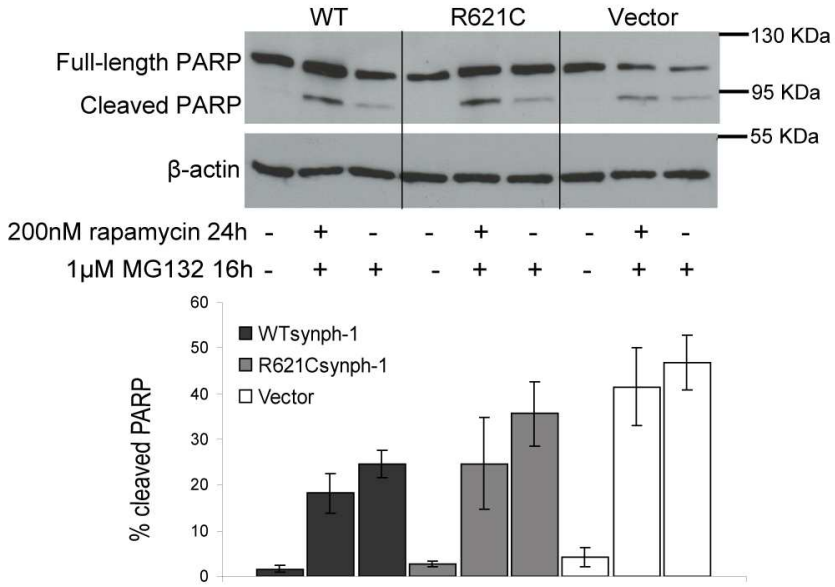
WT
R621C
Vector
Full-length PARP
Cleaved PARP
β-actin
130 KDa
95 KDa
55 KDa
200nM rapamycin 24h - + - - + - - + -
1μM MG132 16h - + + - + + - + +
% cleaved PARP
WTsynph-1
R621Csynph-1
Vector
0
10
20
30
40
50
60

Figure 6

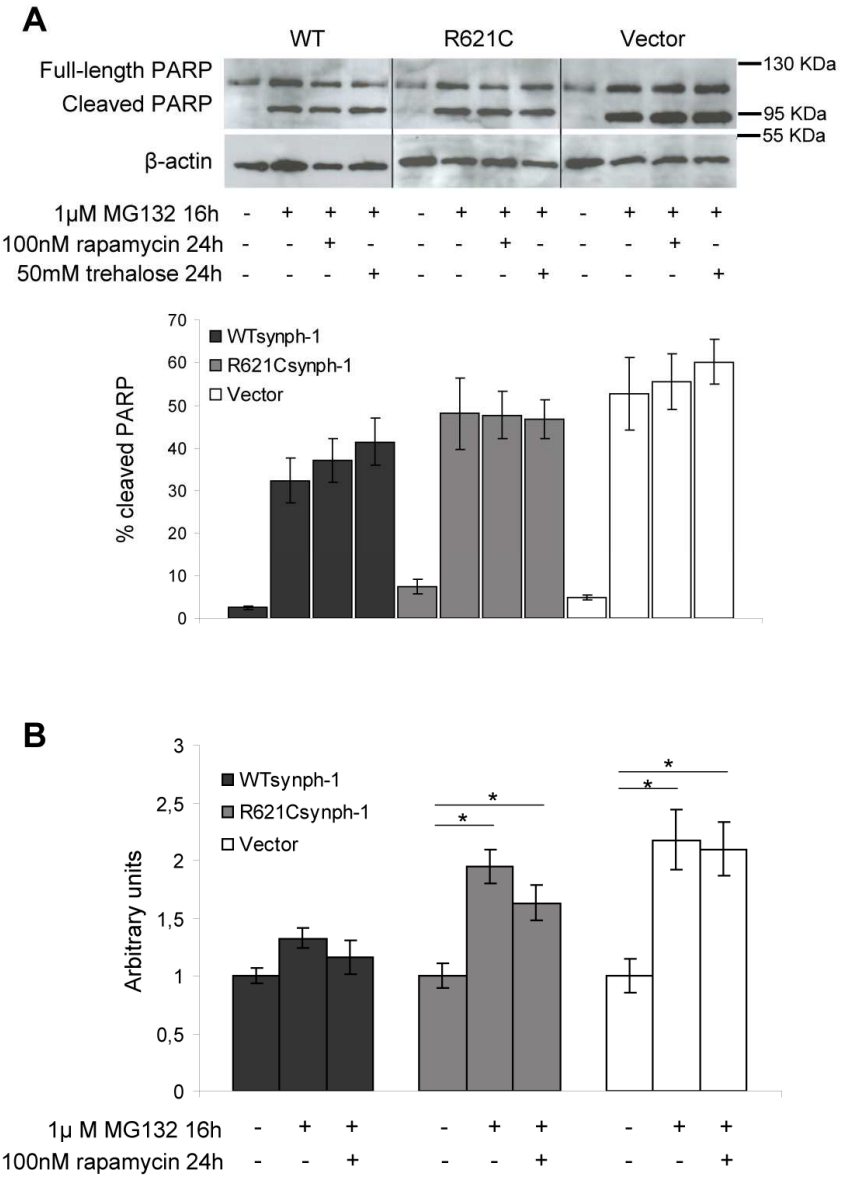
A
WT
R621C
Vector
Full-length PARP
Cleaved PARP
β-actin
130 KDa
95 KDa
55 KDa
1μM MG132 16h - + + + - + + + - + + +
100nM rapamycin 24h - - + - - - + - - - + -
50mM trehalose 24h - - - + - - - + - - - +
% cleaved PARP
WTsynph-1
R621Csynph-1
Vector
0
10
20
30
40
50
60
70
B
Arbitrary units
0
0,5
1
1,5
2
2,5
3
*
*
*
*
1μ M MG132 16h - + + - + + - + +
100nM rapamycin 24h - - + - - + - - +

Figure 7

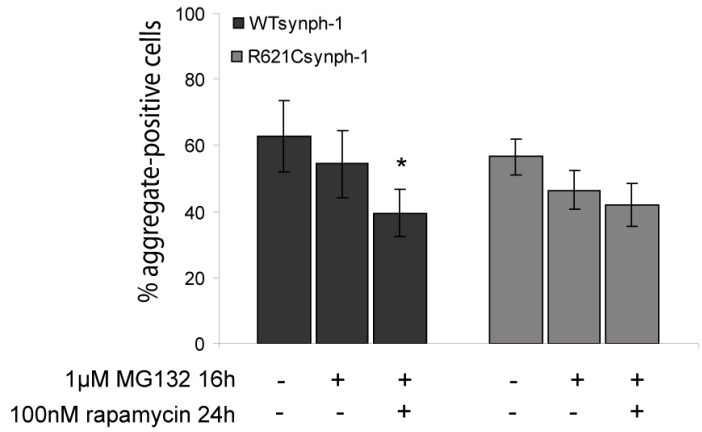
100
80
60
40
20
0
% aggregate-positive cells
WTsynph-1
R621Csynph-1
*
1μM MG132 16h - + + - + +
100nM rapamycin 24h - - + - - +

Figure 8

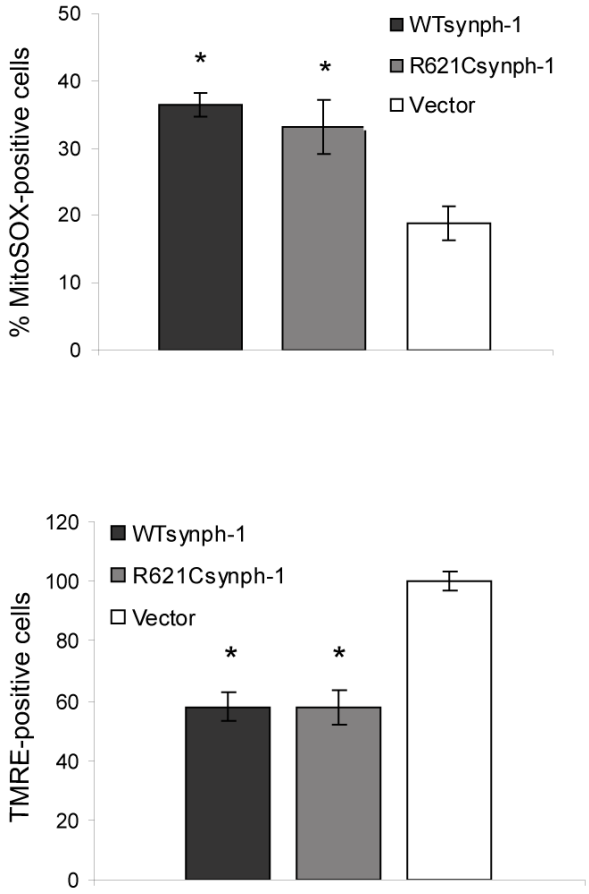
% MitoSOX-positive cells
50
40
30
20
10
0
*
*
WTsynph-1
R621Csynph-1
Vector
TMRE-positive cells
120
100
80
60
40
20
0
*
*
WTsynph-1
R621Csynph-1
Vector

Figure 9

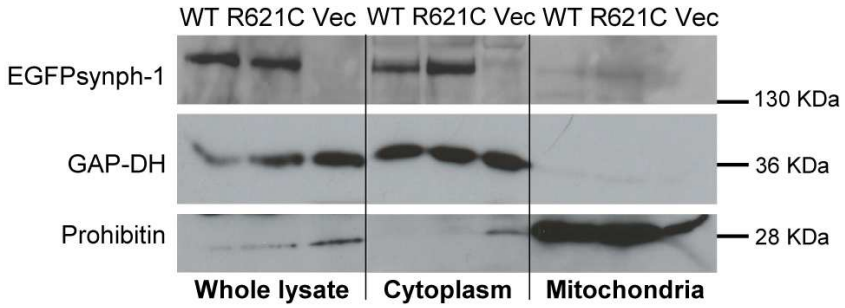

Supplementary figure 1

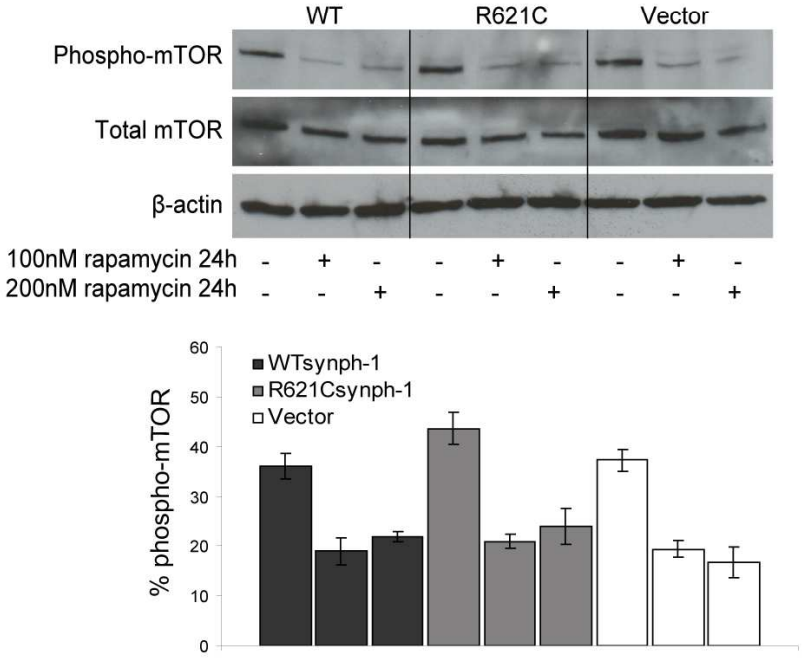

Chapter 3

Modulation of mitochondrial function and morphology by interaction of Omi/HtrA2 with the mitochondrial fusion factor OPA1

Authors:

Nicole Kieper (a,1), Kira M. Holmström (a,1), Dalila Ciceri (1), Fabienne C. Fiesel (1), Hartwig Wolburgb (2), Elena Ziviani (3), Alexander J. Whitworth (3), L. Miguel Martins (4), Philipp J. Kahle (b,1) and Rejko Krüger (b,1)

1: Center of Neurology and Hertie Institute for Clinical Brain Research, Tübingen, Germany; 2: Institute of Pathology, University of Tübingen, Tübingen, Germany; 3: Medical Research Council Centre for Developmental and Biomedical Genetics, University of Sheffield, Sheffield, UK; 4: Cell Death Regulation Laboratory, MRC Toxicology Unit, Leicester, UK

Experimental Cell Research, 2010

Footnotes:

[a] Both authors contributed equally to this work.

[b] To whom correspondence should be addressed: Center of Neurology and Hertie-Institute for Clinical Brain Research, University Clinics Tübingen, Otfried Müller Strasse 27, 72076 Tübingen, Germany. Tel.: +49-7071-2982141; Fax: +49-7071-295260; E-mail: rejko.krueger@uni-tuebingen.de or philipp.kahle@uni-tuebingen.de

Abbreviations used are:

ANT, adenine nucleotide translocator; Drp1, dynamin-related protein 1; Fis1, mitochondrial fission 1 protein; Hsp90, heat shock protein 90; HtrA2, high temperature requirement protein A2; KO, knockout; MEF, mouse embryonic fibroblast; Mfn2, mitofusin 2; MMP, mitochondrial membrane potential; PBS, phosphate-buffered saline; PD, Parkinson's disease; ROS, reactive oxygen species; SD, standard deviation; SEM, standard error of the mean; VDAC1, voltage dependent anion channel; WT, wild-type

Abstract:

Loss of Omi/HtrA2 function leads to nerve cell loss in mouse models and has been linked to neurodegeneration in Parkinson's and Huntington's disease. Omi/HtrA2 is a serine protease released as a pro-apototic factor from the mitochondrial intermembrane space into the cytosol. Under physiological conditions, Omi/HtrA2 is thought to be involved in protection against cellular stress, but the cytological and molecular mechanisms are not clear. Omi/HtrA2 deficiency caused an accumulation of reactive oxygen species and reduced mitochondrial membrane potential. In Omi/HtrA2 knockout mouse embryonic fibroblasts, as well as in Omi/HtrA2 silenced human HeLa cells and *Drosophila* S2R+ cells, we found elongated mitochondria by live cell imaging. Electron microscopy confirmed the mitochondrial morphology alterations and showed abnormal cristae sturcture. Examining the levels of proteins involved in mitochondrial fusion, we found a selective up-regulation of more soluble OPA1 protein. Complementation of knockout cells with wild-type Omi/HtrA2 but not with the protease mutant [S306A]Omi/HtrA2 reversed the mitochondrial elongation phenotype and OPA1 alterations. Finally, co-immunoprecipitation showed direct interaction of Omi/HtrA2 with endogenous OPA1. Thus, we show for the first time a direct effect of loss of Omi/HtrA2 on mitochondrial morphology and demonstrate a novel role of this mitochondrial serine protease in the modulation of OPA1. Our results underscore a critical role of impaired mitochondrial dynamics in neurodegenerative disorders.

Key words: Omi, HtrA2, mitochondria, fusion, OPA1, Parkinson's disease

Introduction:

Omi/HtrA2 (high temperature requirement protein A2) is a nuclear encoded serine protease that localizes to the mitochondrial intermembrane space, and is released into the cytosol upon apoptosis [1]. The pro-apoptotic function of the Omi/HtrA2 protease is at least partially mediated by binding and proteolytic removal of inhibitor of apoptosis proteins [2-4]. However, recent *in vivo* and *in vitro* data indicate that Omi/HtrA2 has physiological cytoprotective role(s) within the mitochondria of non-apoptotic cells. In fact, loss of Omi/HtrA2 may contribute to selective neurodegeneration [5, 6]. Loss of mitochondrial serine protease activity in *mnd2* mice, which is caused by a homozygous point mutation in the Omi/HtrA2 gene, leads to a phenotype with muscular wasting and striatal neurodegeneration [7, 8]. Like in the *mnd2* mutant mice, targeted disruption of the Omi/HtrA2 gene in mice led to progressive, severe striatal neuron loss, consequently resulting in a locomotor phenotype [6]. Finally, mutations in the Omi/HtrA2 gene have been implicated as a susceptibility factor in German and Belgian patients with sporadic Parkinson's disease (PD) [9, 10].

Recent studies in various neurodegenerative diseases have shown that altered mitochondrial function and dynamics take center stage in neuronal viability [11], particulary in PD [12]. Mitochondria are metabolically active and highly dynamic organelles that constantly undergo fusion and fission events in order to maintain integrity. This has not only implications for mitochondrial morphology, but the control of these antagonistic activities is directly linked to

mitochondrial function [13, 14]. Due to the specific energy needs of the nervous system and the non-dividing character of the implicated cell type, disturbed mitochondrial dynamics are critical for the accumulation of dysfunctional mitochondria characterized by increased production of reactive oxygen species (ROS), decreased mitochondrial membrane potential and damaged mitochondrial DNA. In this context proteins that directly modulate mitochondrial fusion have been found mutated in neurodegenerative diseases like Charcot-Marie-Tooth 2A (Mitofusin-2 (Mfn2); [15]) or autosomal-dominant optic nerve atrophy (optic atrophy protein 1 (OPA1); [16, 17]). Mutations in the OPA1 protein as well as increased proteolytic processing of OPA1 lead to impaired mitochondrial fusion and dysfunction of the organelle [18, 19]. Recently, also other PD associated genes, namely Parkin and PINK1, have been directly linked to mitochondrial homeostasis [20] and morphology [21].

Based on the critical involvement of mitochondrial function in neurodegeneration and aging processes and due to the role of mutations in the Omi/HtrA2 gene as possible susceptibility factors in PD [9, 10], we studied the consequences of loss of Omi/HtrA2 protein in fibroblasts from knockout mice [6] as well as in silenced human HeLa and *Drosophila melanogaster* S2R+ cells. We describe for the first time a role of Omi/HtrA2 in the regulation of the key fusion protein OPA1 that is linked to mitochondrial elongation.

Materials and methods:

Cell Lines and Culture

Immortalized mouse embryonic fibroblasts (MEFs) from Omi/HtrA2 knockout (KO) mice and wild type (WT) controls [6] were grown in Dulbecco's modified Eagle's medium (Invitrogen) with added 10% fetal calf serum (Perbio Science) and 1% penicillin/streptomycin (Invitrogen). Both cell lines were kept at the same passage number for experimental consistency.

Stably transfected human embryonic kidney HEK293 cells were generated using pCMV-Tag4 empty vector (Stratagene) or containing human WT Omi/HtrA2-FLAG insert [9]. HEK293 cells were transfected using Fugene6 (Roche), and positive clones selected by the continued addition of 500µg/ml G-418 (Invitrogen) to the growth medium.

A human cell line derived from cervical cancer (HeLa) was used for silencing experiments. HeLa cells were cultured in Dulbecco's modified Eagle's medium (Invitrogen) with added 10% fetal calf serum (Perbio Science). All cells were incubated in a 5 % CO_2 humidified atmosphere at 37°C.

Drosophila S2R+ cells were cultured in Schneider's medium (Invitrogen) supplemented with 5% fetal calf serum (Sigma) and 1% penicillin-streptomycin (Invitrogen-Gibco).

Stably retransfected KO MEF cells were generated using human WT or a protease dead mutant (S306A) of Omi/HtrA2 without the FLAG tag (see above) subcloned into the pcDNA 3.1/Zeo vector (Invitrogen) or empty vector as control. Omi/HtrA2 KO MEF cells were

transfected using Fugene6 (Roche), and positive clones selected by the continued addition of 500µg/ml zeocin (Invivogen) to the growth medium.

Flow Cytometry

For all flow cytometry measurements the cells were harvested using phosphate-buffered saline (PBS) with 2mM EDTA and washed once with PBS after which they were stained with appropriate dyes.

To measure levels of cellular reactive oxygen species (ROS) the cells were stained with 10µM 2',7'-dichlorohydrofluorescein diacetate (Invitrogen) in PBS for 30min at 37°C. The cells were then washed twice with PBS, resuspended in PBS and kept on ice for the measuring procedure. For each sample ~20,000 cells were measured using the 488 argon laser and emission through the FITC filter (530nm) of a CyAn flow cytometer (DakoCytomation).

To measure the levels of mitochondrial superoxide the cells were stained with 5µM MitoSOX Red (Invitrogen) in PBS for 15min at 37°C. The cells were then washed once with PBS and resuspended in PBS. For each sample ~70,000 cells were measured using the 488 argon laser and emission through the PE filter (575nm).

To measure the mitochondrial membrane potential the cells were stained with 100nm MitoTracker Green FM and Mitotracker CM-H_2XRos (Invitrogen) in PBS for 15min at 37°C. The cells were then washed once with PBS and resuspended in PBS. For each sample ~70,000 cells were measured using the 488 argon laser and emission through the PE Texas Red filter (613nm) and the FITC filter (530nm).

For all flow cytometry measurements, KO MEF cells were compared against WT MEF cells and retransfected vector controls were compared against WT Omi/HtrA2 retransfected KO cells. For measurements of mitochondrial ROS the threshold was set at about 50% of the WT signal intensity and the percentage of shift in the fluorescence activated cell sorter (FACS) staining was determined with the Summit version 4.2 software (DakoCytomation). All the presented results are the means of three independent experiments performed in duplicate and are presented as relative change compared to the WT condition.

Analysis of Mitochondrial Morphology

MEF and HeLa cells were stained 10min at 37°C with 125nM MitoTracker Green FM and Hoechst 33342 in DMEM medium (all Invitrogen). The cells were then washed once with PBS and covered with DMEM. For each cell line pictures were taken from live cells using a Cell Observer (Carl Zeiss) at 37°C and 5% CO_2. Each cell was classified into one of the following groups related to the predominant phenotype of mitochondria: elongated, middle sized or fragmented using the same criteria for each picture. For HeLa cells two categories were applicable for scoring: elongated and normal. A number of 100-150 cells were scored per experiment and each experiment was done at least in triplicate. The scoring was done by an unbiased investigator blinded to the genotype and the treatment of the cells.

For *Drosophila* mitochondrial morphology analysis, live cells were incubated with 200μM rhodamine 123 and imaged directly in growing

medium. Quantification of mitochondria length was performed using the ImageJ software as previously described [22].

RNA interference

Silencing of Omi/HtrA2 was performed with HiPerformance siRNA (Qiagen), targeting the following sequence of human Omi/HtrA2, CAGCACCTGCCGTGGTCTATA. A scrambled siRNA was used as control (Qiagen). HeLa cells were transfected with 5nM siRNA on three consecutive days using HiPerFect (Qiagen) according to manufacturer's instruction. Cells were transferred into chamberslides for immunofluorescence after the third transfection and analysed two days later. Protein expression and silencing was verified by Western blot analysis.

Double stranded RNAs were prepared using MEGA script kit (Ambion). Primers used to generate dsRNAs are available upon request. Cells were plated (1.2 x 10^6 per well) in a 6-well plate and treated with 15µg dsRNA in serum-free medium using Effectene (Qiagen). Two hours after dsRNA treatment, complete medium was added to the wells and cells were cultured for 2 days before being imaged.

Electron Microscopy

Omi/HtrA2 KO and WT MEFs were fixed in 2.5% glutaraldehyde in Hank's modified salt solution (HMSS), postfixed in 1% OsO4 in 0.1 M cacodylate buffer, scraped off, centrifuged and dehydrated in a series of ethanol. The 70% ethanol step was saturated with uranyl acetate for contrast enhancement. Dehydration was completed in

propylene oxide and the specimens were embedded in Araldite (Serva). Ultrathin sections were produced on a FCR Reichert Ultracut ultramicrotome (Leica), mounted on pioloform-coated copper grids and contrasted with lead citrate. Specimens were analyzed and documented with an EM 10A electron microscope (Zeiss). Subsequently mitochondria were counted and categorized in 50 cells of each condition.

Western Blot Analysis

Cells were harvested with 2mM EDTA in PBS and lysed with TNE (50mM Tris-HCl [pH 7.4], 150mM NaCl, 1mM EDTA and 10mM NaPP) containing 1% Triton-X (Sigma) and Complete protease inhibitor cocktail (Roche). Protein concentration was measured using Bradford solution (Bio-Rad) in a microplate reader and the protein lysate (20-35µg) was separated by SDS-PAGE. Alternatively 150 000 cells were counted, harvested and lysed directly in Laemmli SDS-PAGE sample buffer (62.5mM Tris-HCl [pH 6.8], 2% sodium dodecyl sulfate (SDS), 5% β-mercaptoethanol, 10% glycerol, 0.01% bromophenol blue) by boiling, before subjecting them to SDS-PAGE. Western blots were analyzed by antibodies against Omi/HtrA2, mitochondrial fission 1 protein (Fis1) (both from Axxora), OPA1 (BD Transduction Laboratories), mitofusin 2 (Mfn2) or β-actin (both from Sigma), adenine nucleotide transporter (ANT) or voltage dependent anion channel-1 (VDAC-1) (both from Calbiochem), prohibitin (NeoMarkers), and heat shock protein 90 (Hsp90; Stressgen).

S2R+ cells were harvested in RIPA buffer (50mM Tris-HCl [pH 7.4], 150mM NaCl,), supplemented with complete protease inhibitor cocktail (Roche). Protein concentration was measured using Bradford solution (Sigma) and the protein lysate (20-30µg) was separated by SDS-PAGE, after addition of loading buffer (50mM TrisHCl; pH 6.8, 2% SDS, 10% glycerol, 1% β-mercaptoethanol, 12.5mM EDTA, 0.02% Bromophenol Blue). Western blots were analyzed using antibodies against Omi/HtrA2 (1:1000, kindly provided by M. Martins) and anti-γ-tubulin (1:10000, Sigma). For detection secondary antibodies conjugated with HRP (Chemicon) were used (1:5000), and immunoreactivity was visualized with ECL chemiluminescence (Amersham).

For densitometric analyses of OPA1 levels on Western Blots the ImageJ software (Rasband, W.S., ImageJ, U.S. National Institutes of Health, USA, http://rsb.info.nih.gov/ij/, 1997-2007) was used. For figure 5B, OPA1 levels were normalized to the loading control and further all samples were compared to Omi/HtrA2 WT MEF levels which were set to 100%. The results represent the mean of comparison of three independent experiments. For the fold change calculation in figure 7D the densitometric analysis of the indicated band was performed for each treatment and these were compared to the untreated controls (0 min of both WT and KO).

Immunoprecipitation

For immunoprecipitation in HEK293 cells stably overexpressing Omi/HtrA2, lysates were made with an immunoprecipitation lysis buffer (50mM HEPES [pH 7.5], 10mM KCl, 50mM NaCl, 1mM

EDTA, 0.5mM EGTA, 1.5mM $MgCl_2$, 10% glycerol, 0.2% NP-40) and were incubated with anti-FLAG agarose beads (Sigma) overnight at 4°C. After 5 washes with lysis buffer the samples were analyzed by Western Blot analysis.

For immunoprecipitation from mouse brain, one hemisphere from a C57/Bl6 mouse was homogenized in homogenization buffer (50mM Tris [pH 7.5], 1% [v/v] NP-40, 2mM EDTA, 100mM NaCl and Complete protease inhibitor cocktail). 10% NP-40 (Fluka) was added and the mixture incubated on ice for 30 min. To remove cell debris the lysates were centrifuged twice after which Protein G agarose alone or pre-incubated with OPA1 antibody was added and incubated overnight at 4°C before it was washed and analyzed by Western blotting.

RT-PCR

Total mRNA was isolated from MEF cells using peqGOLD TriFast reagent following manufacturer's instructions (Peqlab) and 600ng total RNA was reverse transcribed using Transcriptor High Fidelity cDNA Synthesis Kit (Roche) and anchored oligo-dT Primer to exclude non-message RNA from reverse transcription. Two µl of RT reaction was subsequently used as template for transcript amplification in a 25 µl reaction with 5µl 5x GoTaq Buffer, 0.1µl GoTaq Polymerase (Promega) and 2µM specific primers for *OPA1* designed to amplify all isoforms (sense 5'-ACTCAGTTTATGTTCACCAC-3', antisense 5'-AGAGCACACAATATTCAAAC-3') and for *β-actin* (sense 5'-GGGTCAGAAGGACTCCTACG-3', antisense 5'-

GGTCTCAAACATGATCTGGG-3'). The annealing temperature was 48°C for *OPA1* and 52°C for *β-actin* amplification, respectively. Elongation time was 30s in both cases. Cycle number was chosen in the linear range of amplification of each transcript (27 cycles for *OPA1* and 20 cycles for *β-actin*), according to the expression level. Amplified PCR products were resolved by 1% agarose gel ectrophoresis and stained with an ethidium bromide solution (Carl Roth).

For mRNA quantification in *Drosophila* cells, total RNA was extracted using TRI Reagent (Sigma) or RNeasy Mini Kit (Qiagen) following manufacturer's instruction. Total RNA (1.5µg) was reverse-transcribed by using a random decamer primer (RETROscript kit, Ambion). Quantitative real-time PCR was performed using the SYBR Green Master Mix method (Sigma) with a Bio-Rad MyiQ system. Primers used for Omi/HtrA2: Forward- GCCCTGGCGGATAATAGTAA Reverse- GCTGCATACAGGTTAAACTAGGG and the housekeeping gene *GAPDH:* Forward- GCGAACTGAAACTGAACGAG, Reverse- CCAAATCCGTTAATTCCGAT.

Mitochondrial isolation and proteinase K digest

Omi/HtrA2 WT and KO cells were grown to 100% confluence on two 15cm plates, harvested, washed twice with PBS and re-suspended in mitochondrial isolation buffer (MIB) (250mM sucrose, 20mM HEPES [pH 7.5], 3mM EDTA and Complete protease inhibitor cocktail). The cells were disrupted by 25 passes with a glass douncer and subsequently 15 passes through a 20 Gauge needle before they were

centrifuged at 830 x *g* for 10 min. From this the supernatant was retained and the pellet resuspended in MIB and disrupted as before, and again centrifuged at 830 x *g* for 10 min. The combined supernatants were further centrifuged at 16,800 x *g* for 10 min. The supernatant was kept as the cytosolic fraction and the pellet washed twice more with MIB before resuspended in 100µl MIB. The protein concentration was measured using Bradford solution. The purity of the preparation was confirmed by immunoblot analysis. For proteinase K digest, 20µg mitochondria were subjected to 20ng proteinase K (Merck, EC 3.4.21.64) digestion at 37°C for 0, 5, 10, 20, 40 min. The reaction was stopped with 0.8µl stop solution (100mM EDTA, 40mM phenylmethyl-sulphonyl fluoride (PMSF)) before the mitochondria were spun down at 16 000g for 10 min and resuspended in PAGE sample buffer for immunoblot analysis.

Statistical Analysis

Experimental results for mitochondrial morphology were analyzed for statistical significance using the Student's T-test implemented in Microsoft Excel Software. For analysis of the mitochondrial length in *Drosophila* S2R+ cells the significance was determined by ANOVA with a Bonferroni posthoc correction. For statistical significance of the densitometrically analyzed Western blot experiments a one-way ANOVA and a Student Newman-Keuls posthoc correction was performed using GraphPad InStat version 3.00 for Windows 95 (GraphPad Software, San Diego California USA, www.graphpad.com).

Results:

Increased ROS in Omi/HtrA2 KO MEF Cells

First we analyzed the effects of Omi/HtrA2 KO on mitochondrial function and integrity. Dysfunction of mitochondria is typically reflected by disturbed oxidative phosphorylation and leads to the generation of ROS. Intramitochondrial ROS production was quantified using MitoSOX Red, a fluorogenic dye that is targeted to the mitochondria and readily oxidized by superoxide, but not by other ROS- or reactive nitrogen species–generating systems [23]. We found a significant increase in intramitochondrial ROS in MEF cells from Omi/HtrA2 KO mice compared to WT controls (Fig. 1A). Moreover total ROS levels, measured by 2',7'-dichlorohydrofluorescein diacetate conversion, were elevated. An average 15.2% ± 1.2% increase was observed in the Omi/HtrA2 KO MEFs ($p=0.0022$). These results demonstrate substantial oxidative stress occurring in MEF cells devoid of Omi/HtrA2, confirming previously published findings that show increased ROS production in immortalized Omi/HtrA2 KO MEF cells [24]. This could be related to decreased respiration, as shown previously for brain mitochondria isolated from Omi/HtrA2 KO mice [24].

Decreased Mitochondrial Membrane Potential in Omi/HtrA2 KO MEF Cells

We next examined the effects of Omi/HtrA2 knockout on the mitochondrial membrane potential (MMP). We measured the MMP by flow cytometry of cells dual-labeled with MitoTracker Green FM

and Mitotracker CM-H_2Xros (Invitrogen). As Mitotracker Green FM labels all mitochondria independently of membrane potential and Mitotracker CM-H_2XRos is only taken up into mitochondria with an intact membrane potential, a ratio between these two signals allows to determine how many of the cells counted have mitochondria with an intact membrane potential. As this method simultaneously compares mitochondria with an intact membrane potential to all mitochondria it controls for the loss of mitochondrial mass as a potential source for decreased signal. Omi/HtrA2 KO MEF showed a significant decrease in MitoTracker Red/Green signal compared to WT controls (Fig. 1B, C) indicating MMP decrease in the KO cells. These results were confirmed using TMRM as a single dye technique (data not shown), the latter being in line with previous studies [25, 26]. The consistent MMP reduction in Omi/HtrA2 KO MEF cells clearly demonstrates that Omi/HtrA2 is necessary for the maintenance of an intact MMP.

Mitochondrial Morphology Regulated by Omi/HtrA2

Recent data underscore the relevance of mitochondrial dynamics in neurodegeneration. It has been shown that mitochondrial dysfunction leading to free radical generation and loss of energy supply is involved in dynamic morphological alterations of mitochondria [11]. To monitor mitochondrial morphology in living cells we performed fluorescence microscopy based on MitoTracker green and concomitant Hoechst 33342 nuclear staining. This was performed using live cell imaging in order to avoid fixation artefacts. In Omi/HtrA2 KO cells, we found an increased proportion of cells that

display sustained, elongated, net-like structure of mitochondria (Fig. 2A-C).

Mitochondrial ultrastructure was analyzed by electron microscopy. Control MEF cells displayed typical round shaped mitochondria with well-formed cristae (Fig. 2D-F). In contrast, Omi/HtrA2 KO cells exhibited a substantial amount of mitochondria with altered morphology (Fig. 2G-I). Semiquantitative analysis revealed that 44.5% of the mitochondria in Omi/HtrA2 KO MEF cells show these alterations while only 8.6% mitochondria in Omi/HtrA2 WT MEFs have abnormal mitochondrial ultrastructure. Typical alterations were bulged, extended mitochondria, often with less inner membrane structures and no observable cristae structure, including a loss of cristae junctions. At many sites, in particular if the mitochondria were cut longitudinally, we observed a local loss of cristae, whereas the other end of the mitochondrium was still normal. If the part with the lost cristae was cross sectioned, the mitochondrium seemed to be completely devoid of folded inner membrane structures. These alterations of mitochondrial ultrastructure are consistent with the elongated morphology seen with light microscopy (Fig. 2).

To control for cell type and species specific effects, we extended our morphological studies to human HeLa cells and *Drosophila* S2R+ cells. Transient silencing of Omi/HtrA2 in HeLa cells using an siRNA approach resulted in a clear loss of the protein (Fig. 3A) and morphologically a similar phenotype as in MEF cells devoid of Omi/HtrA2, namely elongated mitochondria (Fig. 3B-D). Similarly, the transient silencing of Omi/HtrA2 in *Drosophila* S2R+ cells lead to a loss of both Omi/HtrA2 mRNA (Fig. 3E) and protein (Fig. 3F) and

an elongation of the mitochondria as measured by the length of the mitochondria (Fig. 3G-I). As a comparison, known fission and fusion genes were also silenced (Fig. 3I). The effect of Omi/HtrA2 silencing on mitochondrial morphology was comparable to the effects of silencing the established fission proteins Fis1 and the dynamin-related protein 1 (Drp1) in *Drosophila*. These results clearly underscore a well conserved role of Omi/HtrA2 in regulating mitochondrial morphology.

Mitochondrial morphology relies on Omi/HtrA2 protease function

To investigate whether the altered mitochondrial phenotype seen upon loss of Omi/HtrA2 can be reversed and whether it is dependent on the protease function of the protein, we stably transfected KO MEF cells with empty vector or a plasmid expressing human wt Omi/HtrA2 cDNA. In addition, we generated a protease dead mutant [S306A]Omi/HtrA2 [2-4] and produced the corresponding stably retransfected MEF cell lines. Indeed, retransfection of WT Omi/HtrA2 (Fig. 4A), but not an empty vector (Fig. 4B), was able to revert the mitochondrial phenotype in Omi/HtrA2 KO MEFs to a similar degree as observed in MEFs from wild type littermate controls (Fig. 2C). In contrast, the protease dead mutant was not able to normalize the elongated mitochondrial phenotype (Fig. 4C, D). Quantification of mitochondrial morphology demonstrated the statistical significance of the rescue effect by WT Omi/HtrA2 (Fig. 4D). Interestingly, the level of mitochondrial ROS could also be normalized upon re-transfection of Omi/HtrA2 wt as well as protease-dead (Fig. 4E), suggesting that the morphological phenotype is not due to increased ROS production.

Regulation of mitochondrial morphology appears to depend on Omi/HtrA2 protease activity, whereas mitochondrial ROS production could be related to another function of Omi/HtrA2.

It should be noted that the differences observed between both WT and KO as well as in the vector or wt retransfectants were not due to or did not lead to alterations in the mitochondrial mass as seen by the equal amounts of both the inner membrane protein ANT and the outer membrane protein VDAC1 (Fig. 4F). These results indicate that loss of Omi/HtrA2 leads to disturbed mitochondrial function, without changes in mitochondria mass, and can be rescued by reintroduction of physiological Omi/HtrA2 protein into the KO background.

Omi/HtrA2 Functionally and Physically Interacts with the Mitochondrial Fusion Protein OPA1

Our results suggest an involvement of Omi/HtrA2 in the regulation of mitochondrial morphology. The latter is controlled by mediators of mitochondrial fission, such as Drp1 and Fis1, and by mediators of mitochondrial fusion, such as OPA1 and mitofusins [14]. Interestingly, we discovered a selective increase of OPA1 protein levels, but not in another mitochondrial fusion protein, Mitofusin 2 (Mfn2), in Triton X-100 extracts prepared from Omi/HtrA2 KO MEF, when compared to controls (Fig. 5A). Densitometric quantification of the effect indicates a significant increase in mild detergent extractable OPA1 levels in KO cells (Fig. 5B), without affecting the relative amounts of each isoform. Consistently, we found that retransfection of KO cells with WT Omi/HtrA2 not only rescued the observed mitochondrial phenotype (Fig. 4A, D), but also reverted the increased

OPA1 levels to that seen in WT controls (Fig. 5A, B). This effect was confirmed in HeLa cells treated with Omi/HtrA2 siRNA. These cells also displayed elevated mild detergent-extractable OPA1 levels compared to control siRNA treated cells (Fig. 5C). Importantly, similar to the elongated mitochondrial phenotype, the altered OPA1 protein levels could not be rescued by re-transfection of the protease dead variant of Omi/HtrA2 into the Omi/HtrA2 KO MEF cells (Fig. 5D).

Since these findings were indicative of a functional relation between Omi/HtrA2 and OPA1, we investigated a physical interaction between these two proteins. We observed a direct interaction of overexpressed FLAG-tagged Omi/HtrA2 protein with endogenous OPA1 protein in co-immunoprecipitation experiments using HEK293 cells (Fig. 6A). Moreover, endogenous Omi/HtrA2 was also found to co-immunoprecipitate with OPA1 in lysates from mouse brain (Fig. 6B). Although some OPA1 unspecifically binds to the agarose (and consequently pulls down some Omi/HtrA2) we can detect a clear enrichment of Omi/HtrA2 in the OPA1 immunoprecipitates compared to the control without OPA1 antibody.

Omi/HtrA2 Affects a Triton X-100 Extractable and Proteinase K Labile Pool of OPA1

The effects of Omi/HtrA2 on OPA1 protein levels appeared to occur at the post-translational (protein) level. We found no difference in the mRNA levels of OPA1 between Omi/HtrA2 KO MEF and wild type controls, as determined by semi-quantitative RT-PCR of all isoforms of OPA1 (Fig. 7A).

Interestingly, loss of Omi/HtrA2 influenced preferentially a Triton X-100 soluble pool of OPA1. Under harsher detergent conditions, such as using SDS no difference between Omi/HtrA2 KO MEF cells and WT controls was observed (Fig. 7B, and results not shown). These findings suggest that Omi/HtrA2 influences the extractibility of OPA1 that may be related to the submitochondrial localization. We therefore performed limited proteolysis experiments on isolated mitochondria. This can be used to indirectly investigate the localization of proteins within the mitochondria as the proteinase K digestion consecutively digests mitochondrial proteins starting from the outer membrane. Mitochondrial fractions were derived from Omi/HtrA2 KO and control MEF cells and the relative purity of the subcellular fractions were verified by probing for VDAC1 and Hsp90 respectively (Fig. 7C). Interestingly, the accumulated longer OPA1 isoforms in the Omi/HtrA2 KO cells were degraded more rapidly (Fig. 7D). Further densitometric analysis of the higher molecular weight OPA1 band (marked with an arrow head in Fig. 7D) and the fold change compared to the untreated controls (time point 0; Fig. 7D), clearly indicates that the higher molecular weight band of OPA1 is more rapidly degraded.

Finally, we noted an increase of the small cytosolic pool of OPA1 in the Omi/HtrA2 KO MEF cells in longer exposures (Fig. 7C). Release of OPA1 has been described upon disruption of OPA1 engagement in cristae junctions [27, 28]. We propose that Omi/HtrA2 is involved in OPA1 cristae junction complex maintenance, as Omi/HtrA2 deficient cells show altered mitochondrial ultrastructure and more soluble OPA1 within mitochondria and cytosol. Some of the PK-labile OPA1 could be engaged in mitochondrial fusion, accounting for the observed

mitochondrial elongation in Omi/HtrA2 deficient cells, and the increase in soluble OPA1 release into the cytosol may promote a pre-apoptotic state in Omi/HtrA2 KO MEF cells, consistent with the presence of some activated caspase-3 under basal conditions (data not shown).

Discussion:

Loss of Omi/HtrA2 function has been linked to neurodegeneration in two different neurological disorders, namely Huntington's and Parkinson's disease. Mutations in the Omi/HtrA2 gene that reduced the serine protease activity *in vitro* were found in PD patients and genetic variants that may modulate the expression levels or the stability of Omi/HtrA2 were described in some PD populations [9, 10]. Although the role of some of these genetic variants in Omi/HtrA2 is still debated [29, 30], a potential contribution of Omi/HtrA2 to PD pathogenesis is underscored by its presence in characteristic intraneuronal protein aggregates in PD that not only contain -synuclein protein but also show a specific co-staining with Omi/HtrA2 not observed in other neurodegenerative disorders [9, 31].

Interestingly recent data support a role of loss of Omi/HtrA2 function also in Huntington's disease (HD). Transgenic animal models with overexpression of mutant huntingtin displayed reduced levels of Omi/HtrA2 in affected neurons in the striatum [5]. The relevance of this finding was confirmed in human brains of HD patients that also displayed a selective reduction of Omi/HtrA2 in affected brain regions [5]. The mechanisms how Omi/HtrA2 is involved in the neurodegenerative process are currently however unknown.

Recently altered mitochondrial dynamics were linked to neurodegeneration in PD by the functional characterization of proteins mutated in familial forms of PD (PINK1 and Parkin). Loss of PINK1 or Parkin function was related to dysregulation of the mitochondrial fusion-fission machinery with PINK1 acting upstream of Parkin [21,

32]. Omi/HtrA2 has also been found to be regulated by PINK1 [25], and recent genetic studies in *Drosophila* suggest that Omi/HtrA2 acts downstream of PINK1 but parallel to Parkin in maintaining mitochondrial integrity in *Drosophila* [33, 34]. It was shown that the loss of Omi/HtrA2 leads to a weak mitochondrial phenotype in *Drosophila*, with only mild alterations in mitochondrial integrity upon aging that correlated with progressive motor deficits in these animals [34], which was not described in an independent model [35]. Here we have studied the effects on mitochondrial morphology in Omi/HtrA2 silenced *Drosophila* cells, and found a similar mitochondrial elongation as in mammalian cells.

Our present data indicates that loss of Omi/HtrA2 function leads to changes in mitochondrial morphology by modulation of the interacting fusion protein OPA1, in a mammalian system. Thereby our study provides first mechanistic insight into the physiological role of Omi/HtrA2 in the regulation of mitochondrial dynamics and maintenance of mitochondrial homeostasis and supports the pathogenic relevance of loss of Omi/HtrA2 function in neurodegeneration. The observed interaction of Omi/HtrA2 with OPA1 extends this link to the molecular level and reveals a novel role of Omi/HtrA2 in balancing mitochondrial fusion-fission dynamics. Importantly, the role of Omi/HtrA2 in the regulation of mitochondrial morphology and the effects of the loss of the protein are not transient as we observe the same mitochondrial phenotype in both a models of genetic ablation of Omi/HtrA2, as well as upon transient knock down of the protein. This contrasts with the situation where PINK1 is deleted, where the time point selected for analysis seems crucial for

observing changes in mitochondrial morphology [36]. Furthermore, we showed that the role of Omi/HtrA2 as a modulator of mitochondrial morphology is highly conserved as these effects are independent of cell type and species. In addition, we could clearly show that this is dependent on the serine protease activity of Omi/HtrA2.

In our study, loss of Omi/HtrA2 function was not only related to elongated mitochondrial morphology seen by light microscopy (Fig. 2), but also with differential extractability of the interacting protein OPA1. Remarkably, Omi/HtrA2 appears to influence preferentially a Triton-soluble, proteinase K labile pool of OPA1 protein (Fig. 5 and 7). Further, as OPA1 is known to play a role in maintenance of the inner membrane structure [27, 37], and we see a loss of cristae and cristae junction structures in the KO MEFs (Fig. 2), it is tempting to speculate that the easier extractable material observed represents OPA1 not engaged in the tight complex that seals mitochondrial cristae junctions. Disruption of cristae junctions leads to some cytosolic release of OPA1 [27, 28], and indeed we observe an elevation of a small cytosolic pool of OPA1 specifically in Omi/HtrA2 KO MEF cells. We therefore speculate that Omi/HtrA2 might influence the mitochondrial inner membrane structures and fusion by modulating the localisation of OPA1 to either the cristae junctions or the potentially more easily extractable fusion complex.

Here we present evidence that Omi/HtrA2 is a critical factor for the maintenance of mitochondrial integrity and that loss of Omi/HtrA2 function leads to dysfunctional mitochondria. Indeed, we found that Omi/HtrA2 KO MEFs display an elongated mitochondrial phenotype

and impaired mitochondrial function as indicated by increased ROS levels and reduced mitochondrial membrane potential. Interestingly, the increased ROS levels, unlike the morphology do not seem dependent on protease function, suggesting that these are two separate events but both dependent on the presence of Omi/HtrA2. This also suggests that the increased ROS levels are not the cause of the elongated mitochondria seen in cells devoid of Omi/HtrA2.

In summary we identified for the first time a direct interaction of Omi/HtrA2 with OPA1, a regulatory component of the mitochondrial fusion machinery, and demonstrate consequences of loss of Omi/HtrA2 function on mitochondrial dynamics and integrity that are relevant for different neurodegenerative disorders like Parkinson's and Huntington's disease.

Acknowledgements:

This work was supported by the German Research Council (DFG; KR2119/3-1 to R.K.), German National Genome Research Network (NGFNplus to P.J.K. and R.K.), the Hertie Foundation, the MEFOPA project funded through the European Union research program FP7 (P.J.K. and A.J.W.), and grants from the Wellcome Trust (081987) and the Parkinson's Disease Society (G-0713) (to A.J.W). K. H. is a NEUROTRAIN Early Stage Research Training fellow funded through the European Union research program FP6. We thank Thomas Gasser for support. The authors declare no conflict of interest.

References:

[1] L. Vande Walle, M. Lamkanfi, P. Vandenabeele, The mitochondrial serine protease HtrA2/Omi: an overview, Cell death and differentiation 15 (2008) 453-460.

[2] R. Hegde, S.M. Srinivasula, Z. Zhang, R. Wassell, R. Mukattash, L. Cilenti, G. DuBois, Y. Lazebnik, A.S. Zervos, T. Fernandes-Alnemri, E.S. Alnemri, Identification of Omi/HtrA2 as a mitochondrial apoptotic serine protease that disrupts inhibitor of apoptosis protein-caspase interaction, The Journal of biological chemistry 277 (2002) 432-438.

[3] L.M. Martins, I. Iaccarino, T. Tenev, S. Gschmeissner, N.F. Totty, N.R. Lemoine, J. Savopoulos, C.W. Gray, C.L. Creasy, C. Dingwall, J. Downward, The serine protease Omi/HtrA2 regulates apoptosis by binding XIAP through a reaper-like motif, The Journal of biological chemistry 277 (2002) 439-444.

[4] A.M. Verhagen, J. Silke, P.G. Ekert, M. Pakusch, H. Kaufmann, L.M. Connolly, C.L. Day, A. Tikoo, R. Burke, C. Wrobel, R.L. Moritz, R.J. Simpson, D.L. Vaux, HtrA2 promotes cell death through its serine protease activity and its ability to antagonize inhibitor of apoptosis proteins, The Journal of biological chemistry 277 (2002) 445-454.

[5] R. Inagaki, K. Tagawa, M.L. Qi, Y. Enokido, H. Ito, T. Tamura, S. Shimizu, K. Oyanagi, N. Arai, I. Kanazawa, E.E. Wanker, H. Okazawa, Omi / HtrA2 is relevant to the selective

vulnerability of striatal neurons in Huntington's disease, The European journal of neuroscience 28 (2008) 30-40.

[6] L.M. Martins, A. Morrison, K. Klupsch, V. Fedele, N. Moisoi, P. Teismann, A. Abuin, E. Grau, M. Geppert, G.P. Livi, C.L. Creasy, A. Martin, I. Hargreaves, S.J. Heales, H. Okada, S. Brandner, J.B. Schulz, T. Mak, J. Downward, Neuroprotective role of the Reaper-related serine protease HtrA2/Omi revealed by targeted deletion in mice, Molecular and cellular biology 24 (2004) 9848-9862.

[7] J.M. Jones, P. Datta, S.M. Srinivasula, W. Ji, S. Gupta, Z. Zhang, E. Davies, G. Hajnoczky, T.L. Saunders, M.L. Van Keuren, T. Fernandes-Alnemri, M.H. Meisler, E.S. Alnemri, Loss of Omi mitochondrial protease activity causes the neuromuscular disorder of mnd2 mutant mice, Nature 425 (2003) 721-727.

[8] S. Rathke-Hartlieb, U. Schlomann, P. Heimann, M.H. Meisler, H. Jockusch, J.W. Bartsch, Progressive loss of striatal neurons causes motor dysfunction in MND2 mutant mice and is not prevented by Bcl-2, Experimental neurology 175 (2002) 87-97.

[9] K.M. Strauss, L.M. Martins, H. Plun-Favreau, F.P. Marx, S. Kautzmann, D. Berg, T. Gasser, Z. Wszolek, T. Muller, A. Bornemann, H. Wolburg, J. Downward, O. Riess, J.B. Schulz, R. Kruger, Loss of function mutations in the gene encoding Omi/HtrA2 in Parkinson's disease, Human molecular genetics 14 (2005) 2099-2111.

[10] V. Bogaerts, K. Nuytemans, J. Reumers, P. Pals, S. Engelborghs, B. Pickut, E. Corsmit, K. Peeters, J. Schymkowitz, P.P. De Deyn, P. Cras, F. Rousseau, J. Theuns, C. Van Broeckhoven, Genetic variability in the mitochondrial serine protease HTRA2 contributes to risk for Parkinson disease, Human mutation 29 (2008) 832-840.

[11] W. Mandemakers, V.A. Morais, B. De Strooper, A cell biological perspective on mitochondrial dysfunction in Parkinson disease and other neurodegenerative diseases, Journal of cell science 120 (2007) 1707-1716.

[12] V.S. Van Laar, S.B. Berman, Mitochondrial dynamics in Parkinson's disease, Experimental neurology 218 (2009) 247-256.

[13] S. Lee, S.Y. Jeong, W.C. Lim, S. Kim, Y.Y. Park, X. Sun, R.J. Youle, H. Cho, Mitochondrial fission and fusion mediators, hFis1 and OPA1, modulate cellular senescence, The Journal of biological chemistry 282 (2007) 22977-22983.

[14] K.L. Cerveny, Y. Tamura, Z. Zhang, R.E. Jensen, H. Sesaki, Regulation of mitochondrial fusion and division, Trends in cell biology 17 (2007) 563-569.

[15] K. Kijima, C. Numakura, H. Izumino, K. Umetsu, A. Nezu, T. Shiiki, M. Ogawa, Y. Ishizaki, T. Kitamura, Y. Shozawa, K. Hayasaka, Mitochondrial GTPase mitofusin 2 mutation in Charcot-Marie-Tooth neuropathy type 2A, Human genetics 116 (2005) 23-27.

[16] C. Delettre, G. Lenaers, J.M. Griffoin, N. Gigarel, C. Lorenzo, P. Belenguer, L. Pelloquin, J. Grosgeorge, C. Turc-Carel, E.

Perret, C. Astarie-Dequeker, L. Lasquellec, B. Arnaud, B. Ducommun, J. Kaplan, C.P. Hamel, Nuclear gene OPA1, encoding a mitochondrial dynamin-related protein, is mutated in dominant optic atrophy, Nature genetics 26 (2000) 207-210.

[17] C. Alexander, M. Votruba, U.E. Pesch, D.L. Thiselton, S. Mayer, A. Moore, M. Rodriguez, U. Kellner, B. Leo-Kottler, G. Auburger, S.S. Bhattacharya, B. Wissinger, OPA1, encoding a dynamin-related GTPase, is mutated in autosomal dominant optic atrophy linked to chromosome 3q28, Nature genetics 26 (2000) 211-215.

[18] C. Zanna, A. Ghelli, A.M. Porcelli, M. Karbowski, R.J. Youle, S. Schimpf, B. Wissinger, M. Pinti, A. Cossarizza, S. Vidoni, M.L. Valentino, M. Rugolo, V. Carelli, OPA1 mutations associated with dominant optic atrophy impair oxidative phosphorylation and mitochondrial fusion, Brain 131 (2008) 352-367.

[19] S. Duvezin-Caubet, R. Jagasia, J. Wagener, S. Hofmann, A. Trifunovic, A. Hansson, A. Chomyn, M.F. Bauer, G. Attardi, N.G. Larsson, W. Neupert, A.S. Reichert, Proteolytic processing of OPA1 links mitochondrial dysfunction to alterations in mitochondrial morphology, The Journal of biological chemistry 281 (2006) 37972-37979.

[20] D. Narendra, A. Tanaka, D.F. Suen, R.J. Youle, Parkin-induced mitophagy in the pathogenesis of Parkinson disease, Autophagy 5 (2009).

[21] N. Exner, B. Treske, D. Paquet, K. Holmstrom, C. Schiesling, S. Gispert, I. Carballo-Carbajal, D. Berg, H.H. Hoepken, T.

Gasser, R. Kruger, K.F. Winklhofer, F. Vogel, A.S. Reichert, G. Auburger, P.J. Kahle, B. Schmid, C. Haass, Loss-of-function of human PINK1 results in mitochondrial pathology and can be rescued by parkin, J Neurosci 27 (2007) 12413-12418.

[22] K.J. De Vos, M.P. Sheetz, Visualization and quantification of mitochondrial dynamics in living animal cells, Methods in cell biology 80 (2007) 627-682.

[23] P. Mukhopadhyay, M. Rajesh, K. Yoshihiro, G. Hasko, P. Pacher, Simple quantitative detection of mitochondrial superoxide production in live cells, Biochemical and biophysical research communications 358 (2007) 203-208.

[24] N. Moisoi, K. Klupsch, V. Fedele, P. East, S. Sharma, A. Renton, H. Plun-Favreau, R.E. Edwards, P. Teismann, M.D. Esposti, A.D. Morrison, N.W. Wood, J. Downward, L.M. Martins, Mitochondrial dysfunction triggered by loss of HtrA2 results in the activation of a brain-specific transcriptional stress response, Cell death and differentiation 16 (2009) 449-464.

[25] H. Plun-Favreau, K. Klupsch, N. Moisoi, S. Gandhi, S. Kjaer, D. Frith, K. Harvey, E. Deas, R.J. Harvey, N. McDonald, N.W. Wood, L.M. Martins, J. Downward, The mitochondrial protease HtrA2 is regulated by Parkinson's disease-associated kinase PINK1, Nature cell biology 9 (2007) 1243-1252.

[26] S. Krick, S. Shi, W. Ju, C. Faul, S.Y. Tsai, P. Mundel, E.P. Bottinger, Mpv17l protects against mitochondrial oxidative stress and apoptosis by activation of Omi/HtrA2 protease,

Proceedings of the National Academy of Sciences of the United States of America 105 (2008) 14106-14111.

[27] C. Frezza, S. Cipolat, O. Martins de Brito, M. Micaroni, G.V. Beznoussenko, T. Rudka, D. Bartoli, R.S. Polishuck, N.N. Danial, B. De Strooper, L. Scorrano, OPA1 controls apoptotic cristae remodeling independently from mitochondrial fusion, Cell 126 (2006) 177-189.

[28] D. Zhang, C. Lu, M. Whiteman, B. Chance, J.S. Armstrong, The mitochondrial permeability transition regulates cytochrome c release for apoptosis during endoplasmic reticulum stress by remodeling the cristae junction, The Journal of biological chemistry 283 (2008) 3476-3486.

[29] J. Simon-Sanchez, A.B. Singleton, Sequencing analysis of OMI/HTRA2 shows previously reported pathogenic mutations in neurologically normal controls, Human molecular genetics 17 (2008) 1988-1993.

[30] O.A. Ross, A.I. Soto, C. Vilarino-Guell, M.G. Heckman, N.N. Diehl, M.M. Hulihan, J.O. Aasly, S. Sando, J.M. Gibson, T. Lynch, A. Krygowska-Wajs, G. Opala, M. Barcikowska, K. Czyzewski, R.J. Uitti, Z.K. Wszolek, M.J. Farrer, Genetic variation of Omi/HtrA2 and Parkinson's disease, Parkinsonism & related disorders 14 (2008) 539-543.

[31] Y. Kawamoto, Y. Kobayashi, Y. Suzuki, H. Inoue, H. Tomimoto, I. Akiguchi, H. Budka, L.M. Martins, J. Downward, R. Takahashi, Accumulation of HtrA2/Omi in neuronal and glial inclusions in brains with alpha-

synucleinopathies, Journal of neuropathology and experimental neurology 67 (2008) 984-993.

[32] A.C. Poole, R.E. Thomas, L.A. Andrews, H.M. McBride, A.J. Whitworth, L.J. Pallanck, The PINK1/Parkin pathway regulates mitochondrial morphology, Proceedings of the National Academy of Sciences of the United States of America 105 (2008) 1638-1643.

[33] A.J. Whitworth, J.R. Lee, V.M. Ho, R. Flick, R. Chowdhury, G.A. McQuibban, Rhomboid-7 and HtrA2/Omi act in a common pathway with the Parkinson's disease factors Pink1 and Parkin, Disease models & mechanisms 1 (2008) 168-174; discussion 173.

[34] L.S. Tain, R.B. Chowdhury, R.N. Tao, H. Plun-Favreau, N. Moisoi, L.M. Martins, J. Downward, A.J. Whitworth, N. Tapon, Drosophila HtrA2 is dispensable for apoptosis but acts downstream of PINK1 independently from Parkin, Cell death and differentiation (2009).

[35] J. Yun, J.H. Cao, M.W. Dodson, I.E. Clark, P. Kapahi, R.B. Chowdhury, M. Guo, Loss-of-function analysis suggests that Omi/HtrA2 is not an essential component of the PINK1/PARKIN pathway in vivo, J Neurosci 28 (2008) 14500-14510.

[36] A.K. Lutz, N. Exner, M.E. Fett, J.S. Schlehe, K. Kloos, K. Lammermann, B. Brunner, A. Kurz-Drexler, F. Vogel, A.S. Reichert, L. Bouman, D. Vogt-Weisenhorn, W. Wurst, J. Tatzelt, C. Haass, K.F. Winklhofer, Loss of parkin or PINK1 function increases Drp1-dependent mitochondrial

fragmentation, The Journal of biological chemistry 284 (2009) 22938-22951.

[37] R. Yamaguchi, L. Lartigue, G. Perkins, R.T. Scott, A. Dixit, Y. Kushnareva, T. Kuwana, M.H. Ellisman, D.D. Newmeyer, Opa1-mediated cristae opening is Bax/Bak and BH3 dependent, required for apoptosis, and independent of Bak oligomerization, Molecular cell 31 (2008) 557-569.

Figure legends:

Fig 1. Analysis of ROS levels and mitochondrial membrane potential in Omi/HtrA2 WT and KO MEF cells. (A) Mitochondrial ROS levels were analyzed by staining with the fluorescent dye MitoSOX. (* $p<0.006$). (B, C) MMP was determined by a double staining with Mitotracker GreenFM and Mitotracker CM-H_2XRos. (B) The ratio of Mitotracker GreenFM to Mitotracker CM-H_2XRos staining was measured as a readout for mitochondrial membrane potential (MMP) (* $p<0.003$). (C) Scattergraph representative of an Omi/HtrA2 WT (left graph) and KO (right graph) MEF MMP measurement. The selected area in blue represents the measured cells with intact MMP. The loss of signal in the marked area indicates a decrease in MMP. All results are given as relative comparisons to WT. The results represent the mean of three independent experiments. Error bars show the standard deviation (SD).

Fig 2. Effects of Omi/HtrA2 on mitochondrial morphology in MEF cells. (A, B) Live Omi/HtrA2 WT (A) and KO (B) MEF cells were concomitantly stained with Mitotracker GreenFM and Hoechst 33342 for 10min. Size bar corresponds to 10µm. (C) Mitochondrial morphology was classified into 3 categories: elongated, middle sized and fragmented. The results are shown as the percentage of WT (dark bars) and KO (light bars) cells with mitochondria falling into these categories as scored by an observer blinded to the MEF cell genotype (* $p<0.05$). Error bars show the SD. (D-I) Electron microscopy shows that mitochondria in MEF KO cells (G-I) differed from control MEF

WT cells (D-F) by failure to form elaborated cristae structures. Examples of mitochondria with a local loss of cristae structures (arrow in H and I) or a complete loss of folded inner membrane structures (asterisk in H and arrow in G).

Fig 3. Mitochondrial morphology in Omi/HtrA2 silenced HeLa and S2R+ cells. (A) Treatment of HeLa cells with Omi/HtrA2 siRNA greatly reduced the levels of Omi/HtrA2 protein compared to non-transfected (-) and control siRNA treated cells (ctrl). Re-probing the Western blot for β-actin confirmed equal loading. (B-D) The mitochondrial morphology was investigated in HeLa cells transfected with control siRNA (B) or Omi/HtrA2 siRNA (C). The mitochondria were scored in each cell as either elongated or normal and quantified (D). Error bars show the SD; * $p<0.005$. Size bar corresponds to 10µm. (E) Quantitative real-time PCR measurement of *Omi/HtrA2* knockdown in S2R+ cells compared to control. (F) Western blot of Omi/HtrA2 levels in S2R+ control and Omi/HtrA2 dsRNA treated cells. γ-Tubulin was used as a loading control. (G-I) S2R+ cells treated with control (ctrl) (G) or *Omi/HtrA2* (H) dsRNAs stained with mitochondrial dye rhodamine123 dye. Size bars correspond to 5µm. (I) Mitochondrial length was quantified and compared to knock down of known fission and fusion factors (Mfn/Marf, OPA1, Drp1, Fis1) (** $P<0.01$, *** $P<0.001$). Error bars show the standard error of the mean (SEM).

Fig 4. Retransfection of KO MEFs with human WT Omi/HtrA2 rescues the phenotype. (A-D) The mitochondrial morphology of

Omi/HtrA2 KO MEF cells stably overexpressing either human WT Omi/HtrA2 (A), empty vector (B) or a synthetic protease dead mutant of Omi/HtrA2 (C) was investigated using the same procedure as in Fig. 2. Size bar corresponds to 10µm. In the quantification (D) error bars indicate the SEM (* $p<0.05$). (E) Stably retransfected MEF cells were stained with the fluorescent dye MitoSOX to investigate the levels of intramitochondrial ROS. The procedure was the same as was used for the WT and KO cells. The result is the mean of three independent experiments and a relative comparison of Omi/HtrA2 KO retransfected with vector compared to those retransfected with WT or S306A Omi/HtrA2, where WT was set to 1 (* $p<0.06$). Error bars indicate the SD. (F) WT and KO MEF cells as well as KO MEFs retransfected with either WT Omi/HtrA2 or empty vector were lysed with 1% Triton X-100 in TNE. The stable overexpression of human Omi/HtrA2 leads to expression of an ≈50kDa precursor that is efficiently processed to the ≈35kDa mature form co-migrating with the endogenous Omi/HtrA2, which is completely absent in KO MEF cells and vector controls when analyzed by Western blot. To investigate whether there is a change in the mitochondrial membrane mass, the relative amounts of the outer membrane protein VDAC and inner membrane protein ANT were also probed. β-Actin was used as a loading control.

Fig 5. Effects of Omi/HtrA2 on OPA1 protein levels in mouse and human cell lines. (A, B) Omi/HtrA2 WT and KO MEF cells, as well as with WT Omi/HtrA2 and vector stably re-transfected KO cells, were lysed with 1% Triton X-100 in buffer and subjected to

immunoblotting. (A) Western blots were probed for the mitochondrial fusion protein OPA1 and Mfn2. β-Actin was used as a loading control. (B) Densitometric analysis of OPA1 band intensities, after 1% Triton X-100 in TNE extraction, in three independent experiments is depicted here (n.s.= not significant, * $p<0.05$, ** $p<0.01$). Error bars indicate the SD. (C) Effects of Omi/HtrA2 on OPA1 levels were reproduced in HeLa cells. The silencing efficiency as well as the corresponding changes in OPA1 levels were detected in untreated, control or Omi/HtrA2 silenced HeLa cells lysed with 1% Triton X-100 in buffer and subjected to Western blot analysis using antibodies against OPA1, Omi/HtrA2 and β-actin as a loading control. (D) Omi/HtrA2 KO and WT MEF cells were stably retransfected with either control vector, wt or a protease dead from of Omi/HtrA2 (S306A), and the cells were cells lysed with 1% Triton X-100 buffer and subjected to Western blot analysis using antibodies against OPA1, Omi/HtrA2 and β-actin as a loading control.

Fig 6. Omi/HtrA2 physically interacts with OPA1. (A) HEK293 cells were stably transfected with FLAG-tagged Omi/HtrA2 (+) while untransfected cells (-) were used as controls. Lysates were subjected to Western blot analysis directly (inputs) or after incubation over night with anti-FLAG coupled agarose. Immunoblots were probed with anti-OPA1 and anti-Omi/HtrA2 as indicated. The asterisk marks the recombinant form of Omi/HtrA2. The input sample was taken before adding the agarose. (B) Co-immunoprecipitation of endogenous Omi/HtrA2 and OPA1 in lysates from C57/Bl6 mouse brain. Lysates were subjected to Western blot analysis directly (inputs) or after

incubation overnight with either protein G agarose alone (-) or with anti-OPA1 bound to protein G agarose (+). Immunoblots were probed with anti-OPA1 and anti-Omi/HtrA2 as indicated.

Fig 7. Differences in OPA1 levels are due to protein accessibility. (A) Semi-quantitative RT-PCR was performed on mRNA isolated from Omi/HtrA2 WT or KO and re-transfected MEF cells. There are no differences in the *OPA1* mRNA levels (upper panel). Amplification of *β-actin* served as loading control (lower panel). (B) For analysis of the full cell content, 150 000 control and Omi/HtrA2 KO MEF cells were harvested, lysed directly in Laemmli SDS-PAGE sample buffer and analyzed by Western blot. Immunoblots were probed with anti-OPA1 (short and long exposure), anti-Omi/HtrA2 and β-actin was used as a loading control. (C) Mitochondrial and cytosolic fractions prepared from Omi/HtrA2 WT and KO cells were subjected to Western blotting and analyzed for localisation of both OPA1 and Omi/HtrA2. The purity of the cytosolic (Cyto) and mitochondrial (Mito) fractions was assessed by probing for Hsp90 and VDAC1 respectively. (D) Mitochondria isolated from control (left lanes) or Omi/HtrA2 KO (right lanes) MEF cells were subjected to proteinase K digestion for indicated time points. Western blots were prepared and probed with anti-OPA1 and anti-Omi/HtrA2 as indicated. The outer membrane associated protein Fis1 was rapidly degraded whereas the inner membrane protein prohibitin was shielded. The higher molecular weight OPA1 band densitometrically analysed (arrow head) is indicated and the fold change compared to untreated (time point 0) is shown below the Western blot (D).

Figure 1

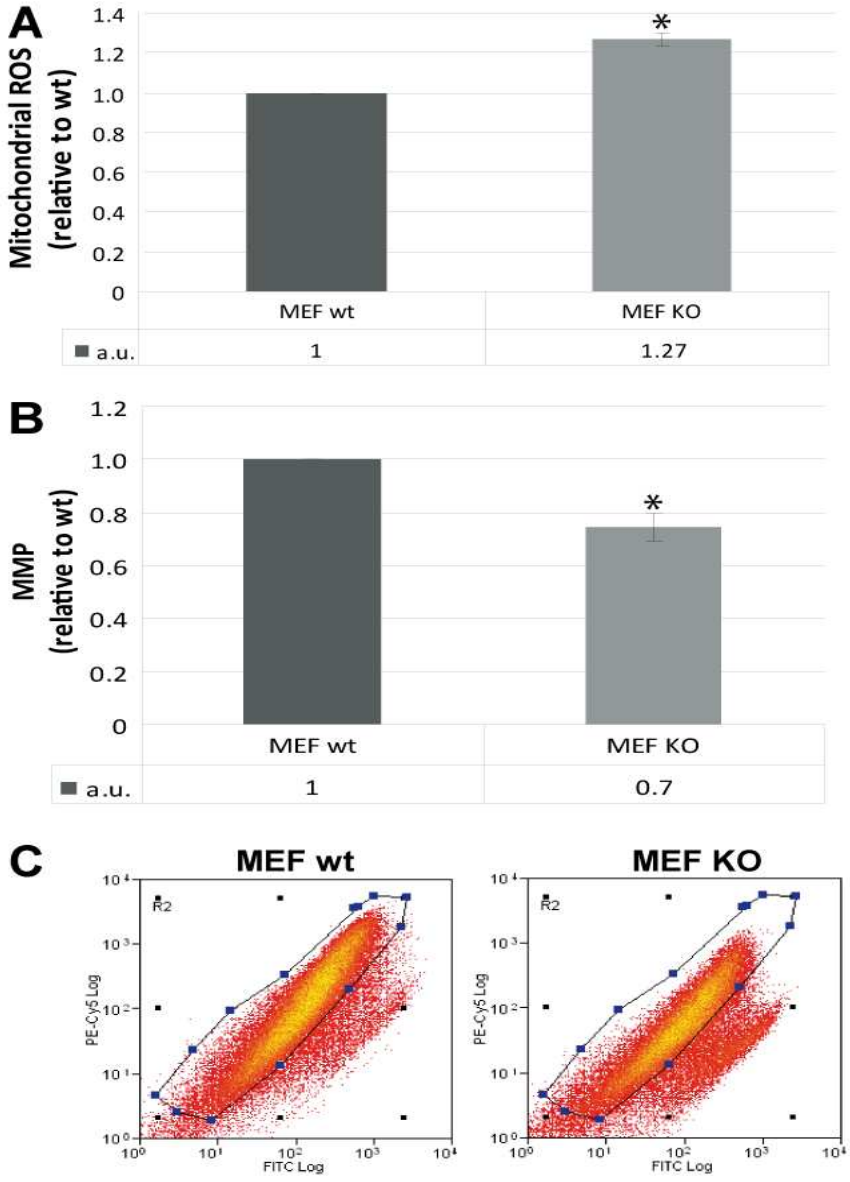
A
Mitochondrial ROS (relative to wt)
1.4
1.2
1.0
0.8
0.6
0.4
0.2
0
*
MEF wt
MEF KO
a.u.
1
1.27
B
MMP (relative to wt)
1.2
1.0
0.8
0.6
0.4
0.2
0
*
MEF wt
MEF KO
a.u.
1
0.7
C
MEF wt
MEF KO
R2
PE-Cy5 Log
FITC Log

Figure 2

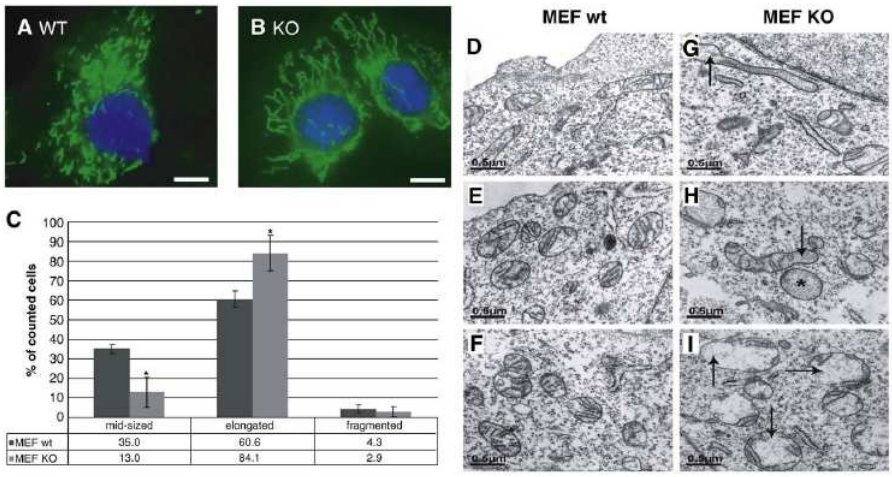
A WT
B KO
C
% of counted cells
100
90
80
70
60
50
40
30
20
10
0
mid-sized
elongated
fragmented
MEF wt 35.0 60.6 4.3
MEF KO 13.0 84.1 2.9
MEF wt
MEF KO
D
E
F
G
H
I
0.5µm

Figure 3

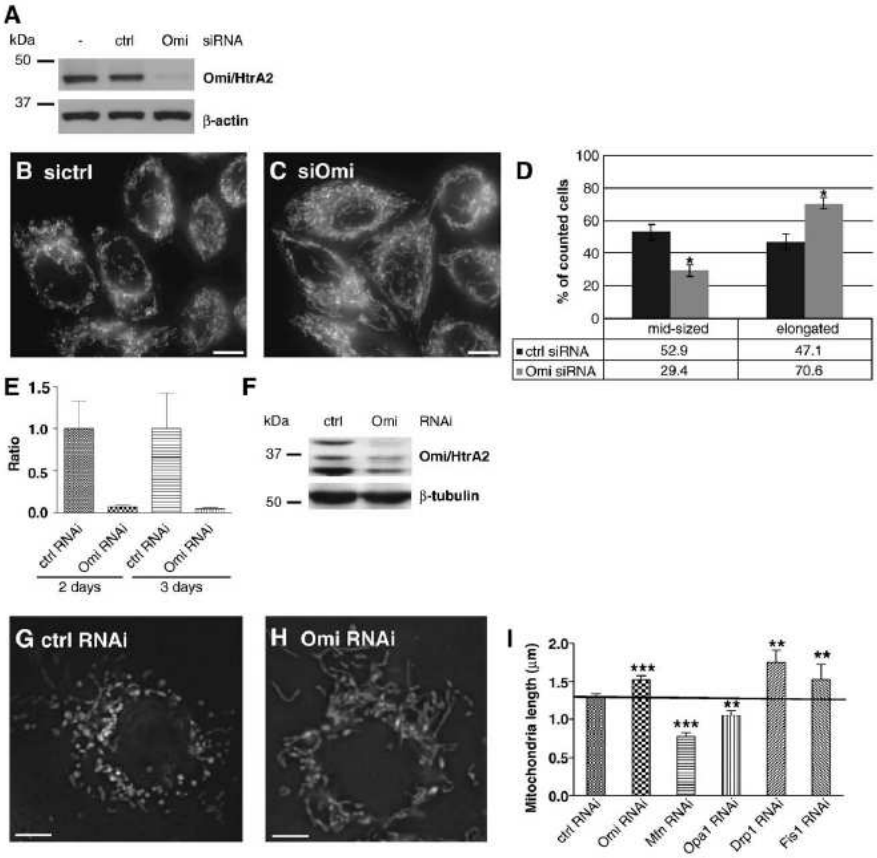
A
kDa
-
ctrl
Omi
siRNA
50
Omi/HtrA2
37
β-actin
B sictrl
C siOmi
D
% of counted cells
100
80
60
40
20
0
mid-sized
elongated
ctrl siRNA
52.9
47.1
Omi siRNA
29.4
70.6
E
Ratio
1.5
1.0
0.5
0.0
ctrl RNAi
Omi RNAi
ctrl RNAi
Omi RNAi
2 days
3 days
F
kDa
ctrl
Omi
RNAi
37
Omi/HtrA2
50
β-tubulin
G ctrl RNAi
H Omi RNAi
I
Mitochondria length (μm)
2.0
1.5
1.0
0.5
0.0
ctrl RNAi
Omi RNAi
Mfn RNAi
Opa1 RNAi
Drp1 RNAi
Fis1 RNAi

Figure 4

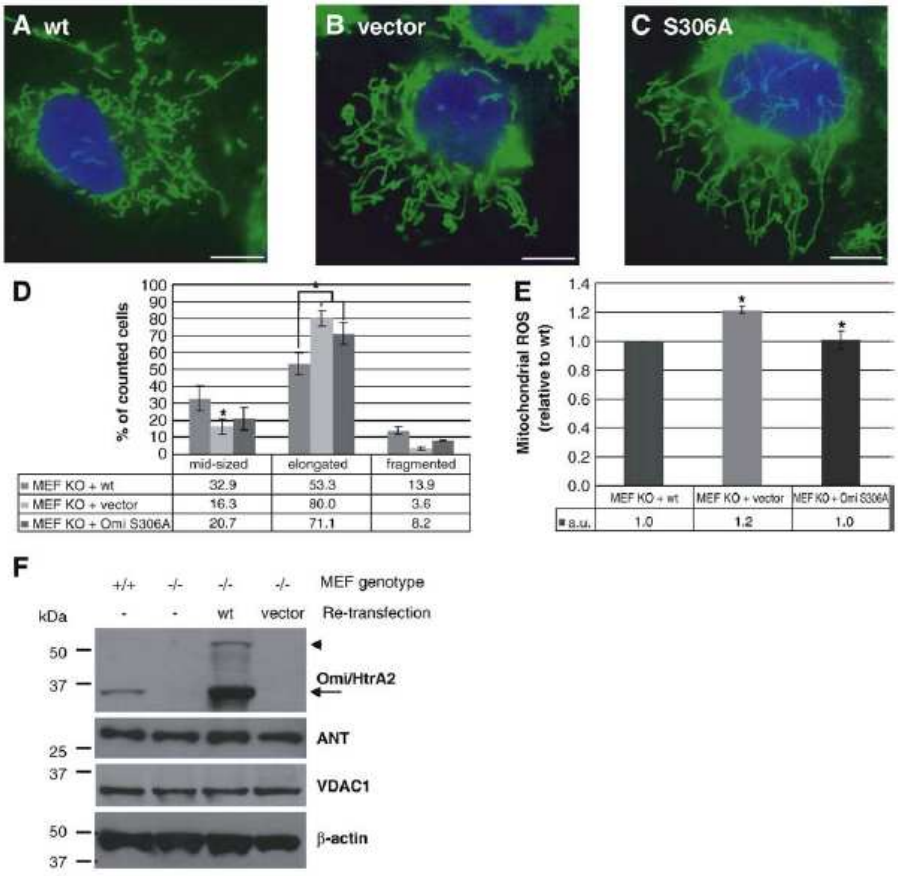
A wt
B vector
C S306A
D
% of counted cells
mid-sized
elongated
fragmented
MEF KO + wt 32.9 53.3 13.9
MEF KO + vector 16.3 80.0 3.6
MEF KO + Omi S306A 20.7 71.1 8.2
E
Mitochondrial ROS (relative to wt)
MEF KO + wt
MEF KO + vector
MEF KO + Omi S306A
a.u. 1.0 1.2 1.0
F
MEF genotype
+/+ -/- -/- -/-
kDa
Re-transfection
- - wt vector
Omi/HtrA2
ANT
VDAC1
β-actin

Figure 5

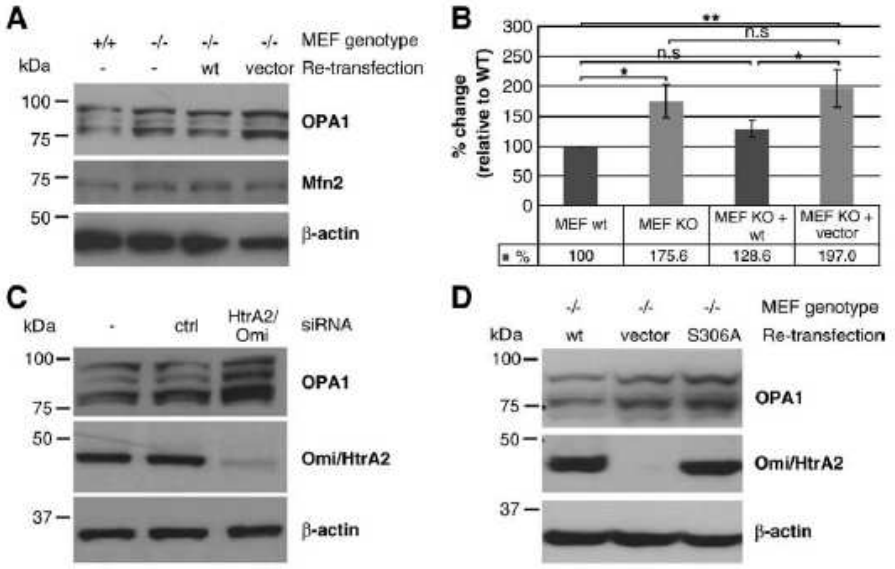
A
+/+ -/- -/- -/- MEF genotype
kDa - - wt vector Re-transfection
100
75
OPA1
75
Mfn2
50
β-actin
B
% change (relative to WT)
300
250
200
150
100
50
0
**
n.s
n.s
*
*
MEF wt
MEF KO
MEF KO + wt
MEF KO + vector
n % 100 175.6 128.6 197.0
C
kDa - ctrl HtrA2/ Omi siRNA
100
75
OPA1
50
Omi/HtrA2
37
β-actin
D
-/- -/- -/- MEF genotype
kDa wt vector S306A Re-transfection
100
75
OPA1
50
Omi/HtrA2
37
β-actin

Figure 6

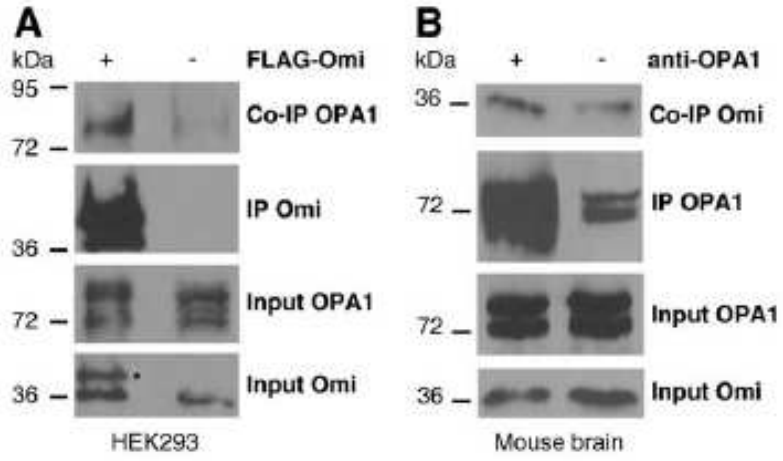
A
kDa
+
-
FLAG-Omi
95
72
Co-IP OPA1
IP Omi
36
72
Input OPA1
36
Input Omi
HEK293
B
kDa
+
-
anti-OPA1
36
Co-IP Omi
72
IP OPA1
72
Input OPA1
36
Input Omi
Mouse brain

Figure 7

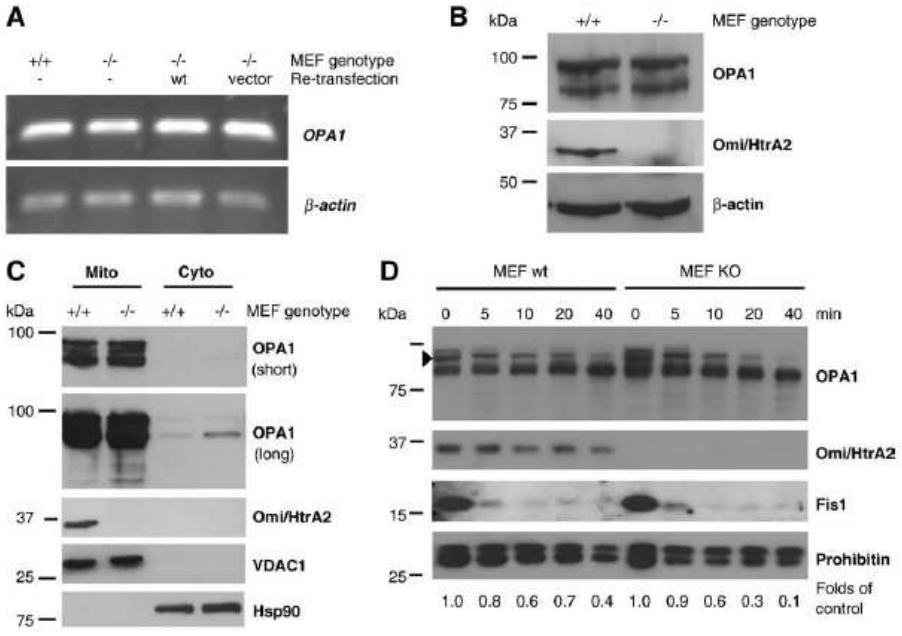
A
+/+ -/- -/- -/- MEF genotype
- - wt vector Re-transfection
OPA1
β-actin
B
kDa +/+ -/- MEF genotype
100
75
37
50
OPA1
Omi/HtrA2
β-actin
C
Mito
Cyto
kDa +/+ -/- +/+ -/- MEF genotype
100
100
37
25
75
OPA1 (short)
OPA1 (long)
Omi/HtrA2
VDAC1
Hsp90
D
MEF wt
MEF KO
kDa 0 5 10 20 40 0 5 10 20 40 min
75
37
15
25
OPA1
Omi/HtrA2
Fis1
Prohibitin
1.0 0.8 0.6 0.7 0.4 1.0 0.9 0.6 0.3 0.1
Folds of control

Chapter 4
Summary and conclusions

4.1 Summary

Several lines of genetic, post-mortem and experimental evidence suggest that protein aggregation and mitochondrial dysfunctions are closely associated with PD. The study of synphilin-1 (that is present in LB in the neurons of PD patients, as mentioned in the introduction) and HtrA2/Omi (that seems to have a role in maintaining the mitochondrial homeostasis in neurons, as mentioned above) may provide new insights on these pathogenetic mechanisms of PD.

Here we confirmed previous reports suggesting that synphilin-1-positive inclusions fulfil the criteria of aggresomes (Marx et al., 2003; Tanaka et al., 2004). We observed that synphilin-1-positive inclusions in cells stably overexpressing wild type and R621C synphilin-1 co-localize with the marker of centrosome γ-tubulin. In addition, MG132-induced inhibition of the proteasome caused an increased number of inclusions compared to untreated cells.

The autophagy inducers rapamycin and trehalose were effective in reducing the number of aggregates formed by WT and R621C mutant synphilin-1 by acting specifically on autophagic pathways. However, neither rapamycin nor trehalose was able to rescue synphilin-1 overexpressing cells from MG132-induced toxicity. Interestingly, we observed a protective effect of overexpressed WT synphilin-1 against apoptosis due to proteasome inhibition. Moreover, WT synphilin-1 overexpressing cells displayed an effective rapamycin-induced degradation of inclusions after pro-apoptotic treatment with MG132,

while no significant clearance of aggregates formed by R621C mutant synphilin-1 was observed in the same conditions.

Overexpression of both WT and R621C synphilin-1 led to increased levels of intramitochondrial ROS and decreased mitochondrial membrane potential compared to controls. These mitochondrial dysfunctions were not prevented by pharmacological activation of autophagy and they resulted independent from synphilin-1 aggregation.

Taken together, our data support a role of synphilin-1 in modulating the formation of aggresome-like inclusions that can be degraded via autophagy. Moreover, we confirmed interesting findings suggesting a protective role of WT synphilin-1 against apoptosis (Giaime et al., 2006). On the other hand, synphilin-1 overexpression resulted toxic for mitochondria.

Loss of HtrA2/Omi caused increased levels of mitochondrial ROS and decreased mitochondrial membrane potential in Mouse Embryonic Fibroblasts (MEF) cells from HtrA2/Omi knockout (KO) mice. Moreover, lack of HtrA2/Omi expression was responsible for increased amounts of elongated mitochondria in HtrA2/Omi KO MEF cells, as well as in human HeLa cells and in *Drosphila melanogaster* S2R+ cells, after transient silencing of HtrA2/Omi with siRNA. A critical role of the protease function of HtrA2/Omi for regulation of mitochondrial morphology was shown by effective rescue experiments with wild-type HtrA2/Omi expression in the KO background. In contrast, protease deficient HtrA2/Omi was unable to rescue the mitochondrial functional alterations.

HtrA2/Omi appeared to interact with the mitochondrial fusion protein OPA1 in both HEK293 cell and lysates from mouse brains. In addition, significant increase in mild detergent-extractable OPA1 levels was observed in both HtrA2/Omi KO MEF cells and HeLa cells treated with HtrA2/Omi siRNA, suggesting that HtrA2/Omi modulates the expression of a soluble pool of OPA1. The OPA1 protein levels were not altered by expressing a protease-defective variant of HtrA2/Omi.

To conclude, we reported evidence of a critical involvement of HtrA2/Omi in the maintenance of mitochondrial integrity, morphology and function.

4.2 Conclusions and future perspectives

Our findings support the concept of a cross-talk between pathological protein aggregation, dysfunctions of the UPS and mitochondrial impairments in the pathogenesis of PD. Therefore, future therapies for PD that focus on modulation of the formation of protein inclusions may not be effective to provide protection from cell death in the presence of mitochondrial abnormalities and proteasome impairments.

On the other hand, various publications reported protective effects of autophagy activation against subsequent stress insults in different cell lines, in the absence of any overexpressed aggregate-prone protein (Ravikumar et al., 2006; Pan et al., 2008; Pan et al., 2009).

It was suggested that a compensatory stimulation of autophagy triggered by the failure of the UPS to effectively clear protein aggregates may occur in the early stages of PD degeneration. This "compensatory stage" may be followed by a failure stage, in which autophagic mechanisms lead to cell death accompanied by accumulation of aggregates and autophagic vesicles (Martinez-Vicente and Cuervo, 2007). Indeed, in post-mortem PD brains signs of apoptosis (Hirsch et al., 1999; Nair et al., 2006; Tatton et al., 2003) as well as increased amounts of autophagic vacuoles and autophagy-related structures were observed (Anglade et al., 1997).

Taken together, current concepts suggest that potential treatments aimed to stimulate the autophagy-dependent clearance of protein inclusions should be started in the earliest stages of the disease, before

the onset of mitochondrial dysfunctions, UPS failure, and activation of apoptotic pathways in the surviving neurons of the substantia nigra.

Our results confirmed previous publications showing a protective effect of WT synphilin-1 against apoptosis, possibly mediated by its C-terminal fragment. In this context, possible new therapeutic strategies for PD could focus either on the enhancement of WT synphilin-1 expression or on mimicking the activities of the C-terminal fragments of synphilin-1.

Unfortunately, it is well known that PD begins years before patients and clinicians notice the first motor signs and at the time of the diagnosis it is possible that more than 50% of the neurons in the substantia nigra are already lost (Schapira et al., 2009). In this perspective, the discovery of new early markers of PD would be really helpful. Since we observed mitochondrial impairment in our cellular model also in basal conditions, in the absence of any sign of cell death, we suggest that the evaluations of mitochondrial parameters could be a potential early marker.

The involvement of HtrA2/Omi in PD is supported by studies on mice (Jones et al., 2003; Martins et al., 2004). However, the relevance of the protein in the pathogenesis of PD in humans is not yet well defined. We provided some insight about the physiological functions of HtrA2/Omi within the mitochondria, showing that loss of HtrA2/Omi causes mitochondrial impairment and altered morphology. Moreover, we suggested that modulation of mitochondrial morphology by HtrA2/Omi could be mediated by its direct interaction with the fusion protein OPA1.

These data highlight the connection between mitochondrial morphology and function, suggesting that potential therapeutic approaches based on restoring mitochondrial functions may not be sufficient if they can't preserve also the structure of mitochondria.

In this context, we speculate that early treatments favouring the maintenance of mitochondrial homeostasis, such as anti-oxidants, could be beneficial for PD patients.

4.3 References of chapter 4

Anglade P, Vyas S, Javoy-Agid F, Herrero MT, Michel PP, Marquez J, Mouatt-Prigent A, Ruberg M, Hirsch EC, Agid Y (1997) Apoptosis and autophagy in nigral neurons of patients with Parkinson's disease. Histol Histopathol 12:25-31.

Giaime E, Sunyach C, Herrant M, Grosso S, Auberger P, McLean PJ, Checler F, da Costa CA (2006) Caspase-3-derived C-terminal product of synphilin-1 displays antiapoptotic function via modulation of the p53-dependent cell death pathway. J Biol Chem 281:11515-11522.

Hirsch EC, Hunot S, Faucheux B, Agid Y, Mizuno Y, Mochizuki H, Tatton WG, Tatton N, Olanow WC (1999) Dopaminergic neurons degenerate by apoptosis in Parkinson's disease. Mov Disord 14:383-385.

Jones JM, Datta P, Srinivasula SM, Ji W, Gupta S, Zhang Z, Davies E, Hajnoczky G, Saunders TL, Van Keuren ML, Fernandes-Alnemri T, Meisler MH, Alnemri ES (2003) Loss of Omi mitochondrial protease activity causes the neuromuscular disorder of mnd2 mutant mice. Nature 425:721-727.

Martinez-Vicente M, Cuervo AM (2007) Autophagy and neurodegeneration: when the cleaning crew goes on strike. Lancet Neurol 6:352-361.

Martins LM, Morrison A, Klupsch K, Fedele V, Moisoi N, Teismann P, Abuin A, Grau E, Geppert M, Livi GP, Creasy CL, Martin A, Hargreaves I, Heales SJ, Okada H, Brandner S, Schulz JB,

Mak T, Downward J (2004) Neuroprotective role of the Reaper-related serine protease HtrA2/Omi revealed by targeted deletion in mice. Mol Cell Biol 24:9848-9862.

Marx FP, Holzmann C, Strauss KM, Li L, Eberhardt O, Gerhardt E, Cookson MR, Hernandez D, Farrer MJ, Kachergus J, Engelender S, Ross CA, Berger K, Schols L, Schulz JB, Riess O, Kruger R (2003) Identification and functional characterization of a novel R621C mutation in the synphilin-1 gene in Parkinson's disease. Hum Mol Genet 12:1223-1231.

Nair VD, McNaught KS, Gonzalez-Maeso J, Sealfon SC, Olanow CW (2006) p53 mediates nontranscriptional cell death in dopaminergic cells in response to proteasome inhibition. J Biol Chem 281:39550-39560.

Pan T, Kondo S, Zhu W, Xie W, Jankovic J, Le W (2008) Neuroprotection of rapamycin in lactacystin-induced neurodegeneration via autophagy enhancement. Neurobiol Dis 32:16-25.

Pan T, Rawal P, Wu Y, Xie W, Jankovic J, Le W (2009) Rapamycin protects against rotenone-induced apoptosis through autophagy induction. Neuroscience 164:541-551.

Ravikumar B, Berger Z, Vacher C, O'Kane CJ, Rubinsztein DC (2006) Rapamycin pre-treatment protects against apoptosis. Hum Mol Genet 15:1209-1216.

Schapira AH, Agid Y, Barone P, Jenner P, Lemke MR, Poewe W, Rascol O, Reichmann H, Tolosa E (2009) Perspectives on recent advances in the understanding and treatment of Parkinson's disease. Eur J Neurol 16:1090-1099.

Tanaka M, Kim YM, Lee G, Junn E, Iwatsubo T, Mouradian MM (2004) Aggresomes formed by alpha-synuclein and synphilin-1 are cytoprotective. J Biol Chem 279:4625-4631.

Tatton WG, Chalmers-Redman R, Brown D, Tatton N (2003) Apoptosis in Parkinson's disease: signals for neuronal degradation. Ann Neurol 53 Suppl 3:S61-70; discussion S70-62.

Publications